University of Zurich[UZH]

Retreat of the Turtmanngletscher and succession of Larix decidua Mill. since the LIA using geomorphological mapping and dendrochronological analysis

GEO 511 Master's Thesis

Author
Ariane Dieth
18-732-255

Supervised by
Dr. Isabelle Gärtner-Roer

Faculty representative
Prof. Dr. Andreas Vieli

30.09.2024
Department of Geography, University of Zurich

Master's Thesis – University of Zurich

Retreat of the Turtmanngletscher and succession of *Larix decidua* Mill. since the LIA using geomorphological mapping and dendrochronological analysis

Author:

Ariane Dieth

Supervised by:

Dr. Isabelle Gärtner-Roer, University of Zurich

Faculty representative:

Dr. Andreas Vieli, University of Zurich

Content

Acknowledgments

I would like to extend my gratitude to my supervisor Dr. Isabelle Gärtner-Roer of the University of Zurich, Department of Geography, for her mentoring during the field work, her feedback, and her oversight during this research.

I am also grateful to the University of Zurich particularly the Department of Geography for providing an academic environment for studying in my masters and writing this thesis.

Special thanks go to Dr. Holger Gärtner of the Swiss Federal Research Institute for Forest, Snow and Landscape (WSL), Research Unit Forest Dynamics, Dendrosciences Group, for his guidance during fieldwork and in the lab, his feedback, and his mentoring during this thesis. Additional thanks go to Loïc Schneider, the lab technician at WSL, for his assistance with questions on my lab work, and to Lisa Marie Yvette Jourdain and Dr. Stefan Klesse at WSL for their help and provision of resources in statistics. I am equally indebted to my fellow students, Flurina Durisch and Isabel Kienbaum, who accompanied me during field campaigns, making the work both productive and enjoyable.

I would also like to acknowledge the landowners, Bergschaft Ems/Gemeinde Oberems, and the local forester for allowing me to collect dendrochronological samples in the study site of the Turtmann Valley which was crucial for my thesis.

On a personal note, I extend my heartfelt thanks to my friends and fellow students Leonora Seiler, Bahri Mindik and Sebastian Quinten who shared the journey of writing a master's thesis with me. Their friendship and their encouragement while simultaneously writing their own thesis were greatly appreciated during this period.

Abstract

This thesis examines the landscape evolution of the southern Turtmann Valley, in Switzerland, focusing on the retreat of the Turtmanngletscher since the Little Ice Age (LIA). Through a combination of geomorphological mapping, glacier extent reconstructions and dendrochronological analysis of *Larix decidua* Mill., the study investigates processes shaping the landscape and the tree establishment in the proglacial area. The methods used included geomorphological mapping through aerial images and different maps and mapping of glacier extents through historical maps and aerial images, both in a GIS environment. Further methods were tree-ring width measurements with a correlation analysis on the relationship of the tree-ring width and temperature resp. precipitation, and the approach of a chronosequence by the determination of the minimum age of the sampled *L. decidua* Mill. The resulting geomorphological map presents the interactions between different processes in an alpine valley following deglaciation in the late Holocene. The findings reveal that the Turtmanngletscher reached its maximum extent in the mid-19th century followed by a period of retreat with minor readvances in the 1920s and 1980s. While geomorphological mapping clearly identified the frontal "LIA" moraine at the focus site, dendrochronological dating of these landforms was limited, as tree establishment in the area occurred only after significant glacier retreat. Geomorphic processes, such as gravitational and periglacial disturbances, were found to delay tree establishment in parts of the proglacial area following the Turtmanngletscher's retreat from its maximum extent during the LIA. Tree growth patterns of *L. decidua* Mill. were found to correlate with temperature, while precipitation had less impact. As a final result, the response of tree growth to climatic conditions could be used to validate glacier extent mapping. In conclusion, this thesis contributes to understanding the landscape evolution of the southern Turtmann valley as a post-glacial landscape by highlighting the connection of geomorphology, climate and succession of larch trees.

List of Figures

List of Tables

List of Tables in the Appendix

1. Introduction

In high mountain environments, glaciers have long been the dominant forces grinding down bedrock and carving out valleys during the past glaciations of the Pleistocene. The most recent effects of glaciers on the landscape were made after the last glacial maximum (LGM) around 18'000 years ago which was followed by a warming period known as the Holocene (Le Roy et al., 2024). This chaotic period, marked by climatic fluctuations, is divided into different sub-periods that feature colder or warmer temperatures where the landscape was influenced through on-going glacier retreats and readvances. One of such cooling period during the Holocene was the Little Ice Age (LIA) after which the current warming period began. Multiple dates for the start and the end of this period have been suggested in studies, with a general consensus in the Alps placing the period between approx. the years 1260 to 1860 (Le Roy et al., 2024; Wanner et al., 2022). The last maximum glaciation of the Holocene occurred at the end of the LIA, with glacier advances around the mid-19th century (Zemp and Paul, 2008). Since the end of the LIA, glaciers have retreated significantly due to global climate (Le Roy et al., 2024). This retreat is particularly evident in alpine environments, where steep topography and dynamic climatic conditions have contributed to rapid ice loss (Dikau et al., 2019). Given that glaciers serve as long-term freshwater reservoirs and their retreat can destabilise valley slopes, understanding their historical behavior is crucial for predicting future changes and the impact of deglaciation on the evolving landscape (Zhu et al., 2013). As glaciers vanish, they expose new surfaces to the dynamic processes of erosion and sediment transport in a proglacial area where geomorphic processes and ecological succession unfold (Eichel, 2017).

Ecological succession follows a pattern from pioneer microbiological ecosystem over herb species to shrub and tree species. This primary succession and the establishment of vegetation of later stages of succession in recently deglaciated terrains are influenced by a complex interplay of factors (Moris et al., 2017). Topography, climatic conditions, soil development, disturbances and microsite conditions all play a critical role in determining the trajectory of vegetation development (Eichel et al., 2013; Garbarino et al., 2010; Wojcik et al., 2021). In a proglacial area, trees like European larch trees (*L. decidua* Mill.) often colonise moraine surfaces and establish where conditions allow (D'Amico et al., 2010). By dating the germination age of these trees, an indirect method of dating of moraines and glacier retreat can be applied, often where no previous absolute dating of the landform exists. Thus, the minimum age of a landscape can be derived by examining the time it took for a glacier to retreat and for trees to establish (Le Roy et al., 2024; Rheintaler, 2024; Yang et al., 2021). Additionally, the correlation between tree growth and climatic parameters such as temperature and precipitation can be analysed in tree-ring width growth offering information on the climate and glacier fluctuations in the proglacial area (Gärtner and Heinrich, 2013).

The southern Turtmann Valley in Switzerland presents an ideal case for studying these processes. Since the retreat of the Turtmanngletscher after the LIA's maximum advance in 1850, the valley has undergone significant geomorphological and ecological changes (Dikau et al., 2019). Proglacial areas in the valley are subject to ongoing gravitational, periglacial, fluvial, and erosional processes (Eichel, 2017; Messenzehl et al., 2018). Vegetation succession is advancing across this newly exposed terrain from distant valley areas to the glacier forefield which provides an opportunity to examine the dynamics of landscape and ecological development. The cluster of *L. decidua* Mill. established in the proglacial area at the location of the hypothesised terminus of the Turtmanngletscher during the last maximum advance of the LIA is ideal for studying these dynamics.

Previous studies have largely focused on broader patterns of glacier retreat and the climatic drivers behind these landscape changes, but there remains a critical need to explore the detailed geomorphological and ecological processes that follow deglaciation (Le Roy et al., 2024; Rheintaler, 2024; Wanner et al., 2022; Zemp and Paul, 2008). In the Turtmann Valley, prior research has examined glacier retreat patterns and geomorphic processes in a large scale (Otto and Dikau, 2004; Messenzehl et al., 2017) or specific aspects of vegetation succession, such as the colonisation of lateral moraines (Eichel et al., 2013; Eichel, 2017). However, there remains a gap in understanding the connection between the establishment of larch trees and glacier retreat. Given that geomorphic processes influence both the landscape development of the main valley floor and tree establishment, understanding the interactions between these processes such as landslides, permafrost degradation, changes in meltwater streams and other geomorphic processes with the deglaciated ground is crucial.

This thesis aims to address this research gap by analysing tree age distributions in relation to landscape features, such as the frontal moraine of the last maximum extent of the Turtmanngletscher in the LIA, and in relation to climatic conditions. By using dendrochronology to date European Larch trees (*L. decidua* Mill.) in the proglacial area, together with geomorphic processes across the southern Turtmann Valley, this research seeks to reconstruct the sequence of landscape development in the southern Turtmann valley since the LIA and provide new insights into the factors driving these changes by exploring following research questions:

1. What can geomorphological mapping, glacier extents since the Little Ice Age, and a dendrochronological analysis of European Larch trees (*Larix decidua* Mill). tell about the landscape development of the southern Turtmann Valley and the glacial history of the Turtmanngletscher?
2. Where was the terminus of Turtmanngletscher in the Little Ice Age, and how did the landscape in the proglacial area develop afterwards?
3. Can the frontal moraines from the Little Ice Age be identified and dated using dendrochronological methods (minimum age determination)?

By answering these questions, this thesis aims to enhance the understanding of landscape evolution in high mountain environments and provide insights into the complex interactions between glacial history, geomorphology, and dendrochronology. This is especially needed in the context of ongoing climate change.

2. Theory

This master thesis covers two disciplines in physical geography – geomorphology and dendrochronology – that are complex and full of many sub-disciplines. Both were mostly developed around the early 20th century when more technological and methodological advances were made (Chandler et al., 2018; Schweingruber, 1996). Geomorphology describes and classifies relief shapes on the Earth's surface and aims to understand the processes responsible for shaping these relief forms (Dikau et al., 2019). Dendrochronology studies the growth of trees and tries to analyse past climatic conditions, environmental changes and historical events by examining the tree rings (Schweingruber, 1996). As both disciplines covered in this master thesis are complex, a short historic context, relevant theories to the methods used in this master thesis and important theories used for the discussion are covered in the following chapter.

2.1 Geomorphology

2.1.1 History of Geomorphology

The discipline of geomorphology is connected to quaternary geology and has been part of the early earth sciences although it was not named a sub-discipline until later. In the 18th century scientists like J. Hutton with "Theory of the Earth" (1788) and J. Playfair with "Illustrations of the Huttonian Theory of the Earth" (1802) established the idea that the Earth's surface is shaped by ongoing observable processes rather than sudden catastrophic events. However, at that time these theories were not accepted yet because in the religious climate. It was more preffered to believe in the theory of catastrophic events due to their part in the bible. These geologists laid the foundation for other scientists in the 19th century such as C. Lyell with "Principles of Geology" (1830) and W.M. Davis with "The Geographical Cycle" (1900) who developed the discipline of geomorphology in the western cultures. Davis' idea of different stages of development of the landscape with his categories of "youth", "maturity" and "old age" influenced geology at that time especially in the English-speaking regions. The Germans A. Penck and W. Penck had some opposing ideas to Davis which are further described by Oldroyd and Grapes (2008) but not described here in this master thesis as this would cover too much detail of the history of geomorphology and glacial geomorphology. The Ice Age theory and theories how glaciers have shaped the Earth's surface were presented by L. Agassiz together with J. Bettannier in "Études sur les Glacier" (1840). The three-volume work "Die Alpen im Eiszeitalter" (1901/1909) by A. Penck and E. Brückner is based on early scientists like Agassiz and Bettannier and it was influential for glacial geomorphological mapping and field mapping in glaciated areas for the future (Chandler et al., 2018; Haritashya et al., 2022; Oldroyd and Grapes, 2008).

2.1.2 Geomorphological mapping

Field mapping was already an established approach in the late 19th and early 20th century to record the study area and landforms on topographic maps (Haritashya et al., 2022). With time, new methods to map the real landscape was developed next to the traditional exclusive field mapping. A good practice nowadays is to use remote sensing such as aerial photographs to analyse a study site and map before and after a field campaign (Theler et al., 2010). In the field, printouts can be brought and scientists can directly map onto them. With GPS the exact location of a landform can be noted down and loaded into a GIS software later in the office. The geographic information system (GIS) provides a fast way on how to work and calculate with different layers to make a geomorphological map (Theler et al., 2010). A workflow for ideal field mapping can be found in Chandler et al. (2018). In recent years, artificial intelligence and machine learning are more common in many sciences. Using only remote sensing and letting the machine describe the landscape can help in systematic approaches covering big areas but for other areas where details or complex relationship between natural processes want to be studied, a great part of the interpretation could be lost. The interpretation of the landscape can only be done by processing the observations and information cognitively which is closely related to the human as described by Brierley et al. (2021) (see **Figure 1**). "Reading the landscape" is namely influenced by known concepts, assumptions made possible by experiences and intuition, situational context (environmental, cultural, and historical) and cognition in general. Additional to only data and observations from field surveys, sedimentological, chronological and remote sensing data should be considered for interpretations in geomorphological mapping. Often, previous knowledge and experiences influence hypotheses and what is expected to see in a landscape. This can lead to a confirmation bias – the tendency to seize upon information that confirms the preferred position and initial hypothesis. To counteract this bias, having an approach of multiple working hypotheses and maintaining an open mind during field campaigns is essential (Alden, 2019. These multiple working hypotheses involves a lot of different assumptions and theories from previous studies. In the end, the geomorphological map shows the interpretation made by the scientist with evidence supporting the conclusions although in the context the scientist is in. Therefore, interpretations should undergo validation and verification to assess the reliability of the conclusions (Alden, 2019; Brierley et al., 2021; Chandler et al., 2018; Couper, 2022; Haritashya et al., 2022).

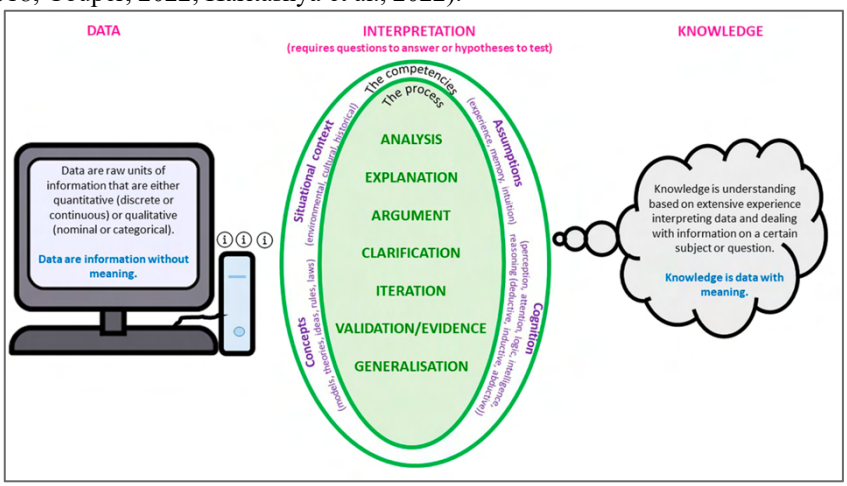

FIGURE 1: A SCHEMA OF HOW INTERPRETATION OF DATA IS INFLUENCED THROUGH DIFFERENT FACTORS (FROM BIERLEY ET AL., 2021).

The scientific framing and knowledge behind the interpretation should be considered when reading a geomorphological map. Hence, the next chapter goes into a short theory on glaciology and geomorphology in an alpine proglacial area to illustrate the background knowledge for this thesis.

2.1.3 Glaciology and geomorphology in an alpine proglacial area

Most glaciers in an alpine terrain are either valley or cirque glacier. The proglacial area is defined as the area between the un- or metastable state of a landscape and a new equilibrium state. This is usually between the glacier tongue where deglaciation occurs and a land system with semi-stable periglacial or non-glacial conditions. Oftentimes, the boundary of the present-day proglacial area is defined to be at the location of the frontal and lateral moraines of the Little Ice Age (LIA) because since the maximum extent of the LIA around the 1850s, glaciers have mostly retreated and the land systems became ice-free (Heckmann et al., 2019; Zemp et al., 2008).

Erosion of a landscape as well as accumulation of new sediment in an alpine proglacial area is influenced by glacier movement. A glacier can move through internal ice deformation due to the own mass of a glacier. Basal gliding is another type of glacier movement and is caused by sufficient high temperature and sufficient pressure at the lower part of the ice mass. These factors lead to a meltwater layer at the ice-ground boundary and enables sliding on the surface. Alpine glaciers are mostly temperate glaciers (ice temperature around 0°C) and therefore, basal movement is a more prominent glacier movement and leads to a lot of glacial erosion at the base (Haritashya et al., 2022; Dikau et al., 2019). Glacial erosion results from several processes including abrasion, compression, the fracturing of solid rock and erosion through transported rock debris at the glacier basal zone. Additionally, glaciofluvial processes due to meltwater shape the land surface. However, the geomorphology of a typical alpine proglacial area is influenced by more than just the glacial movement with the retreats and advances of the glacier. The topography and geology are crucial for the strength of glacial erosion in shaping a surface. Chemical weathering and physical weathering are autogenic erosional processes happening everywhere in a mountain valley. In addition to weathering, other processes influence the relief. In geomorphology the concept of "process domains" by Montgomery (1999) is used often to categorise areas of land surface where one or multiple processes are responsible for the detachment, transport and accumulation of material. Next to the above-mentioned glacial and glacio-fluvial process domain these can namely be periglacial, gravitational, fluvial or slope-aquatic, aeolian, organic and anthropogenic process domains. However, in deglaciated valleys, process domains that only are within glacial geomorphology are important for shaping the landscape. Thus, for example aeolian processes are less the drivers of shaping the landscape than the other processes even though wind can be a factor in snow drift and snow accumulation or seed dispersal for succession of vegetation. Thus, these processes are interconnected with each other (Brardinoni and Hassan, 2006; Dikau et al., 2019; Haritashya et al., 2022; Heckmann et al., 2019).

As it is possible to categorise and map landforms and land surface with countless different concepts and models, the approach by Eichel (2017) which is based on Montgomery (1999) and Dikau et al. (2019) is used in this master thesis, while other concepts and models are not reviewed. **Table 1** shows an overview of different process domains in an alpine proglacial area with different landforms that are relevant for this master thesis adapted from Eichel (2017) and added with content from Dikau et al. (2019). However, this list is not complete with all geomorphological landforms that could exist in an alpine setting.

TABLE 1: AN OVERVIEW ON DIFFERENT PROCESS DOMAINS, PROCESSES AND LANDFORMS IN AN ALPINE PROGLACIAL AREA, ADAPTED FROM EICHEL (2017) AND DIKAU ET AL. (2019). IN BLUE A TYPICAL LANDFORM FOR THE CORRESPONDING PROCESS IS DESCRIBED.

Process domain	Process	Description
Glacial	Erosion through glacier movement	U-valley: glacially shaped valley in an U-shape with the valley floor above sea level and it is the most frequent morphological landform built through linear glacial erosion.
		Striation: linear grooves or scratches on a rock surface that are in the direction of the glacier's movement. They are created through rocks and debris embedded in the ice that scrape the bedrock.
		Crescentic and lunate fracture: semi-circular, crescent-shaped fractures and hollow forms in solid rock, often on polished rock surfaces.
		Chattermark: a series of small, crescent-shaped fractures on a rock surface that are created by the pressure of hard rocks or debris embedded in a glacier as it moves over the underlying bedrock.
		Polished rock surface: smooth rock surfaces formed by abrasion where rough edges are grinded and a shiny smooth surface is left.
	Plucking and abrasion	Roche moutonnée: a ridge of solid rock shaped by glacier ice with a flat windward side (abrasion) and a steep leeward side (plucking).
	Accumulation through glacier movement	Basal moraine / basal till: glacial drift in the valley floor that is deposited underneath the glacier and made of till sediment.
		Moraine: wall-like, glaciogenic relief forms that occur at the edges of glaciers through sediment accumulation. This group of landforms can also include moraines that occur in the ice mass itself and on the ice mass or that can be composed of sediments that are not of glacial origin. In the alps most visible are usually lateral moraines (at the side of a glacier) and frontal moraines (end moraine that is at the edge where the glacier tongue was).
Periglacial	Freezing and thawing	Permafrost ground: soil, rock or sediment that remains at or below 0°C for at least two consecutive years.
		Rock glacier: lobate or tongue-shaped landform composed of a mixture of ice and rock debris that moves slowly downslope. It forms in periglacial environments where rock debris accumulates and is mixed with ice which drives the gradual flow of the mass due to gravity.
		Protalus rampart: a ridge or mound of rock debris that accumulates at the base of a steep slope typically below a snow or ice patch. It forms when loose rocks and debris are dislodged by freeze-thaw action and then roll or slide down the slope and are halted by the edge of the persistent snow or ice creating a distinct linear accumulation.
	Cryoturbation	soil movement due to frost action
	bound solifluction	slow downslope movement of soil mass due to diurnal and annual frost creep and gelifluction under vegetation cover such as a lobate landform with vegetation / turf-banked solifluction lobe.
	unbound solifluction	slow downslope movement of soil mass due to freeze-thaw processes (needle-ice creep, diurnal and annual frost creep and gelifluction) such as a lobate landform without vegetation / stone-banked solifluction lobe.

TABLE 1 (CONTINUED): AN OVERVIEW ON DIFFERENT PROCESS DOMAINS, PROCESSES AND LANDFORMS IN AN ALPINE PROGLACIAL AREA, ADAPTED FROM EICHEL (2017) AND DIKAU ET AL. (2019). IN BLUE A TYPICAL LANDFORM FOR THE CORRESPONDING PROCESS IS DESCRIBED.

Process domain	Process	Description
Gravitational	Landsliding	Downward movement of slope material resulting from a failure along a well-defined shear plane, includes fall or slide of individual clasts, translational debris sliding and rotational slides (slumps). The landform in this thesis often just called a landslide deposit.
		Rock avalanche: rapid, large-scale movement of rock material down a slope and it involves the disintegration of a large volume of rock into smaller fragments which flow down the slope at high-speed forming a chaotic and highly destructive debris deposit.
		Debris flow: mixture of fines, larger sediment and water moving downslope triggered by intensive rainfall or rapid snowmelt.
		Rock fall: sudden and freefall release of individual rocks or a small cluster of rocks from a steep slope or cliff. This occurs when rock material detaches due to weathering, freeze-thaw cycles or other natural processes.
(nival)		Snow avalanche: rapid and often large-scale downslope movement of snow, sometimes mixed with ice and debris, triggered by factors such as heavy snowfall, wind, temperature changes, or human activity.
Fluvial	water and soil erosional processes	processes eroding slope material by running water
		Gully channel: a narrow, steep-sided trench or channel formed on a hillside or slope by the concentrated flow of water typically during heavy rainfall or rapid snowmelt.
		Inter-gully wall: ridge-like landform produced by a combination of debris flows and soil erosional processes ("gullying") between gully channels.
	water erosional processes	Fluvial channel: a channel in the ground that is created through erosion. There can be active channels which have continuously water flowing and inactive channels which are not active anymore or not active in the observational period.
		Gorge: deep narrow valley with steep vertical walls craved through erosion of a river over a long time period. It can be built through a subglacial meltwater river.
	sediment deposition	Sandur: a broad flat area of sediment deposited by meltwater streams flowing from a glacier and composed of sand, gravel and other debris that have been carried and spread out by the water as it flows away from the glacier. It is sometimes also called glacier outwash plain.
		Delta: an outwash plain in the shape of a delta with multiple rivers and streams.
Anthropogenic		Multiple landforms that are shaped and created through human activity can be visible in a proglacial area. These include artificial or dammed lakes, hiking paths and streets, artificial hills and more.

2.2 Dendrochronology

2.2.1 Dendrochronology

The science of dendrochronology covers all scientific topics where tree rings are used for an accurate age determination. The principle of crossdating which is considered to be the base for dendrochronological studies was founded by A.E. Douglass in 1919 when he cross-dated different trees for purposes in meteorology (Gärtner and Heinrich, 2013). In this method, patterns in tree-ring growth of trees from the same region or study site are compared as they usually show similar growth patterns due to the shared environmental conditions. By aligning these patterns, a precise chronological sequence can be established to ensure that each ring is assigned to its exact calendar year (see **Figure 2**). For example, if there were multiple very dry years and a tree exhibits thin rings during this period, another tree of the same species in the same site shows low growth as well. Hence, these patterns can be compared and the age can be validated. In a typical dendrochronological study, firstly two samples per tree are crossdated visually and with statistical measures such as Gleichläufigkeit (no English term) to identify and correct any errors in measuring tree-ring widths and in ring counting which could be detected as missing or false rings. Gleichläufigkeit is a statistical measure of how well the patterns of tree-ring growth of two different samples from year to year are synchronous and supports crossdating. Secondly, the sample is crossdated with an existing chronology from the region or the other sampled crossdated tree-ring width curves of trees in the same site to build up a new chronology. This new principle at that time made it possible to accurately date tree rings to the calendar year and to use wooden samples newly in multiple disciplines such as climatology, archaeology and geomorphology (Crang et al., 2018; Gärtner and Heinrich, 2013; Schweingruber, 1996; Wilford et al., 2005).

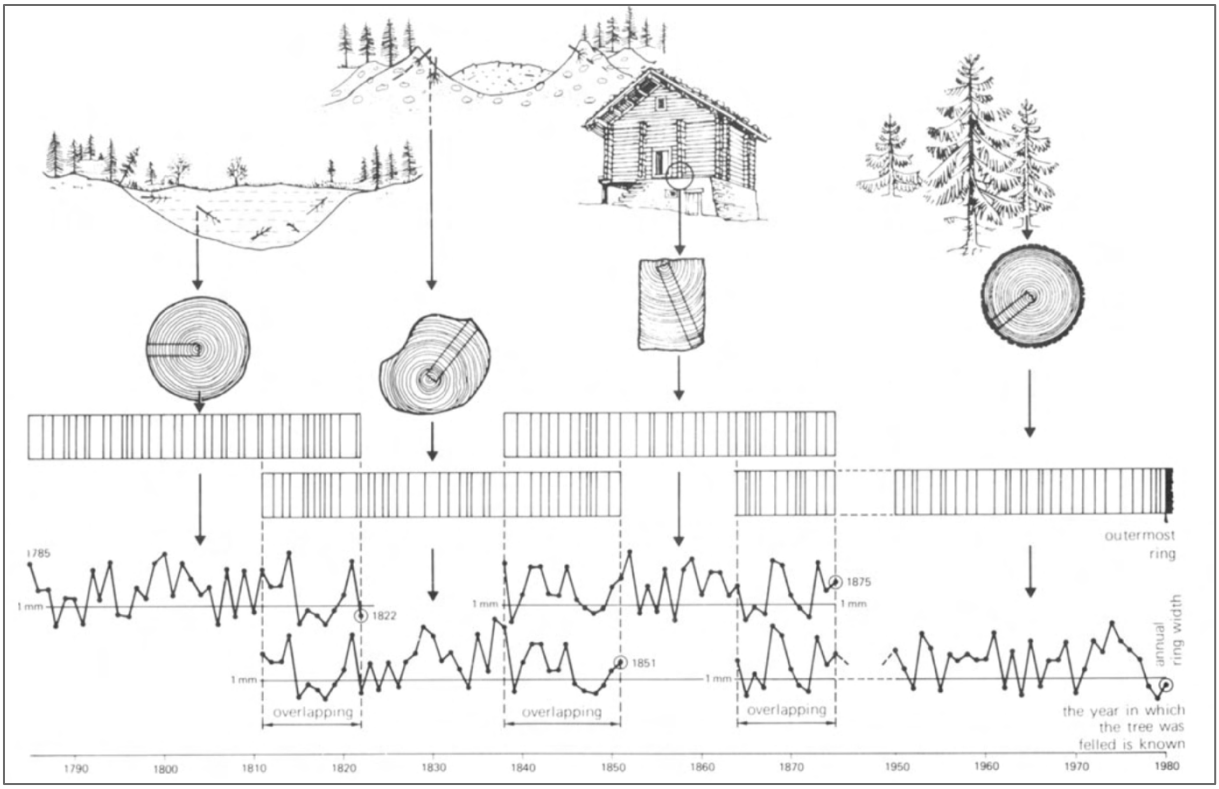

FIGURE 2 A SCHEMA FOR CROSSDATING DIFFERENT SAMPLES WITH EACH OTHER (FROM SCHWEINGRUBER, 1988).

Dendroecology is the study field which uses tree-ring data in environmental studies which cover topics such as geomorphic processes, water level changes, temperature and precipitation reconstruction or glacier fluctuations whereas all consider the growth responses of the trees to the respective environmental factors at the study site. Temperature and precipitation can be reconstructed by analysing the annual variations in tree ring width, wood density or isotopes at all locations where temperature or precipitation is the dominating factor controlling growth. In geomorphological analyses, a common use of tree-ring width measurements is used to study the response of tree growth to disturbances such as avalanches, landslides, debris flows, soil creep and other geomorphic processes. By determining the minimum age of a tree or a shrub in a previously glaciated valley, the succession of vegetation in said valley and the glacier fluctuations can be analysed. Since the start of dendrochronology, studies have grown more complex going beyond counting tree rings which is why knowledge about tree growth and wood anatomy had to improve alongside the development of dendroecological studies (Gärtner et al., 2015; Gärtner and Heinrich, 2013; Wilford et al., 2005).

2.2.2 Tree Growth

In general, trees in climates with seasons exhibit growth by formation of rings with some exceptions (see Schweingruber, 1996: 45). Although growth rings may be visible in these trees named by Schweingruber (1996) but they might not be annual. Trees in the Alps show seasonal cycles with rapid growth in spring, slowing of the growth over the summer, a cease in growth in autumn and no growth in winter. The period when a tree is growing is called growing season or vegetation period. Wood production and metabolism is stilled or reduced in winter to invest energetic resources into other parts (Newson, 2022a). Typically, tree growth does not occur simultaneously in all parts, it follows a sequence: first in the branches, then in the stem, and finally in the roots. Primary growth results in the elongation of the tree and occurs at the tips of roots and shoots. In the secondary growth, the stem, roots, and branches thicken to guarantee nutrient transport and support the new weight and height. The formation of wood in the secondary growth happens from outwards towards the centre during the growing season and involves different amounts and types of cells. The layer of living actively dividing cells is called vascular cambium and is situated between the phloem (bark) and the xylem (wood). During the growing season the cambium is producing phloem cells towards the outside of the cambial layer and xylem cells towards the inside. Softwoods resp. conifers, such as European larch tree (*Larix decidua*) or Stone Pine (*Pinus cembra*), and hardwoods resp. deciduous trees, such as Silver Birch (*Betula pendula*) or European Beech (*Fagus sylvatica*), have different processes and cells involved in tree growth. The biggest difference is the presence of vessel elements and fibres in hardwoods whereas softwoods lack these cell types. For this master thesis, only the tree growth of softwoods is described as there is a lot of literature on tree growth and wood anatomy of hardwoods available and not relevant for this thesis where only *L. decidua Mill.* is studied (Crang et al., 2018; Gärtner and Heinrich, 2013; Newson, 2022a and 2022b; Schweingruber, 1983; Schweingruber, 1996).

In terms of conifers, the xylem cells are parenchyma (storage) cells forming the rays and tracheids. The long tubular tracheids can transport water and provide structural support. In the spring, the cambium is more active, producing large, thin-walled tracheids which are designed for efficient water and nutrient transport. As the season progresses the cambium produces flattened, thick-walled tracheids for structural strength. This differentiation of the size and thickness of tracheids during the growing seasons leads to the visibility of a tree ring with the large thin-walled tracheids called earlywood and the small thick-walled tracheids called latewood as it is visible **Figure 3** (Crang et al., 2018; Gärtner and Heinrich, 2013; Newson, 2022b).

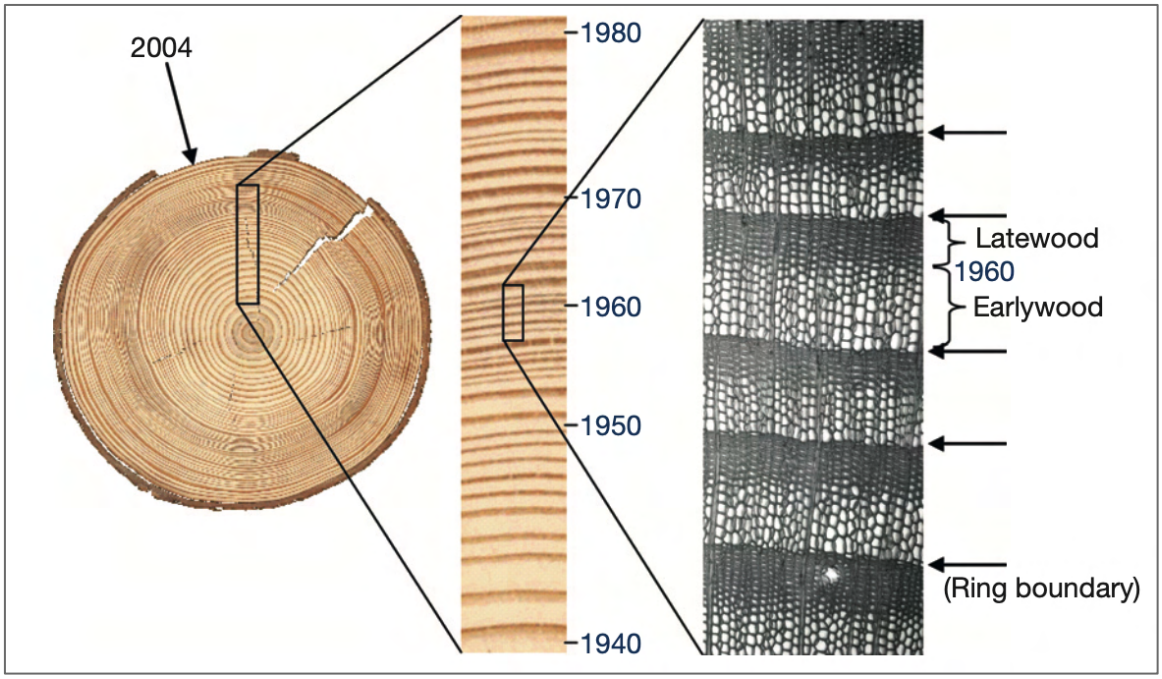

FIGURE 3 MACROSCOPIC AND MICROSCOPIC VIEW OF ANNUAL TREE RINGS IN CONIFERS WITH THE EARLYWOOD AND LATEWOOD VISIBLE IN THE IMAGE OF THE THIN SECTION (FROM GÄRTNER AND HEINRICH, 2013).

The wood-anatomical structure of each species is primarily determined by genetics and can be varied by environmental factors. The degree to which a tree is influenced by environmental factors is called sensitivity and depends on the species (Schweingruber, 1996). It can be observed by ring width variations or density fluctuations within the annual rings. Environmental factors can be temperature, water availability, light availability, nutrient supply, wind, competition, air and soil pollution and environmental disturbances such as mechanical load or damages to parts of the tree caused for instance by soil creep, avalanches, landslides and other gravitational processes. In general, a characteristic sequence of narrower or wider rings in trees in the same region which can be determined by crossdating reflect the environmental conditions that mostly influence tree growth in that specific region. Intra-annual rings might be formed when environmental conditions change rapidly during the active vegetation period. If a tree is disturbed by external factors and thus tilted or bent, reaction wood is formed. In conifers compression wood which usually consists of rounded cells with thick cell walls might be formed on the other side of the stem. Tension wood on the side of the disturbance is built in hardwood. There are other disturbances that can lead to growth suppression, scars in the tissue or other wood anatomical changes visible in tree rings. Environmental conditions do not only influence tree growth only in detail but also in the distribution, abundance and species composition of trees in an area (Frank et al, 2022; Gärtner and Heinrich, 2013; Newson, 2022; Schweingruber 1988; Schweingruber, 1996).

2.2.3 Ecological succession and chronosequence

Destructive events such as avalanches, debris flow and landslides can cause significant damage or even complete destruction of trees in an area. Additionally, land surface can be laid bare by forest fires and through glacier retreat. The recolonisation of vegetation and trees in this denuded area happens successively through different species compositions over time. This succession is closely linked to the frequency of such destructive events and can be distinguished by two types. Primary successions begin on severely disturbed land surfaces with new substrates such as raw soils, rock debris, river gravel or moraines (e.g. after volcanic eruption, after glacier retreat). Secondary successions begin on areas that are less severely disturbed and might have some soil organic matter left or are still covered by vegetation (e.g. forest fire, fallow land) (Gärtner and Heinrich, 2013; Matthews and Whittaker, 1987; Wojcik et al., 2021).

A glacier forefield is defined as the area between the glacier tongue and the last maximum advance of the glacier. This area typically undergoes a succession of the soil and vegetation due to deglaciation processes. The mineral substrate is successively exposed by the retreating glacier and depending on the geomorphological activity such as rock falls, meltwater streams and other weathering factors, soil is formed. The fast colonisation through soil biota, lichens and plants after a glacier retreat increase the built up of organic matter causing soil formation. The development of ecosystems is influenced by five main factors according to the classical approach described by Wojcik et al. (2021): climate, biota, parent material, topography and time. This supports the approach of the ideal chronosequence where all factors except for time differ minimally and the time since the glacier retreat correlates to the distance to the glacier tongue and development of the ecosystem. If the initial environmental conditions are the same and the sites of a succession are undergoing the same sequence of changes, then the chronosequence with the autogenic development can be used (see case A in **Figure 4**). However, other allogenic factors such as disruptions, different geomorphological activity, anthropogenic influence, and variable environmental conditions can influence the succession in the glacier forefield (see case B, C and D in **Figure 4**). Overall, the autogenic development is the dominant background process for glacier forefield succession (Egli et al., 2010; Eichel et al., 2013; Wojcik et al., 2021).

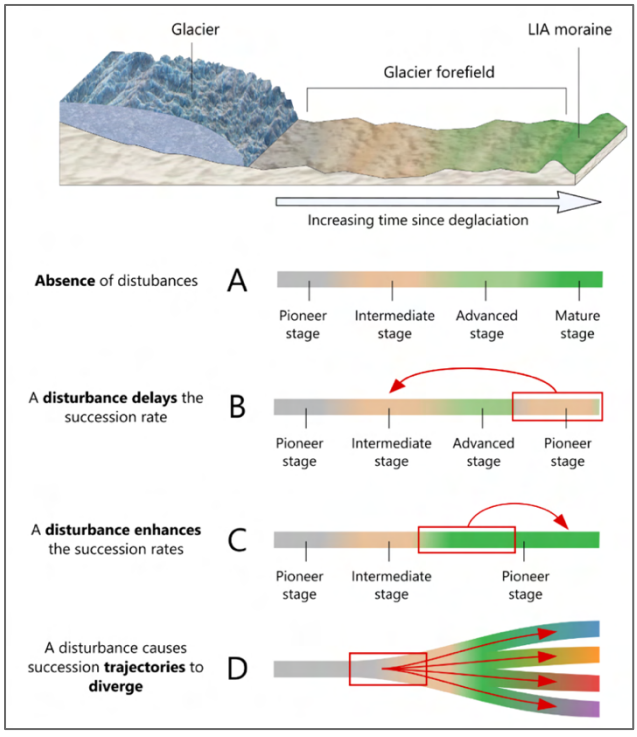

FIGURE 4 SCHEMA OF THE INFLUENCE OF DISTURBANCES ON THE SUCCESSION IN A GLACIER FOREFIELD (FROM WOJCIK ET AL., 2021).

Succession firstly starts with vegetation colonisation by pioneer species and is mostly influenced by abiotic factors such as topography, slope aspect, exposure to weathering processes, hydrology, moisture, sediment characteristics, and geomorphological activity. Pioneer species in a glacier forefield can be herb species such as *Saxifraga aizoides* or *Linaria alpina* near the terminus on moraines in areas with geomorphological activity, as it was the case in the study done by Eichel et al. (2013) and Eichel (2017) in the Turtmann Valley. In active glaciofluvial influenced areas and areas with high to moderate geomorphological activity typical grasses (e.g. *Alopecurus*) and herbs (e.g. *Campanula scheuchzeri*) occur. Further away and with more time for soil development typical herbs and dwarf shrubs start to grow (e.g. *Salix reiculata, Dryas octopetala*). This vegetation cover can stabilise the moving debris. In older and more stabilised terrain with lower geomorphological activity, herbs, shrubs and trees are found (e.g. *Rhododendron ferrugineum, L. decidua* Mill.). As soon as the soil is more developed and environmental conditions enable the growth of other tree species, the competition with the light demanding larch tree can lead to a decrease in the larch stock and an increase in other tree species such as *Pinus Cembra* (Burga et al., 2010; D'Amico, 2014; Eichel et al., 2013; Eichel, 2017).

3. Study site and methods

This master thesis combines methods from geomorphology and dendrochronology. The geomorphological analysis and mapping of the southern Turtmann Valley is the main method to analyse the whole study site with the main valley and hanging valleys, while the dendrochronological analyses on European larch trees (*Larix decidua* Mill.) are used for the focus site in the area of the retreat of the Turtmanngletscher since the Little Ice Age (LIA). Both methods together help in the determination of landforms and processes in the study site and the landscape history of the valley. A fundamental part of this thesis was the fieldwork where analyses of the landscape and sampling of the trees was made. The main field campaign was conducted in the first week of October 2023 and required five days in total. It included the analysis of the study site in the geomorphological context and the sampling of *L. decidua* Mill. in the focus site. The second field campaign at the end of July 2024 was used for the verification and reassessment of the mapped geomorphological landforms and of the interpretations of the growth of the larch trees.

3.1 Study Site

3.1.1 Location

The study site is in the south end of the Turtmann Valley in Canton Valais in southwestern Switzerland (see **Figure 5-A**). It is a neighbouring valley parallel to the west of the Matter Valley and east to the Val d'Anniviers / Val de Zinal. The Turtmann Valley is a 20 km long high alpine valley which spans from the north from the Rhône Valley (at 620 m a.s.l.) over the towns Unterems, Oberems and Ergisch to the south at the Turtmanngletscher and Brunegggletscher (4'150 m a.s.l.). The river Turtmänna flows from the artificial hydropower reservoir, the Turtmannsee, in the proglacial area in the south of the valley until the confluence of the Rhône River. The northern part of the Turtmann Valley is a narrow V-shaped valley shaped by fluvial erosional processes and the further south it gets, the more the valley floor opens to a U-shaped valley. The Turtmanngletscher is positioned at the south end of the valley with the accumulation area at the mountain flanks of the Tête de Milon, Bishorn and Stierbärg. The study site analysed in this master thesis is limited to the proglacial area and the few surrounding hanging valleys with the focus on the main valley covering the distance of the location of the terminus of the Turtmanngletscher during the maximum extent of the LIA (called "focus site" in this thesis) to the current terminus of the glacier. The valley is almost undisturbed from human activity with only two artificial lakes used for hydropower and a few hiking and mountaineering paths, thus making the landscape studied in this master thesis mostly influenced by natural geomorphic processes. The geomorphological analysis spans over a distance of 3.5 km with an area of 9.0 km^2 and from an altitude of 3'500 m a.s.l. from the mountain peaks to 2'000 m a.s.l. in the valley floor. However, the focus site of the terminus of the frontal "LIA" moraine where the dendrochronological samples were taken, spans over an area of 0.2 km^2 at an altitude of 2'050 to 2'200 m a.s.l. (see **Figure 5-B** and **Figure 5-C**).

◄ **FIGURE 5 A)** THE LOCATION OF THE TURTMANN VALLEY IN SWITZERLAND. **B)** THE SOUTH OF THE TURTMANN VALLEY WHERE THIS MASTER THESIS IS FOCUSED ON. THE WHOLE AREA FROM THE WESTERN TO THE EASTERN MOUNTAIN FLANKS IS ANALYSED IN THE GEOMORPHOLOGICAL CONTEXT WITH FOCUSING ON THE LOCATION OF THE FRONTAL "LIA" MORAINE, CALLED THE FOCUS SITE (WHITE SQUARE). **C)** THE STUDY SITE FOR THE DENDROCHRONOLOGICAL ANALYSIS IS FOCUSED ON THE AREA BETWEEN THE TURTMANNSEE AND THE FRONTAL MORAINE OF THE TERMINUS OF THE TURTMANNGLETSCHER DURING THE MAXIMUM OF THE LIA. SAMPLES FROM LIVING TREES WERE TAKEN IN THE FOCUS SITE (MARKED BY THE WHITE OUTLINE) (ARIANE DIETH, 2024).

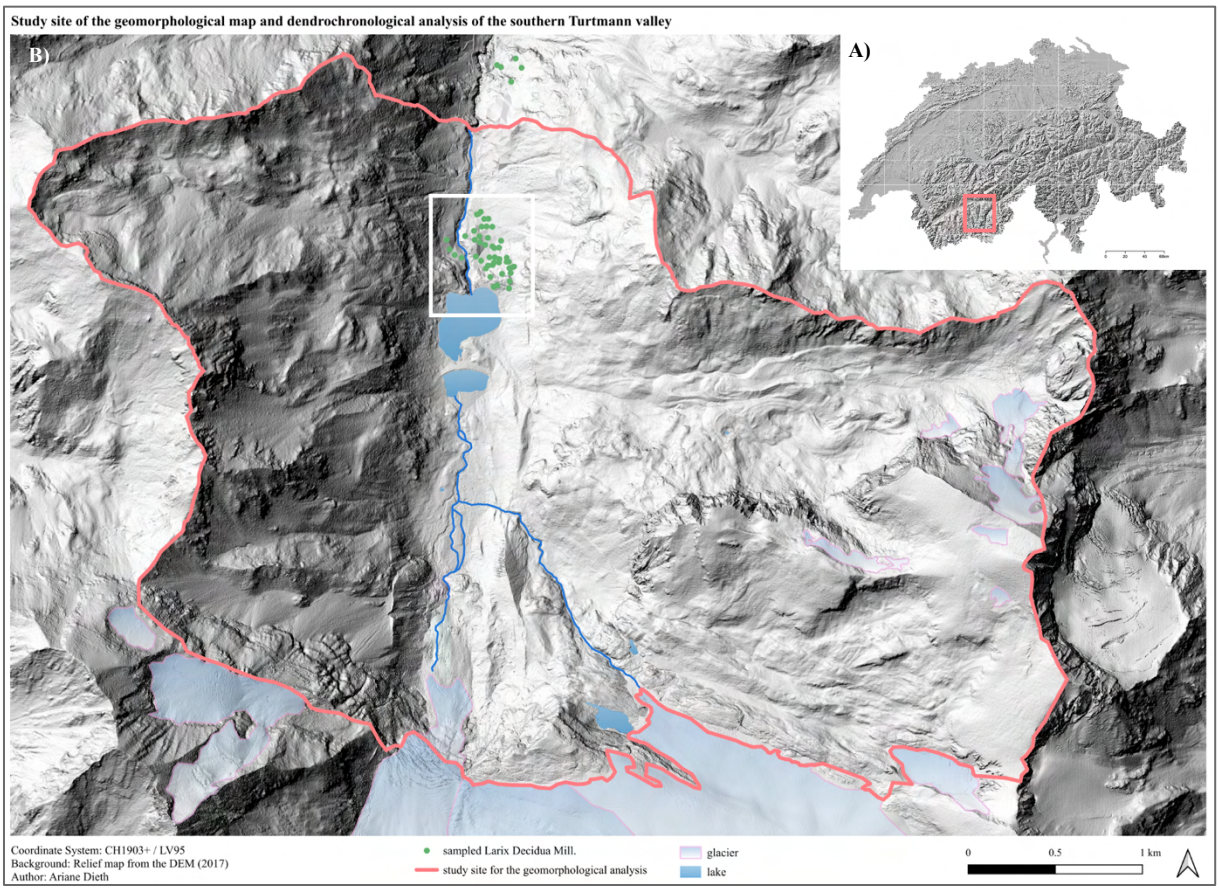
Study site of the geomorphological map and dendrochronological analysis of the southern Turtmann valley
B)
A)
Coordinate System: CH1903+ / LV95
Background: Relief map from the DEM (2017)
Author: Ariane Dieth
sampled Larix Decidua Mill.
study site for the geomorphological analysis
glacier
lake
0
0.5
1 km


C)

3.1.2 Climate

As the study site is in an inner alpine setting, the climate is intramontane with an annual precipitation of approx. 600 – 9'000 mm at 2'000 m a.s.l. (Gärtner-Roer et al., 2013). The mean annual air temperature (MAAT) for the time period from 2000 to 2023 is 6.3°C and the temperature for the growing season of *L. decidua* Mill. (1st of June until 1st of October) is 12.5°C measured at the Grächen weather station at an elevation of 1'605 m a.s.l. (MeteoSchweiz, 2023). The growing season is derived from Moser et al. (2009) and Saderi et al. (2019). However, for the study site the MAAT would need to be adapted with the environmental lapse rate of 0.53°C decrease per 100 m elevation gain, concluded by Rist et al. (2020) in the Rhône valley in a distance of approx. 20 km from the study site. Therefore, calculated with this environmental lapse rate the MAAT between the years 2000 and 2023 for the Turtmann Valley at the focus site (at 2'005 m a.s.l.) is 4.1°C and the temperature during the growing season is 10.4°C. According to Dikau et al. (2019: 439) the MAAT measured at the weather station at the dam wall of the reservoir lake (Turtmannsee) is 1.8°C (elevation of 2'180 m a.s.l.). There is no measurement of snow cover in the Turtmann Valley but in the Rhône Valley there were 250 snow cover days at an elevation of 2'600 m a.s.l. (Rist et al., 2020). The treeline in the study site is at an altitude of 2'400 m a.s.l. and the timberline at approx. 2'200 m a.s.l. However, the treeline is influenced by grazing during the summer months and might vary at different parts of the valley (Gärtner-Roer et al., 2013).

3.1.3 Geology

Most of the Turtmann Valley consist of the basement nappe from the middle Penninic belonging to the Briançon-unit and is represented by the Siviez-Mischabel-Decke. Further south and in higher elevation where the Turtmannngletscher is now located, the tectonic unit from the upper Penninic is represented by the Tsate-Decke and again further south and in higher elevation at the flanks of the Les Diablons, Tête de Milon and Bishorn is the Dent-Blanche-Decke which represents the lower Austroalpine nappe. The peak of the Turtmannspitze at the west flank of the Turtmann Valley is also part of the Tsate-Decke. The most prominent nappe in the study site, the Siviez-Mischabel-Decke, consists of mica shists and gneiss (Bearth, 1980; Iten, 1948; Marthaler et al., 2008). In **Figure 6**, the geology of the study site is visible through both sheets "1307 Vissoie" and "1308 St. Niklaus" of the Geology Atlas of Switzerland GA25. During the Quaternary, glaciations and deglaciations influenced the relief of the Turtmann Valley, leading to a lot of sediment deposits and moraines which are accumulated as till (Dikau et al., 2019).

FIGURE 6 GEOLOGY OF THE SOUTHERN TURTMANN VALLEY. THE MAP WAS CREATED BY STITCHING TOGETHER THE SHEETS "1307 VISSOIE" AND "1308 ST. NIKLAUS" FROM THE GEOLOGICAL ATLAS OF SWITZERLAND GA25 (FROM SWISSTOPO, 2024G).
THE LEGEND CAN BE ACCESSED IN SWISSTOPO (2024G).

3.1.4 Vegetation

Due to the study site being in a high-mountainous area where deglaciation processes occur, the vegetation mostly consist of pioneer species and species at different succession stages. The vegetation cover of the proglacial area of the Turtmanngletscher was studied by Eichel et al. (2013) and Eichel (2017). In the glacier forefield typical species are herbs such as *Saxifraga aizoides*, grass *Alopercurus* species, dwarf shrubs such as *Salix reticulata* or *Dryas octopetala*. The further away from the glacier tongue and the young terrain, pioneer species get replaced by typical succession vegetation. *Larix decidua Mill.* is the most prominent tree species in the study site and the only species that samples were taken from in this master thesis. Some *Pinus Cembra* are located in the study site as well as some individual specimens of *Betula Pendula* (Eichel et al., 2013; **Figure 7**).

The European Larch tree (*L. Decidua* Mill.*)* is a pioneer species in subalpine and mountainous settings as it is growing very fast. This tree species is dependent on light availability in all growing stages and the young trees are flexible. Thus, *L. decidua* often grows in disturbed soils that form through avalanches and landslides or in glacial forelands. The large deciduous coniferous tree can reach up until 50 metres and can turn up to 800 years old in optimal conditions. However, the larch trees studied in this master thesis are much smaller and younger (as seen by the dating results in **4.3.2**). In high elevations in the Alps *L. decidua* forms the upper tree limit as it is a very cold and wind tolerant tree during winter. Thus, individual trees or specimens grouped in small cohorts can be found up to an altitude of 2'500 m a.s.l. (Da Ronch et al., 2016). Continental conditions are most suitable for whole larch forests to form because this species has more resilience than other species in the subalpine region (Moris et al., 2017). Temperature is the most influential factor in the growth of *L. decidua* by determining the onset of growth, although light availability is determining further wood formation processes as well (Moser et al., 2009). According to a study by Moser et al. (2009) done in the Lötschental in Canton Valais (in 26 km distance to the study site), the onset of growth varies by an increase of approx. 3-4 days/100 m towards the valley floor. In this thesis, the growing season for *L. decidua* Mill. in the Turtmann Valley is defined as the period between June and October (Saderi et al., 2019). However, due to the altitude of 2'150 m a.s.l., the actual number of days with favourable growing conditions is likely reduced to around a minimum of 101 days as colder conditions early in June and later in October limit the effective growing period. This corresponds to the study by Moser et al. (2009) that found a similar duration of growth onset in the nearby Lötschental region.

FIGURE 7 An overview of the most common trees in the study site with **A)** *L. decidua* Mill. of which the samples for the dendrochronological analysis were taken (here sample L005) and not-sampled trees **B)** *Pinus Cembra* and **C)** *Betula Pendula* (Ariane Dieth, 2023).

3.2 Geomorphological Mapping

In this study, geomorphological mapping was conducted using a combination of remote sensing imagery, topographic data and field work. The mapping process began with collecting data from open sources such as the Geoportal of Switzerland (Swisstopo, n.d.) which were then analysed to identify key geomorphological features in the study site. These features were then digitized within a GIS environment ensuring accurate spatial representation. By doing field campaigns, some of the digital observations could be validated and cross-referenced with the situation in the study site. A similar approach to field mapping is described in Chandler et al. (2018).

3.2.1 Field Work

Before conducting the fieldwork, the study site was analysed with maps and aerial images from Swisstopo and existing geomorphological data from previous studies to get a first impression on the landscape and geomorphology. Previous to the field campaign in October 2023 a visit to the Turtmann Valley in September 2023 was done where photos of the valley were taken along the hiking path on the east valley shoulders while walking from Holustei located at 2'619'938 °N, 1'114'150 °E (CH1903+ / LV95) to the SAC Turtmann hut at 2'620'146, °N, 1'112'104 °E (CH1903+ / LV95). These photos should help to have some base in the geomorphological mapping and analysis of the study site when being back in the office.

The field campaign took part in the first week of October 2023. The main aim was mostly to take samples for the dendrochronological analysis. However, also the first interpretation of the landscape as well as discussions with the supervisor I. Gärtner-Roer on the landscape and geomorphology was done in these days. On the first day in the field, the first impressions from theory were cross-referenced with the observations and interpretations on site. The lateral and frontal moraines from the maximum extent of the LIA and other geomorphological landforms in the glacier forefield were noted down on printed out maps. A lot of photos were taken from different angles and places to be used for further analysis and mapping back in the office. Based on the observations of the landscape on the first day of the field work, the area of larch trees to be sampled was chosen (see **3.1.1**).

After different drafts and analyses in GIS as well as consulting studies on the Turtmann Valley, another short field campaign for the geomorphological map was done at the end of July 2024. The aim was to cross-check areas and landforms that were mapped but where there was still some uncertainty of the accuracy left. A lot of photos were taken, and notes written down to be able to check on the findings and observations when being back at the office.

3.2.2 GIS

The open-source free software QGIS (version 3.34.3-Prizren) was used for the geomorphological map (QGIS, 2024). As the main base map for the geomorphological analysis, the orthophoto of 2020 was used (Swisstopo, 2024a). A shaded relief out of the digital elevation model swissALTI^{3D} was made in QGIS using the toolbox which was then also used as a base of the geomorphological analysis of the Turtmann Valley (Swisstopo, 2017). Other basic maps used for analysing the landscape development of the Turtmann Valley were provided on the online platform map.geo.admin of Swisstopo (n.d.) and are summarised in **Table A 1** in the Appendix. If not mentioned otherwise, the official Swiss coordinate system CH1903+ / LV95 is used. Literature and studies done in the Turtmann Valley were used as sources for analysing the landscape (see **Table 2**). Especially the studies of Eichel et al. (2013), Eichel (2017) and Otto and Dikau (2004) were used most for reference and decision-making. Otherwise, decisions were made on own observations and photos during the fieldwork.

For the mapping of the glacier extent the same resources as for the geomorphological mapping were used with having the main focus on using historic orthophotos, historic maps, and knowledge from previous studies (see **Table 2**; Swisstopo 2024b to 2024d). The data on glacier length changes of Glacier Monitoring Switzerland (GLAMOS, 1881-2023.) was only used for the validation of the geomorphological mapping and glacier extent mapping in addition to the other methods. Modelling the glacier extent with the data from GLAMOS would have gone over the scope of this master thesis and was thus excluded.

TABLE 2 AN OVERVIEW OF THE MAPS OF THE TURTMANN VALLEY THAT WERE USED FOR THE GEOMORPHOLOGICAL ANALYSIS AND THE MAPPING OF THE GLACIER EXTENTS OF THE SOUTHERN TURTMANN VALLEY.

Content	Data Type	Provided by
Geomorphological map with vegetation classes of the forefield of the Turtmanngletscher	Geomorphological map 1:20'000	Eichel et al. (2013); Eichel (2017)
Geomorphological maps from 1986 to 1989 of the NW corner of the forefield of the Turtmanngletscher, photos	Geomorphologic map 1:500, photos	van der Meer (1997)
Elevation map with mapped talus slopes in the whole Turtmann Valley	Elevation map with mapped talus slopes 1:50'000	Messenzehl et al. (2017)
Geomorphological maps of the Hungerlitälli and Grüobtälli and permafrost distribution	Geomorphological maps 1:5'000	Van Tatenhove and Dikau (1990)
Tectonic map of the Zone du Combin	Tectonic map 1:75'000	Iten (1948)
Geomorphological map of the whole Turtmann Valley; photos	Geomorphological map 1:25'000, photos	Otto and Dikau (2004)
Map of sediment storage landform types of the hanging valleys in the whole Turtmann Valley	Map of the sediment landforms 1:50'000	Otto et al. (2009)
Adapted map of Otto et al. (2009) after geomorphological field mapping	Map of the sediment landforms 1:50'000	Messenzehl et al. (2018)
Map of the sediment storage types of the Hungerlitälli	Map of sediment landforms 1:5'000	Otto and Sass (2006)
Geological explanations with cross-sections; Geological Atlas of Switzerland (GA25)	explanatory booklets of the Geological atlas of Switzerland 1:25'000 of the sheets Vissoie (CN 1307) and St. Niklaus (LK 1308)	Marthaler et al. (2008) Bearth (1980) Swisstopo (2024g)

3.2.3 Cartography

The cartographic design of the geomorphological maps focused on clarity and the effective communication of geomorphic processes. Nine different process domains were chosen with two of them mixtures of two process domains to distinguish between various geomorphological units such as glacial, periglacial, fluvial/lacustrine, gravitational and anthropogenic features. The use of a mosaic of process domains was taken from Montgomery (1999) and adapted to the purposes of this thesis with similarities to previous studies done in the Turtmann Valley (Dikau et al., 2019; Eichel, 2017). The landforms were classified and symbolised using the same distinct colours as the process domains. A hierarchical approach was adopted in the map to emphasize the most prominent geomorphological features while maintaining the ability to present finer details when needed. The scale selection was carefully considered to balance the map's readability with the level of detail required for analysis. Smaller excerpts of the map were made for the discussion to analyse the landscape development and added with images as examples (Chandler et al., 2018).

3.3 Dendrochronology

The methods used for dendrochronological analysis in the study area are described in the following chapter. This includes the sampling strategy, sample preparation and tree-ring width measurement, followed by the detailed procedures for data analysis including the statistical methods used to assess the relationship between tree growth and climate variables. An explanation of the tools and software used throughout the process and an outline of the steps taken to minimize errors and improve the reliability of the data are provided. Guidelines were given by Schweingruber (1988), Wilford et al. (2005), Gärtner and Nievergelt (2010), Gärtner and Heinrich (2013), Gärtner et al. (2015), Cherubini et al. (2020), Gärtner et al. (2023) and Gärtner et al. (2024).

3.3.1 Sampling

The sampling of the trees during the field campaign took 2.5 days in total. Before the sampling a grid of squares of sizes 50 m x 50 m was put over a map with a scale of 1:5'000. From each square a tree was sampled. To get a variety of different locations it was decided on the first day that at least three trees on the west of the Turtmänna, three trees northern of the frontal "LIA" moraine in the focus site, three trees southern of the focus site on the riegel near the Turtmann lake and at least twenty trees inside the focus site should be taken. Twenty trees were chosen to have enough trees for the study on succession to be statistically possible (see **Figure 5-C**). An individual tree was selected based on its size and location in the grid to get the oldest representative tree in its square. An assumption that usually taller trees and trees with a high circumference are older, was made because they had more time to build up the wood. However, the tree height and stem circumference are not distinct measures for the age of a tree because many other parameters (for instance wind, tree competition, light availability and more) influence tree growth (Schweingruber, 1996).

The trees were sampled with an electric drill and a 5 mm increment corer as described by Gärtner et al. (2023) and provided by the Swiss Federal Institute of Forest, Snow and Landscape (WSL). Three cores were sampled per tree. Two opposing cores (samples -A and -B) were taken in a height of about 1.50 m or less depending on branches, location, and disturbances. They were taken parallel to the slope to get as little disruptions of tree-ring growth as possible (Wilford et al., 2005). The sample number-X is sampled as low as possible perpendicular to the slope to be able to capture the oldest rings of the tree (Gärtner and Heinrich, 2013). As it was done with an electric drill, this was possible up until a height of approx. 20 cm from the ground (Gärtner et al., 2023). The position of the trees was determined in the field by the hand-held GPS and the mobile phone because sometimes the location from the GPS was not clear enough. In cases where these two coordinates did not match, the exact position of the trees was made from field notes and on the base of orthophotos from different years on the Geoportal (Swisstopo, 2024b). In addition, photos were taken in the field of the landscape and some representative trees during the first and second field campaign. **Figure 5-C** in **3.1.1** shows a map and a photo of the sampled trees in the study site. In total, 46 larch trees were sampled in the study area with a total of 138 cores. Five additional trees were cored in the forest further down in the valley to get a long chronology of the Turtmann Valley. Although these five trees are not part of the analysis on succession and are not part of the study site, they were dated.

3.3.2 Sample preparation

The tree cores were prepared and analysed at a lab of the research unit Forest Dynamics at WSL. While preparing and analysing the tree cores a comprehensive logbook was written alongside which should help to find error sources and keep the data organised.

After the cores were taken with an increment corer in the field, they were put in paper straws to let them dry and prevent them from rotting (Cherubini et al., 2020; Gärtner et al., 2015). This made them transportable and left time to not continue immediately with the further steps. To make it possible to see the growth of narrow rings, the core samples require preparations. Usually, this is done by gluing them to a wooden support and then sanding them (Schweingruber 1988; Wilford et al., 2005). However, in this thesis, 3D-printed plastic holders called GSC-holders were used instead of the wooden support holders. This approach was piloted as a new method at the dendrochronological lab at WSL (Gärtner et al., 2024). Normally, the cores would be glued with a water-based wood glue individually to wooden supports (Wilford et al., 2005). It is essential to hold the cores in place by tape during the drying process to prevent them from changing their shape and becoming curved on the support holder. There are two types of GSC-holders with a length of 10 cm and 20 cm. They can be assembled when a core exceeds 20 cm in length. Since the sampled trees had small radii, both types of holders were primarily used separately. The approach with the GSC-holders instead of the traditional approach was done to skip steps in preparing the samples such as the gluing (Gärtner et al., 2024).

In contrast to sanding the cores to observe the tree rings, the plane surface can be cut. This is done with the core-microtome – a device created at the WSL as an alternative to the classic sanding method (Gärtner and Nievergelt, 2010; Gärtner et al., 2023 and 2024). The core-microtome consists of a blade holder that is attached to a sledge and a sample holder that is on adjustable positioning table (see **Figure 8**, Gärtner and Nievergelt, 2010). In this thesis, the cores with the GSC-holders were placed on the adjustable sample holder. The positioning table with the sample can be lifted up at intervals of 10 - 20 µm while the blade holder on the sledge slides over the sample at a horizontal angle of approx. 45°. As a result, layers of wood of the core can be cut away until the desired surface is reached (Gärtner and Nievergelt, 2010; Gärtner et al., 2015).

It is important that the entire core is cut evenly for the further steps in the measurements (see **3.3.3)**. A critical aspect of cutting a tree core with a core-microtome is the freshness of the tree sample. The cell walls of the tree cores should be sufficiently soft to prevent breakage of the core during cutting. Therefore, cutting the tree cores as soon as they arrive in the laboratory is advisable. Alternatively, if the sample preparations are delayed by a few days, the tree cores can be moistened by putting them in a beaker filled with water or brushing the top surface with water (Gärtner and Nievergelt, 2010). In this thesis, the sampled cores were all put in a beaker with water for approx. 5 minutes before cutting, as the sample preparations were done a few days or weeks after arrival from the field campaign (see **Figure 9**). Detailed comments on this process and indications of tree cores that broke despite precautions were written in the logbook and used for later analysis of individual tree cores. The advantages of cutting the surface of the tree cores with a core-microtome are multiple. Once cut, the cells forming the tree rings are openly visible and not filled with swarf. By cutting the surface with the core-microtome, the surface is uniform. The resulting flat surface of the tree core is then suitable for the measurement of the tree-ring width (Gärtner and Nievergelt, 2010; Gärtner et al., 2024).

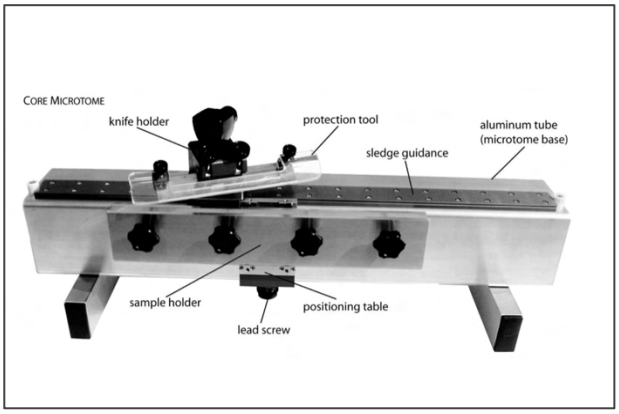

FIGURE 8 THE CORE-MICROTOME AND ITS FEATURES (FROM GÄRTNER AND NIEVERGELT, 2010).

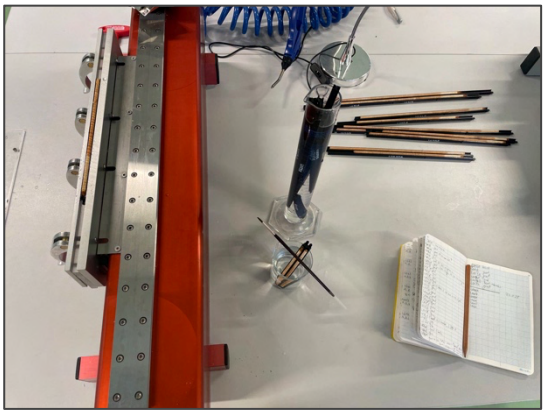

FIGURE 9 AN OVERVIEW OF THE WORKTABLE WITH THE CORE-MICROTOME. A CORE IS MOUNTED ON THE CORE-MICROTOME WHILE THE NEXT CORES ARE SOFTENING IN VESSELS FILLED WITH WATER (ARIANE DIETH, 2023).

3.3.3 Measurement

The measurement of the tree-ring width can be done partly or fully digitally. In this thesis it was done fully digitally with Skippy and CooRecorder as described by Gärtner et al. (2015) and (2024).

Skippy

After cutting the cores with the core-microtome, the samples were photographed with the image capturing system Skippy (Gärtner and Schneider, n.d.). It is a camera-based imaging system that takes high-resolution photographs of samples (see **Figure 10** and **Figure 11**). A camera (here a Sony Alpha 7R IV; 61MP) is mounted on top of a frame and the sample is placed onto a moving platform. An interval for the moving platform is chosen in the Skippy software to take photographs for each spacing. In this thesis, an interval of 6 mm was chosen. The photos should be taken with a small mm-paper next to the core for the calibration afterwards in the measuring software. After photographing, each photo can be stitched together to a panorama image in the program called PTGui (New House Internet Services BV, n.d.). By carefully assessing the images while stitching them together, blurry photographs can be removed before putting together the panorama image to have clearly visible tree rings in the photos for measurements afterwards. The panorama images are saved as TIF-File to keep the high resolution of the photographs and to be able to load them into the next software called CooRecorder (Gärtner et al., 2015 and 2024).

FIGURE 10 THE SET-UP OF SKIPPY (ARIANE DIETH, 2023).

FIGURE 11 THE OUTPUT OF SKIPPY, HERE A STITCHED IMAGE OF THE SAMPLE L013A (ARIANE DIETH, 2024).

CooRecorder

The tree-ring width measurements were done with the software "CooRecorder" from Cybis Elektronik & Data AB (2023). It is an intuitive software to digitally measure the tree-ring width with high-resolution images. The stitched image from the previous step can be loaded into the program. The image file needs to be in the same folder as the measurement file (.pos) that will be saved from the software. The name of the image file should be short because CooRecorder cannot have an unlimited number of letters or digits in the name of the resulting file. Firstly, the photo had to be calibrated with the mm-paper that is in the photo included to obtain the image resolution for the software. Secondly, points were placed at the tree-ring boundaries in a straight line from the outermost to the innermost ring.

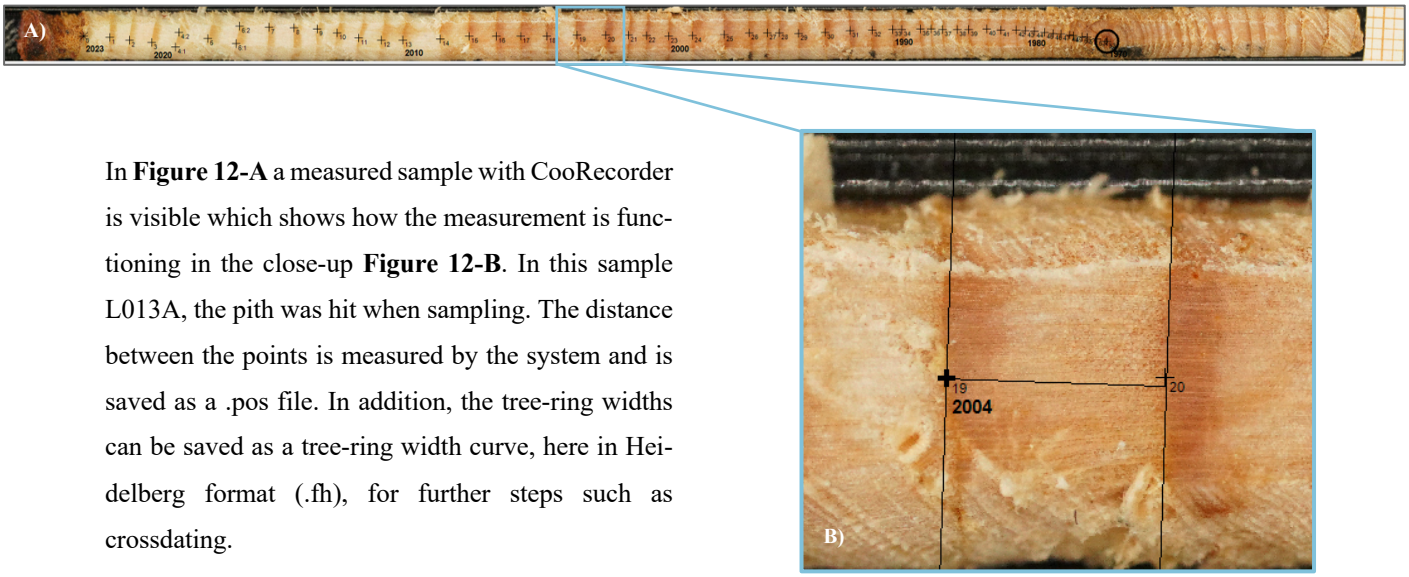

In **Figure 12-A** a measured sample with CooRecorder is visible which shows how the measurement is functioning in the close-up **Figure 12-B**. In this sample L013A, the pith was hit when sampling. The distance between the points is measured by the system and is saved as a .pos file. In addition, the tree-ring widths can be saved as a tree-ring width curve, here in Heidelberg format (.fh), for further steps such as crossdating.

FIGURE 12 A MEASURED AND DATED TREE SAMPLE WITH **A)** THE WHOLE SAMPLE L013A AND **B)** A CLOSE-UP OF A MEASUREMENT OF ONE RING (ARIANE DIETH, 2024).

3.3.4 Analysis of the tree-ring growth

Once the tree-ring widths were accurately measured, the data was prepared for statistical analysis. The primary goal of this analysis was to assess the relationships between tree growth patterns and external climatic factors particularly temperature and precipitation as well as to have accurate dated ages of the tree samples. Using specialised dendrochronological software (e.g., TSAP, Statistic package R and Microsoft Excel), the raw data was processed and cross-dated to ensure consistency. This allowed for the following application of statistical methods such as correlation analysis to determine significant trends and isolate environmental drivers of tree growth.

A first step after measuring the tree-ring widths with CooRecorder, the samples need to be crossdated (see **2.2**). Firstly, the three cores from each tree (samples with suffix -A, -B and -X of each tree) were crossdated with each other to identify errors in counting the tree rings. Secondly, the sampled trees in the study site were then crossdated with each other to obtain a chronology for the study site as no previous chronology of the Turtmann Valley existed. The crossdating in the case of this thesis was therefore used to minimise errors made in the measurement of the tree-ring widths, to build up a chronology and to determine the minimum age of each tree precisely. This first part of the analysis of the tree-ring widths was done in the software TSAP-WIN (Rinntech, n.d.). This software is used to cross date tree-ring width curves visually with some parameters such as "Gleichläufigkeit" (see theory in **2.2**). If a tree ring seemed to be missing in one sample while crossdating the three samples of one individual tree, the

sample was again loaded into CooRecorder. A missing ring was inserted if there has been a previous mistake in measurement and then, the tree-ring width curve was loaded back into TSAP-WIN. However, crossdating the core with the suffix -X together with the other two cores -A and -B from the same tree sometimes showed to be difficult. This can be explained as the two cores -A and -B were taken in a standardised height of approx. 1.5 m and parallel to the slope whereas the core with the suffix -X was taken perpendicular to the slope and as near as possible to the ground to get the minimum age of the tree (Gärtner et al., 2023; Wilford et al., 2005). Because of the position of the sampling, a core with the suffix -X might show different tree-ring widths because of effects of slope disturbances, and might have built reaction wood (Gärtner and Heinrich, 2013; Schweingruber, 1996). This will be further explained in the discussion in **5.3.3**.

The crossdated samples per tree where then crossdated with the other trees in the study site to improve the quality of the age determination and to be able to make observations on patterns in tree growth for the study site later on. Some trees that could previously not be crossdated within each other were defined as outliers (see **Table A 2** in the Appendix). The three samples of L022 and L027 could not be correctly crossdated within each other and with the other trees of the study site, thus, they were excluded from the statistical analysis and the chronology. The outliers L006 and L034 could also not be crossdated within each other in an accurate way, however the sample L006B showed enough Gleichläufigkeit in some years with the majority of the trees in the study site and was included in the statistical analysis. In the same way, the samples L034A and L034X could be crossdated with the majority of the trees in the study site as they showed some Gleichläufigkeit in some years. Therefore, the sample L034A was included in the statistical analysis. The outliers of the trees L006, L022, L027 and L034 as well as other trees that showed curious growing patterns in their tree-ring width measurements are analysed in the discussion in **5.3.1**.

The successfully crossdated trees built up the chronology used for further analysis with the correlation between climatic conditions and tree growth patterns in the focus site. An average tree-ring width curve of the samples with the suffixes -A and -B of the crossdated trees in the study site in the program TSAP-Win (called “time series” and/or “chronology” in **Figure 22** resp. **Figure 23** in the results in **4.3**) was done which is the easiest method to make a chronology for an area (Frank et al., 2022). The samples with the suffix -X were not used for the chronology because the majority of samples showed different growth patterns and these samples were used for the determination of the minimum age. By excluding the mentioned outliers, the aim was to ensure that the correlation analysis accurately reflects the typical growth-climate relationship in the study site. Thus, the final dataset comprised trees that demonstrated consistent growth patterns suitable for statistical analysis and comparison with the climate data.

Comparison with climate data

To analyse the tree-ring growth data with climatic conditions such as temperature and precipitation, files for Microsoft Excel were made of the chronology of the sampled trees in the Turtmann Valley and the mean curve of the outliers. The time series was then illustrated in graphs with the sample depth, showing how many samples make up a value of the tree-ring width. The next step involved preparing the climate data which was obtained from the Grächen weather station at an elevation of 1605 m a.s.l. (MeteoSchweiz, 2023). The yearly mean temperatures were already available. However, the mean temperature for specific months had to be prepared. Hence, the mean temperatures of the months of the growing season of *L. decidua* Mill. (between June and October) for the time period of the grown trees (1949 to 2023) were calculated. In another step, the mean temperatures of the months that correlate with the tree growth of the chronology were calculated. These include the months of May, June, July

and August (see explanations in **4.3.1** and in the discussion in **5.3.1**). Together with these temperature mean values and the yearly precipitation measurements, the chronology as well as the outliers were illustrated in graphs in **4.3.1** and further analysed with the statistical analysis in the discussion in **5.3.1**.

Statistics

The statistical analysis for the investigation of the relationship between tree-ring growth and temperature and precipitation was done in R Studio in multiple steps (Posit PBC, 2024). The R script used was provided by Dr. Stefan Klesse at WSL and adapted for this master thesis (see section "**R Code**" in the Appendix).

In a first step, the tree-ring data had to be obtained from individual CSV files that were extracted from TSAP-Win. Only trees that could be reliably crossdated in the previous step were included in the final analysis (samples with suffix -A and -B without the above-mentioned samples of the outliers; see **Table A 2** in the Appendix). The CVS files that each represent a single tree were put into a list of data frames and then converted into time series object. To ensure consistency and prepare for further analysis, all the time series were combined into a single time series object and afterwards converted to a data frame. The tree-ring data was detrended using a spline method with a 10-year window to show the long-term trends and emphasize inter-annual variability.

The second step involved preparing the climate data which was obtained from the Grächen weather station (MeteoSchweiz, 2023). The CSV file was reshaped in R Studio to have columns representing months and rows representing years. Only data from 1949 onwards was considered for the analysis because the oldest tree of the samples with suffix -A and -B is from the year 1950 (tree L001). Temperature and precipitation data were converted to numeric values and organized into data frames. After, the running averages of the climate data were calculated over various season lengths from one to twelve months.

The third step involved the correlation analysis and the visualisation. The detrended tree-ring widths were correlated with the running averages of temperature and precipitation data. This was achieved using the function "Climateplot_new" which calculated correlations over different seasons and detrended the climate data if necessary. Both Pearson and Spearman correlation methods were used to ensure robustness. The results of the correlation analysis are visualised using contour plots to display the strength and direction of correlations between detrended tree growth and climate variables over different seasons (see **Figure 24** and **Figure 25** in **4.3**). Thus, the visualisation provides an understanding of periods and conditions that significantly affect tree-ring formation in the study site.

As this was done for the tree samples that were included in the chronology, also the same analysis was done for the outliers to obtain graphs for demonstrating their difference in tree-ring growth and to be able to discuss the outliers accordingly. The R script for the analysis of the trees of the chronology of the Turtmann Valley is available in the section "**R Code"** in the Appendix. As the script of the outliers is the same, it is not illustrated in the thesis.

In summary, the methods employed in this study combined geomorphological mapping, GIS analysis, and dendrochronological techniques to investigate the landscape and tree-growth patterns in the Turtmann Valley. A comprehensive dataset was developed through fieldwork, analysis of existing aerial images and maps, laboratory analysis and literature research. The integration of these diverse methodologies ensured that the spatial and temporal aspects of the geomorphological features and tree-ring data were captured and analysed. With the methodology firmly established, the following chapter will present the results of these analyses, offering insights into the geomorphic processes and tree-growth dynamics within the study area.

4. Results

The following chapters present the results of this master thesis starting with the resulted maps of the geomorphological analysis with a short description. The analysis of the different geomorphic process domains and the mapped landforms is done in the discussion in in **5.1** with additional photos in the same chapter for providing examples next to the map. The glacier extents that are discussed in **5.2** are shown as resulted maps in this following chapter. Furthermore, two maps showing the glacier extents as well as some mapped geomorphological landforms and the year of the starting of growth of the sampled trees are found in the same chapter. These maps should provide the base for the synthesis in **5.4** where interplay between glacier extents, geomorphology and dendrochronology will be discussed. Additionally, the results obtained by the analysis of the dendrochronology are visible in the last part of this chapter.

4.1 Geomorphology

4.1.1 Geomorphological map of the southern Turtmann Valley

The resulted geomorphological map covers the area described in **3.1.1** which extends over the main valley floor where the Turtmanngletscher has moved as well as two eastern hanging valleys – the Piipjitelli and the area where the Brunegggletscher is retreating – and three western hanging valleys – Frilitälli, Wängertälli with the Wängeralp and Inners Wängertällli. The geomorphological map in **Figure 14** with the legend in **Figure 13** shows a complete mosaic over the study area with mapped process domains described in **4.1.2** and analysed in **5.1**. Morphologic landforms are overlaid as vetors in the shape of lines or polygons which are described in **4.1.3** and and also analysed in **5.1**.

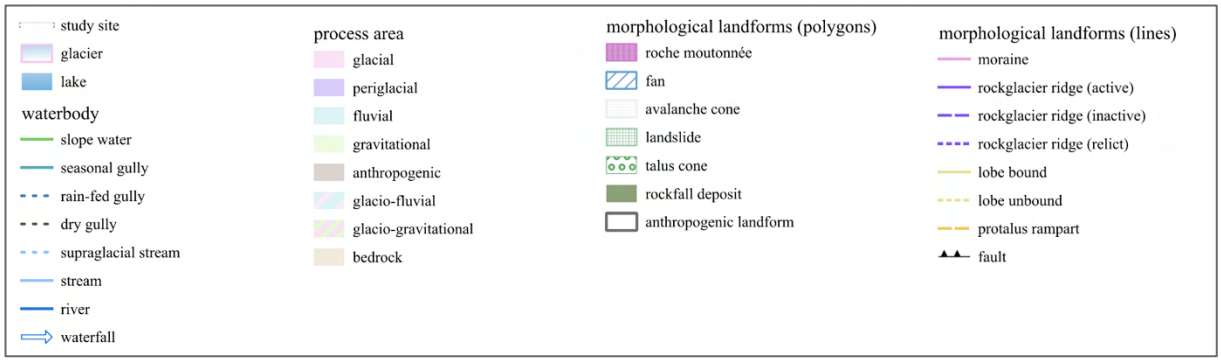

Figure 13 Legend to the geomorphological map of the southern Turtmann Valley with the mapped geomorphological landforms (waterbodies, morphological landforms as polygon and lines) and the process domains seen in **Figure 14** (Ariane Dieth, 2024).

◄ **Figure 14** The resulted geomorphological map of the geomorphological analysis of the southern Turtmann Valley is depicted on the next page. The scale is in 1:17'000 and covers the whole study site with the main valley floor as well as the surrounding hanging valleys (Ariane Dieth, 2024.

Geomorphological map of the southern Turtmann valley

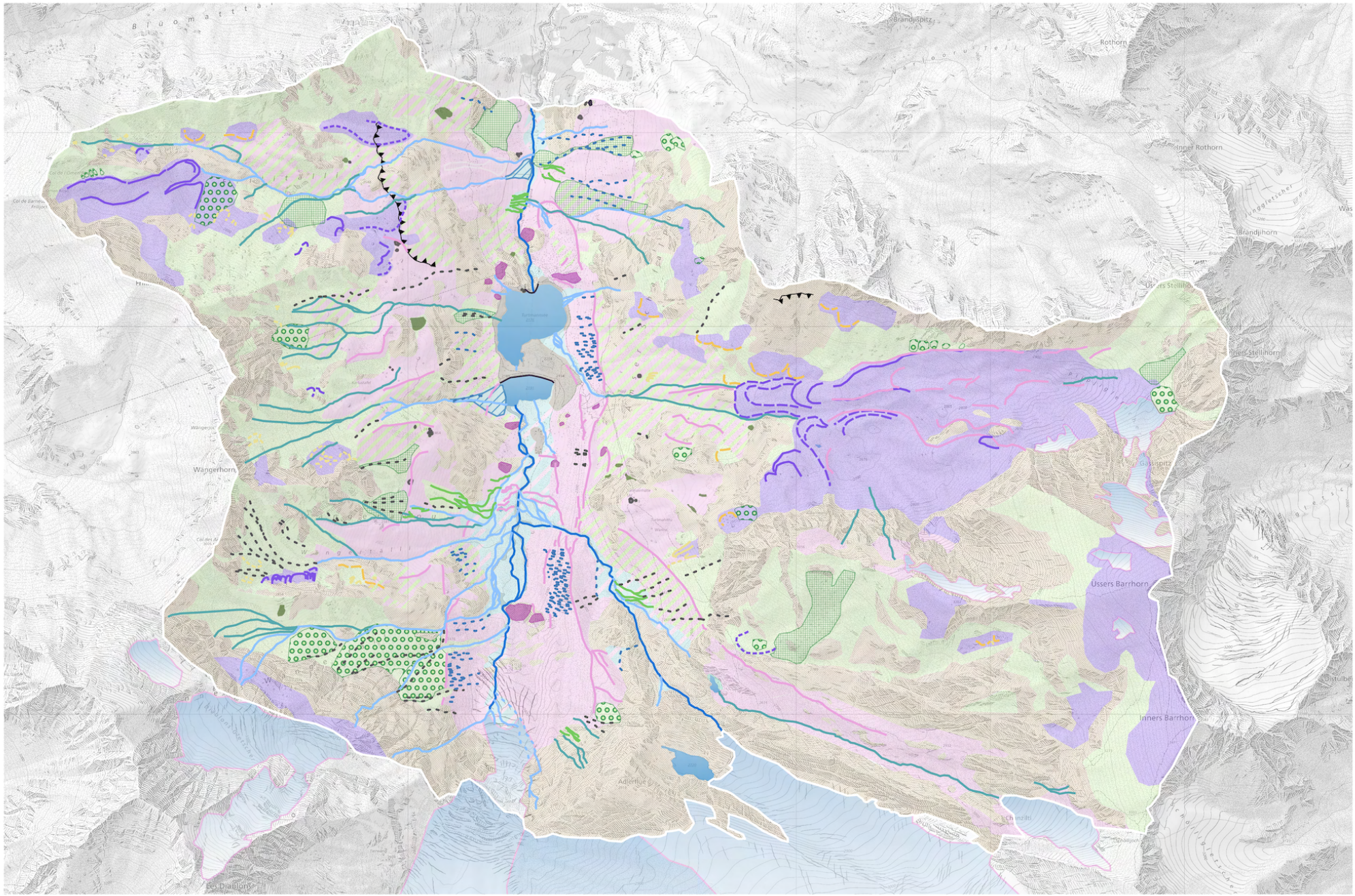

Coordinate System: CH1903+ / LV95
Background: National map of Switzerland 1:10'000 (2017)
Author: Ariane Dieth - based on the Orthophoto of Swisstopo (2020) and different geomorphological maps of the Turtmann proglacial area

0 0.5 1 km

4.1.2 Mapped process domains in the southern Turtmann Valley

In the southern Turtmann Valley nine process domains have been identified including two mixed process domains. These domains are displayed on the final geomorphological map in **Figure 14** with the legend in **Figure 13**, and in **Figure 15** which specifically highlights the process domains. The categorisation of these domains reflects the dominant geomorphic processes in the area. Accordingly, mixed process domains such as glacio-gravitational and glacio-fluvial have been included to be able to show areas where more than one process is important to be mentioned.

The valley floor is primarily composed of till material from glaciation periods which is categorised under the glacial process domain (see definition on basal till **Table 1** in **2.1.3**). The periglacial process domain is located in the hanging valleys where permafrost is often present on north-facing slopes and where relict landforms created by periglacial processes are still evident (as seen in the mapped morphological landforms in **Figure 16**). One of the largest process domains by area is the gravitational domain. The steep slopes of the Turtmann Valley are highly susceptible to avalanches, rockfalls, rockslides and debris flows. The fluvial process domain is situated around the river systems. The anthropogenic process domain is mapped around the hydropower reservoirs and areas where sediment from the construction of these reservoirs has been deposited. Lastly, the "bedrock" process domain is mapped in areas where bedrock is exposed, such as on mountain peaks, steep rocky slopes, and smaller outcrops of bedrock.

◄ **FIGURE 15** THE PROCESS DOMAINS IN THE SOUTHERN TURTMANN VALLEY MAPPED THROUGH THE GEOMORPHOLOGICAL ANALYSIS IOF THE STUDY SITE (ARIANE DIETH, 2024).

Geomorphological process domains in the southern Turtmann valley

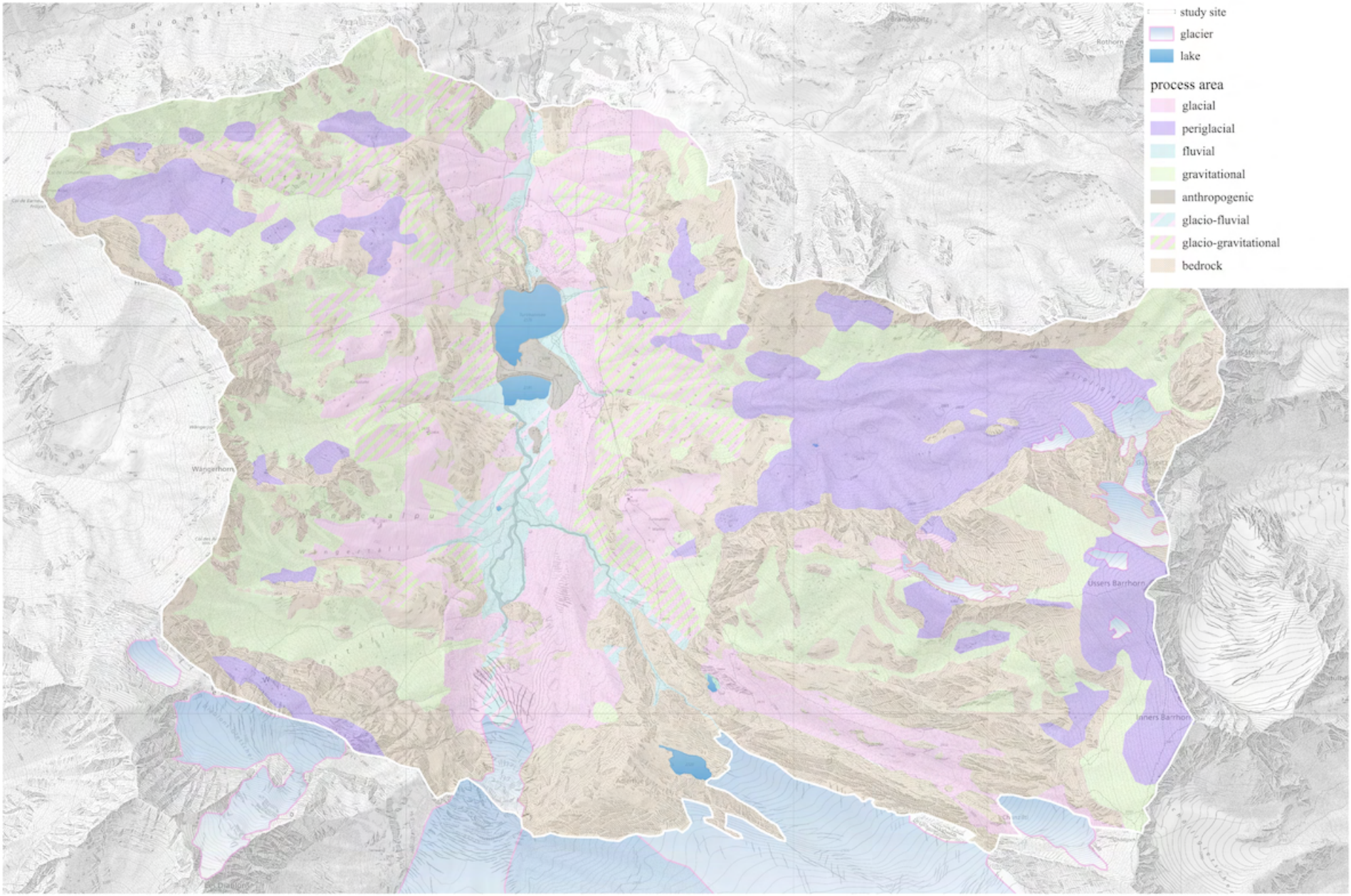

Coordinate System: CH1903+ / LV95
Background: National map of Switzerland 1:10'000 (2017)
Author: Ariane Dieth - based on the Orthophoto of Swisstopo (2020) and different geomorphological maps of the Turtmann proglacial area

0 0.5 1 km

4.1.3 Mapped morphological landforms in the southern Turtmann Valley

The morphological landforms shown in the final geomorphological map (**Figure 14**) are categorised into linear vectors and polygons. Within the glacial process domain, 81 moraine ridges have been mapped, most of which are located in the proglacial area of the Turtmanngletscher. However, some moraine ridges have also been identified in the hanging valleys. In addition to these accumulation landforms, 14 roche moutonnées as erosional landforms have been mapped. Other landforms within the glacial process domain are not included on the map due to its scale but photographs provide an overview of features such as striations and crescentic fractures (see **5.1.2**). In the category of periglacial landforms 109 features have been mapped. These include ridges and lobes of rock glaciers (whether active, inactive, or relict), lobes influenced by freeze-thaw cycles or permafrost (gelifluction and solifluction lobes, though these are not distinguished in this thesis) and protalus ramparts. Gravitational landforms mostly consist of conic-shaped features or features covering an area such as talus cones, rockfall deposits, landslides, avalanche cones and alluvial fans. In total, 53 gravitational landforms have been mapped in addition to the broader gravitational process domain which is characterised by talus slopes and areas with scree and rock deposits. Furthermore, seven buildings that are still standing and in use along with about 15 ruins of alpine pastures have been mapped as anthropogenic landforms. **Figure 16** and **Figure 17** illustrate the different landforms mapped in the Turtmann Valley. Photographs of the various landforms are included in the discussion in **5.1**. where they are analysed and discussed as part of the geomorphological study of the valley, sometimes with excerpts of the geomorphological map.

◄ **FIGURE 16** THE GEOMORPHOLOGICAL LANDFORMS THAT WERE MAPPED AS VECTORS AS LINES IN THE GEOMORPHOLOGICAL MAP ARE SHOWN FOR THE STUDY SITE (ARIANE DIETH, 2024).

◄ **FIGURE 17** MAPPED POLYGONS ARE MOSTLY PART OF THE GRAVITATIONAL PROCESS DOMAIN SHOWING DIFFERENT TYPES OF LANDSLIDES, TALUS CONES AND ROCKFALL DEPOSITS. MULTIPLE ROCHE MOUTONNÉES (IN PURPLE) ARE SHOWN IN THE PROGLACIAL AREA OF THE TURTMANNGLETSCHER (ARIANE DIETH, 2024).

Geomorphological map of the southern Turtmann valley - mapped linear geomorphological landforms

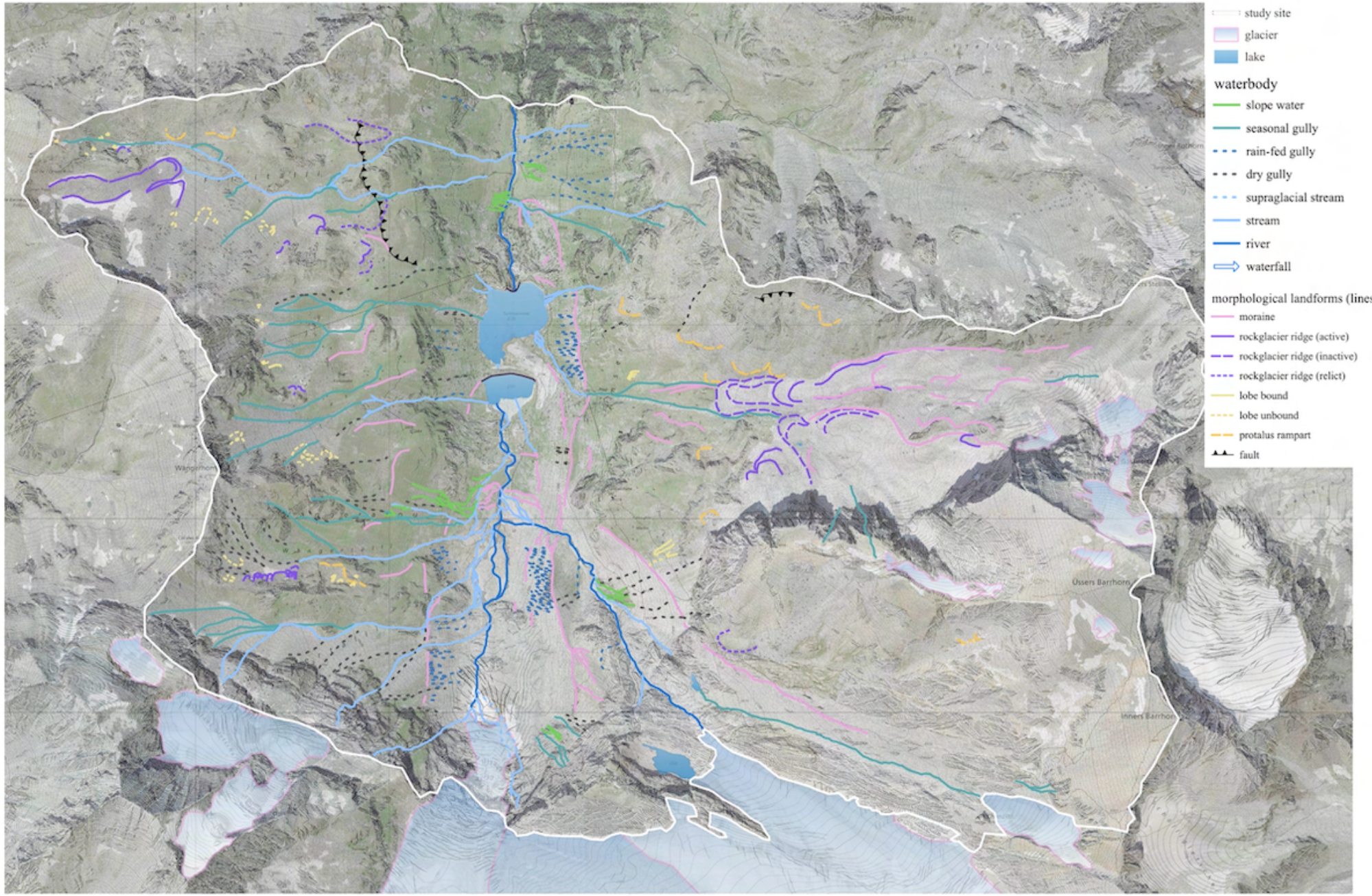

Coordinate System: CH1903+ / LV95
Background: National map of Switzerland 1:10'000 (2017) and Orthophoto (2020)
Author: Ariane Dieth - based on the Orthophoto of Swisstopo (2020) and different geomorphological maps of the Turtmann proglacial area

Geomorphological map of the southern Turtmann valley - mapped polygon geomorphological landforms

Coordinate System: CH1903+ / LV95
Background: National map of Switzerland 1:10'000 (2017) and Orthophoto (2020)
Author: Ariane Dieth - based on the Orthophoto of Swisstopo (2020) and different geomorphological maps of the Turtmann proglacial area

4.2 Glacier extents

The glacier extents were mapped according to conclusions from historic aerial images, historic maps, the GLAMOS data and mapped glacier extents from previous studies. Only the glacier extents in the study site from the frontal "LIA" moraine to the current (2020) location of the glacier tongues of the Turtmanngletscher resp. Bruneggletscher were mapped (see **Figure 18**). The glacier extents of the glaciers in the hanging valley were not mapped as they are not part of the research objectives where the focus lies on the Turtmanngletscher. However, **Figure 19** shows the focus site with the geomorphological situation as well as the dated trees from the dendrochronological analysis. An excerpt of the area around the glacier extents from 1920 to 2005 is illustrated in **Figure 21** together with the moraine ridges as it is discussed in the synthesis in **5.4**. The mapping of the glacier extents as well as the relationship between the geomorphology and the glacier movement is described and analysed in the discussion in **5**.

◄ **FIGURE 18** MAPPED GLACIER EXTENTS AND POSITION OF THE GLACIER TONGUE OF THE TURTMANNGLETSCHER AND BRUNEGGGLETSCHER SINCE THE LITTLE ICE AGE (ARIANE DIETH, 2024).

Extent of the Turtmanngletscher and Brunegggletscher from the LIA (1850) to currently (2020)

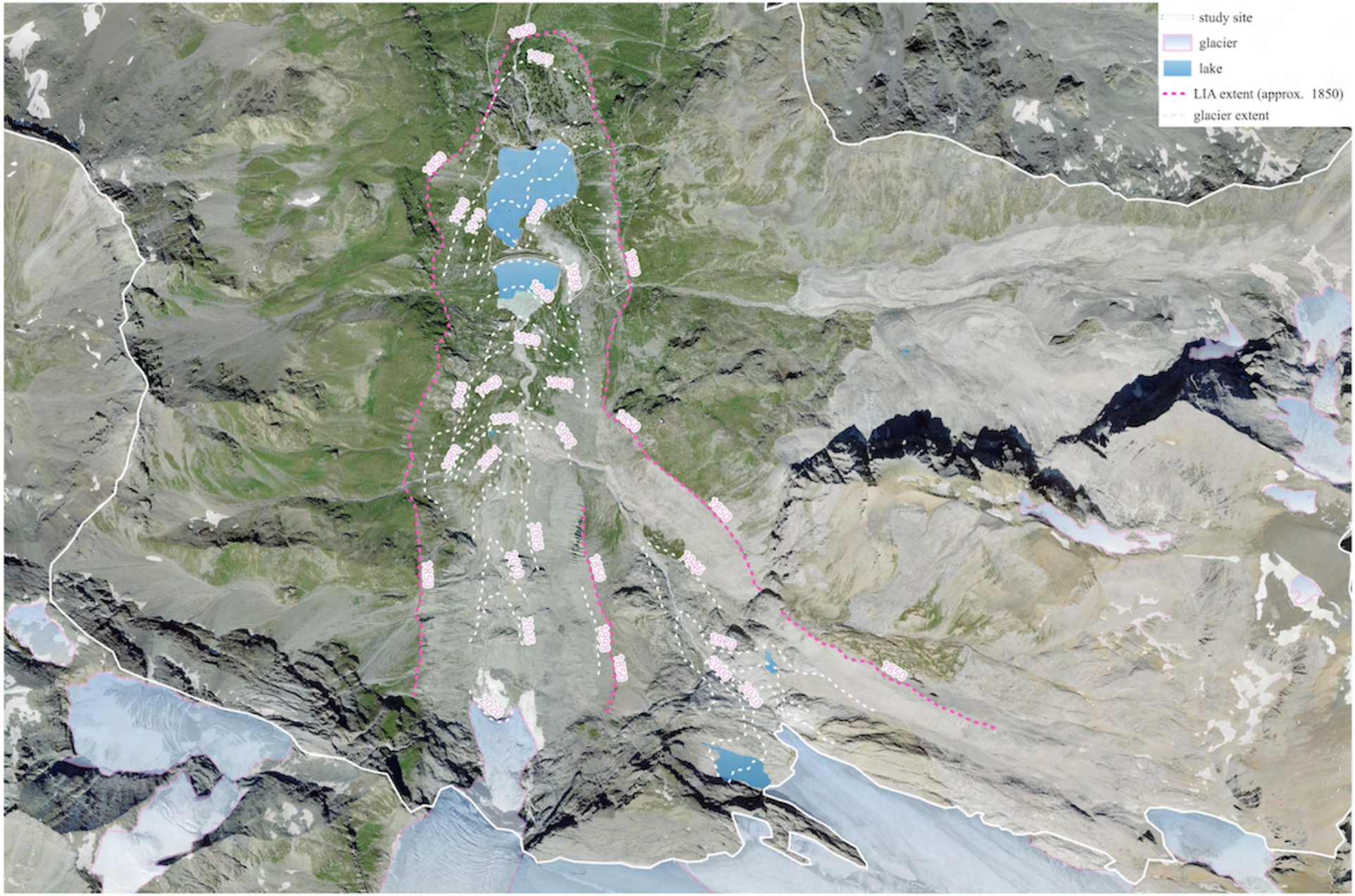

Coordinate System: CH1903+ / LV95
Background: Orthophoto (2020)
Author: Ariane Dieth - based on historic aerial images and maps, GLAMOS data and previous studies in the Turtmann valley

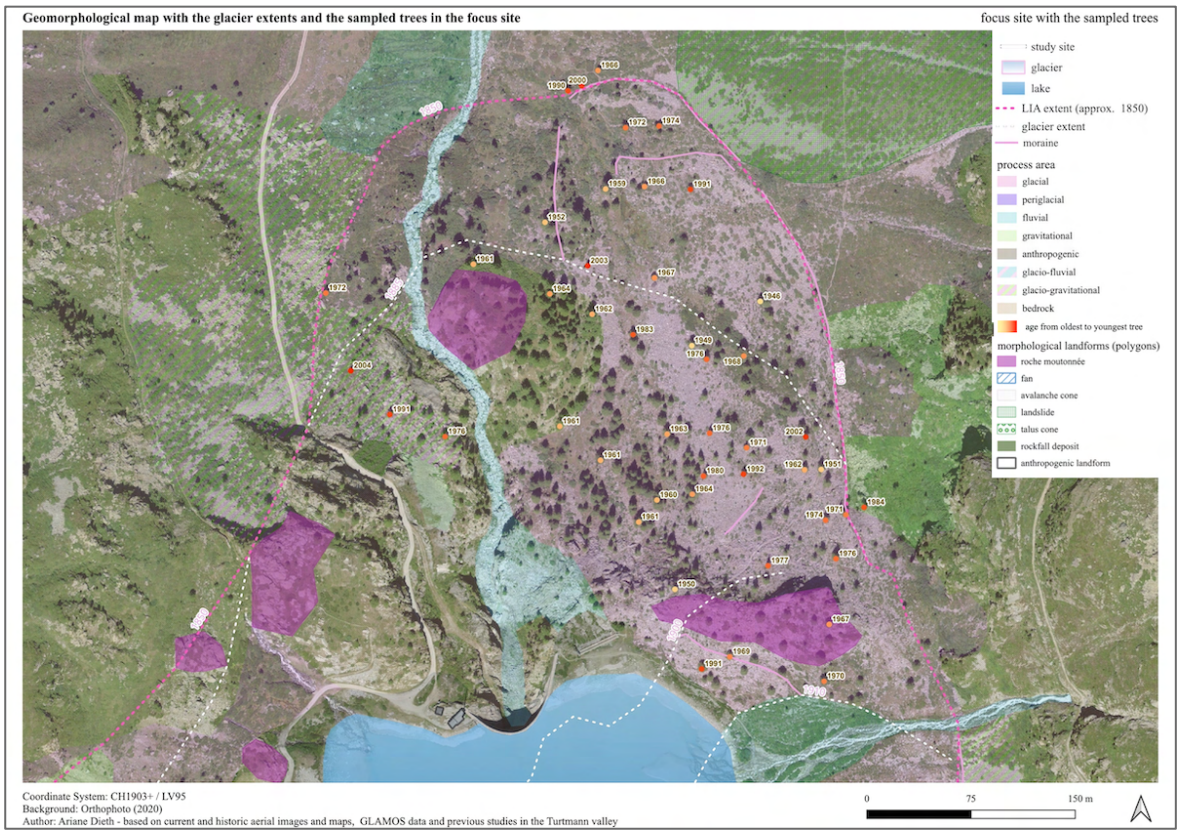

FIGURE 19 THE FOCUS SITE WITH THE MAPPED GLACIER EXTENTS, THE GEOMORPHIC PROCESS DOMAINS, AND SOME GEOMORPHOLOGICAL LANDFORMS. THE SAMPLED TREES ARE MAPPED IN COLOUR FROM YELLOW (OLDEST) TO RED (YOUNGEST) AND HAVE A LABEL WITH THEIR RESPECTIVE AGE (ARIANE DIETH, 2024).

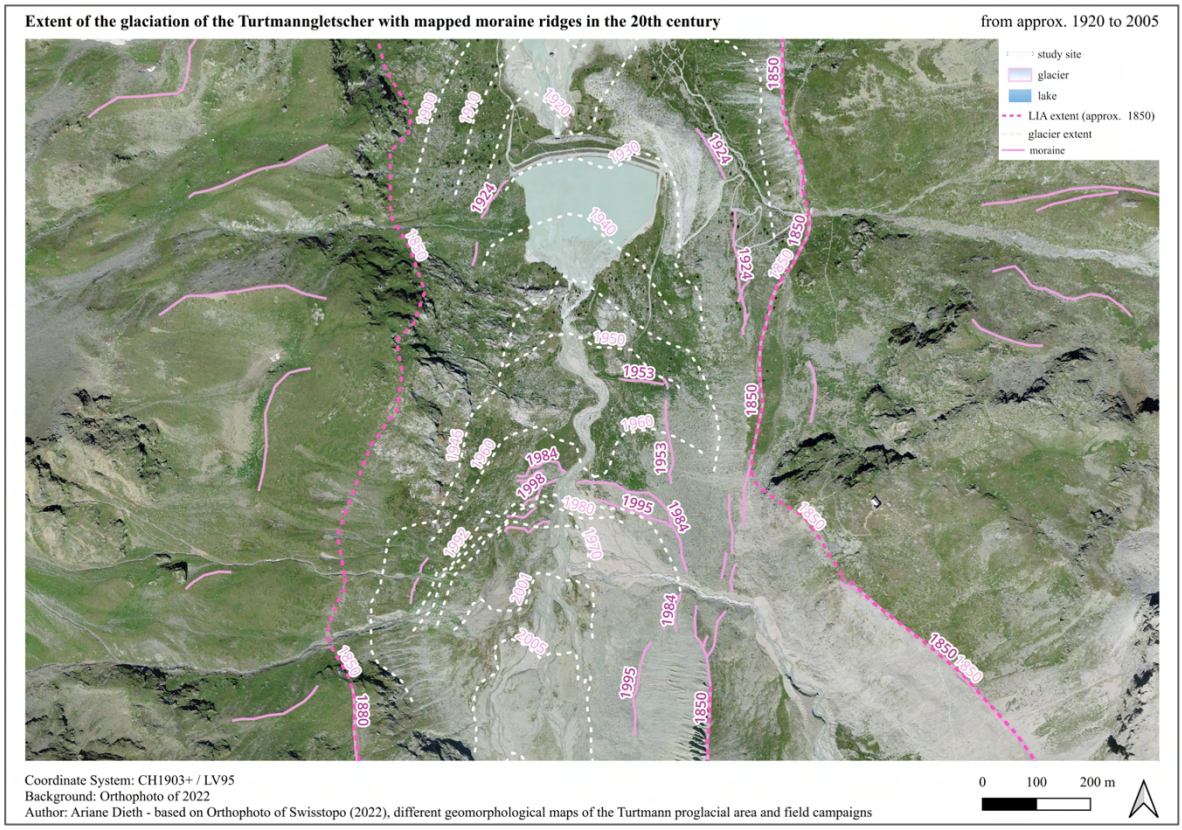

FIGURE 20 THE MAPPED GLACIER EXTENTS AND MORAINE RIDGES FOR THE AREA BETWEEN THE POSITION OF THE GLACIER TONGUE IN THE 1920S AND IN 2005 WITH THE HUGE MORAINE RIDGE OF 1984 VISIBLE IN THE CENTRE OF THE MAP (ARIANE DIETH, 2024).

According to GLAMOS, the Turtmanngletscher retreated 1’682 metres between the years 1885 and 2018 and the Brunegggletscher retreated 1’411 metres between the years 1934 and 2021 (see **Figure 21**). Both glaciers were connected until about the 1930s/1940s as the GLAMOS data, historic maps and historic aerial images suggest (GLAMOS, 1881-2023; Swisstopo, 20204b, 2024c and 2024d).

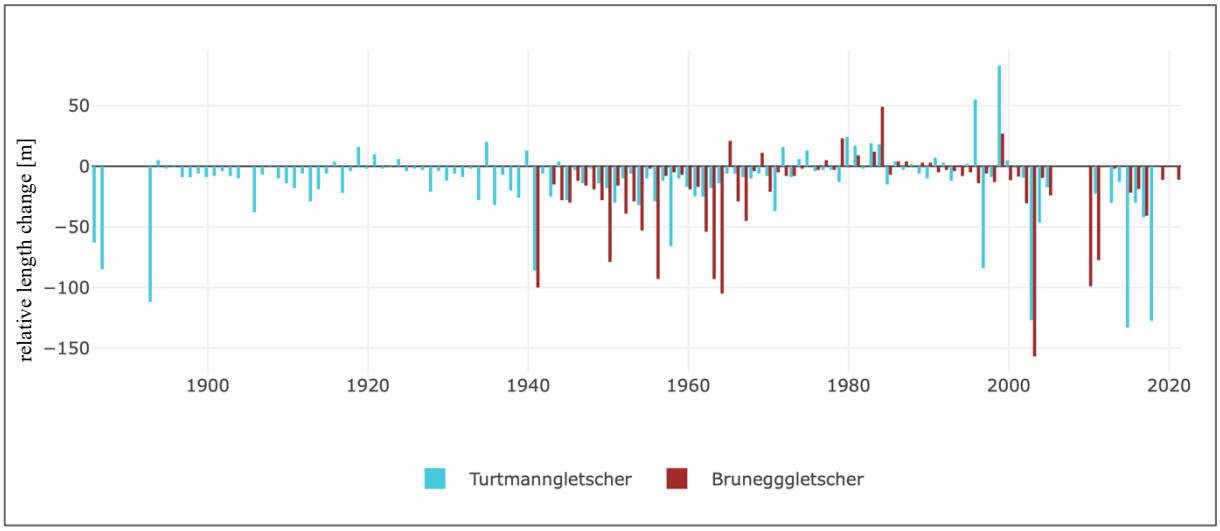

FIGURE 21 RELATIVE GLACIER LENGTH CHANGES OF THE TURTMANNGLETSCHER AND BRUNEGGGLETSCHER SINCE IT WAS RECORDED (FROM: GLAMOS, 1881-2023).

4.3 Dendrochronology

The main aim of the dendrochronological analysis was to obtain the minimum ages of the chosen trees in the study site to determine the the terminus of the Turtmanngletscher during the Little Ice Age (LIA). The expected results show the succession of *L. decidua* Mill. with which a chronosequence can be built and the retreat of the Turtmanngletscher in an area where there is not a high regularity of updates of maps (see **2.2.3**). Additionally, the growth patterns of the trees are analysed in this master thesis to check for effects of climatic parameters such as temperature and precipitation on the growth and succession of trees that would give information on the the climatic conditions that may drive glacier fluctuations in the southern Turtmann Valley in the corresponding years.
The results of the tree growth and the analysis on the correlation with temperature and precipitation will first be shown in chapter **4.3.1** and the minimum ages of the studied trees and spatial distribution of the trees are presented in chapter **4.3.2**.

4.3.1 Relationship between the growth of *L. decidua* Mill. and climate

The growth pattern of the tree rings in comparison with temperature resp. precipitation was done with the samples named with suffixes -A and -B without some samples of the trees defined as outliers as described in **3.3.4**. The samples that make up the chronology are visible in **Table A 2** in the Appendix. First, the results of the chronology of the sampled trees in the Turtmann Valley are presented. After, the result to the outliers is presented. In this chapter, graphs of the time series, sample depth and correlation with temperature resp. precipitation for the detrended and raw chronology are presented.

The chronology of the tree-ring width (TRW) measurement is shown in **Figure 22** as a superimposed curve onto the individual TRW curves in said graph. The tree-ring data was detrended to show the long-term trends and emphasize inter-annual variability. The overall pattern of tree-ring growth visible in **Figure 22** shows relative stability in growth rates over the long term although there are short-term variations. These variations (peaks and troughs) show when the growth of the trees was distinctive from other years. Notable peaks were in the mid-1960s, late 1980s, late 1990s and in the late 2000s. Periods with a decline in growth are in the late 1950s, late 1970s, in the mid-1990s and some years after the year 2000. In the most recent years the growth was stable without noticeable peaks and troughs. There are periods with a larger spread of the single TRW curves (grey in **Figure 22**) which suggest more variability in the growth of the observed trees. This needs to be considered in the interpretation of the results.
Another aspect that needs to be considered is the sample depth which indicates the number of tree samples contributing to the chronology each year (see **Figure 23**). The chronology and the sample depth which indicates the number of tree samples contributing to the chronology each year, are shown. The sample depth starts with only one tree in 1949 and gradually increases over the years reaching a total of 87 samples by 2023. As the sample size grows, the reliability of the mean chronology improves. However, also the composition of the used samples changes. As there are younger tree included in the later years, the mean tree-ring width in the later period raises artificially, giving the appearance of an increase over time. In fact it just reflects a shift in the age distribution of sampled trees as younger trees with wider rings are averaged together with older trees that have narrower rings. This can result in a more flattened trend over time masking the individual biological growth patterns of any single tree. This needs to be considered when interpreting **Figure 26** to **Figure 31** where the chronology is presented together with temperature and precipitation. However, the peaks of the years 1964, 1989, 1994, 1998, 2003, 2010

and 2015 which are also visible in the detrended data (**Figure 22**), are visible in the raw chronology of **Figure 23** and **Figure 26** to **Figure 31**. The troughs of low growth in the late 1950s, in the mid-1970s, after 1980, in the mid-1990s and some years after the year 2000 in the detrended chronology are visible in the years of 1955 to 1957, 1975, 1980/1981, 1995 to 1997, 2002 and 2007. In the raw chronology the years 2013 and 2014 also show low growth which is only slightly visible in the detrended chronology.

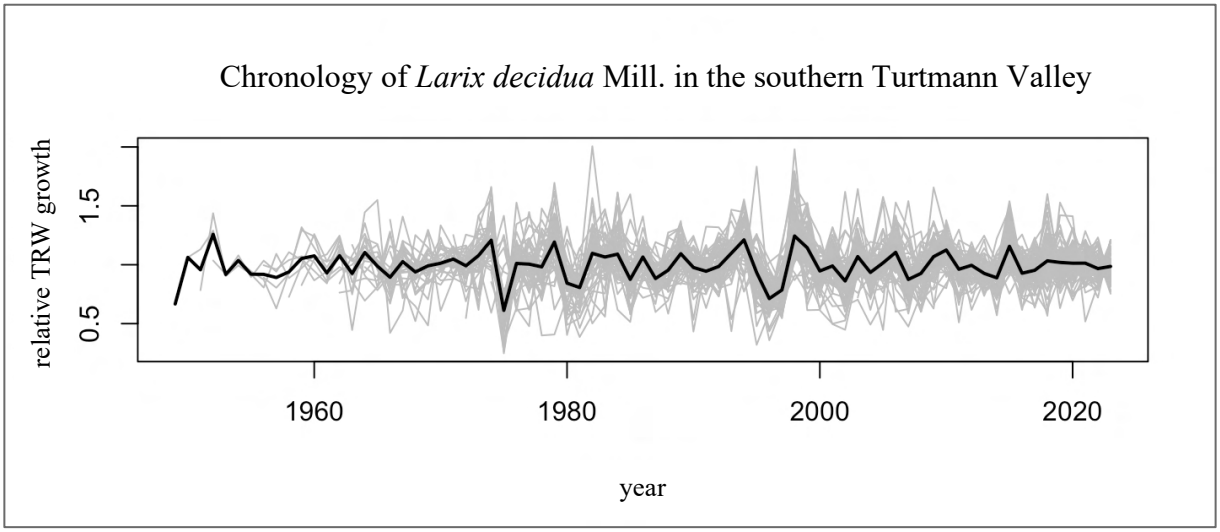

FIGURE 22 THE TIME SERIES OF THE SAMPLES WITH THE SUFFIX -A AND -B OF THE TREES IN THE STUDY SITE WITHOUT THE OUTLIERS. THE X-AXIS IS THE TIMELINE SPANNING FROM 1949 TO 2023. ALTHOUGH THE OLDEST TREE IS DATED TO 1946, THE OLDEST SAMPLE WITH A SUFFIX -A WAS DATED TO 1949. THE Y-AXIS REPRESENTS THE DETRENDED TREE-RING WIDTH VALUES. THESE VALUES CORRESPOND TO RELATIVE GROWTH RATES AND ARE ADJUSTED TO REMOVE LONG-TERM TRENDS. IN GREY THE SINGLE TREE-RING CURVES ARE VISIBLE AND IN BLACK THE MEAN CURVE (CHRONOLOGY) OF THE TIME SERIES IS ILLUSTRATED (ARIANE DIETH, 2024).

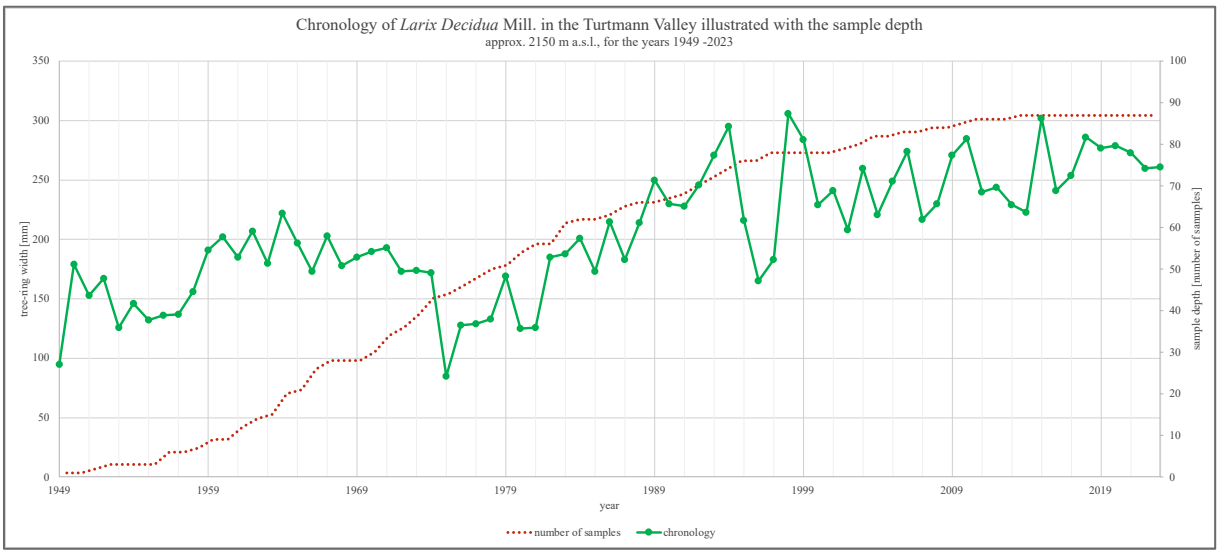

FIGURE 23 THE CHRONOLOGY (GREEN) OVER THE YEARS FROM 1949 TO 2023 IS REPRESENTED IN THIS GRAPH TOGETHER WITH THE SAMPLE DEPTH (RED-DOTTED LINE). THE Y-AXIS ON THE LEFT SHOWS THE TREE-RING WIDTH FOR THE CHRONOLOGY AND THE Y-AXIS ON THE RIGHT SHOWS THE NUMBER OF SAMPLES CONTRIBUTING TO THE CHRONOLOGY. THE CHRONOLOGY IS NOT DETRENDED AND SHOWS THE RAW TREE-RING WIDTH (ARIANE DIETH, 2024).

To be able to interpret the peaks and troughs of the TRW curves and the mean chronology, a correlation with temperature and precipitation was assessed across different months and varying seasonal lengths, as shown in **Figure 24** and **Figure 25**. The correlation values range in both plots from +1 to -1 with positive correlations represented by shades of blue and negative correlations by shades of yellow. The lines of the contour plot help to read the coloured correlation values.

The precipitation plot in **Figure 24** shows overall weak correlation between precipitation and tree growth as the values are mostly below +0.3 or above -0.3. There is a slight negative correlation with a value of -0.3 in July as well as July and June (two months of season lengths) and July, June and May (three months of season lengths) visible in in yellow. This shows that in this period the increase in precipitation is weakly correlated with a decrease in tree-ring growth.

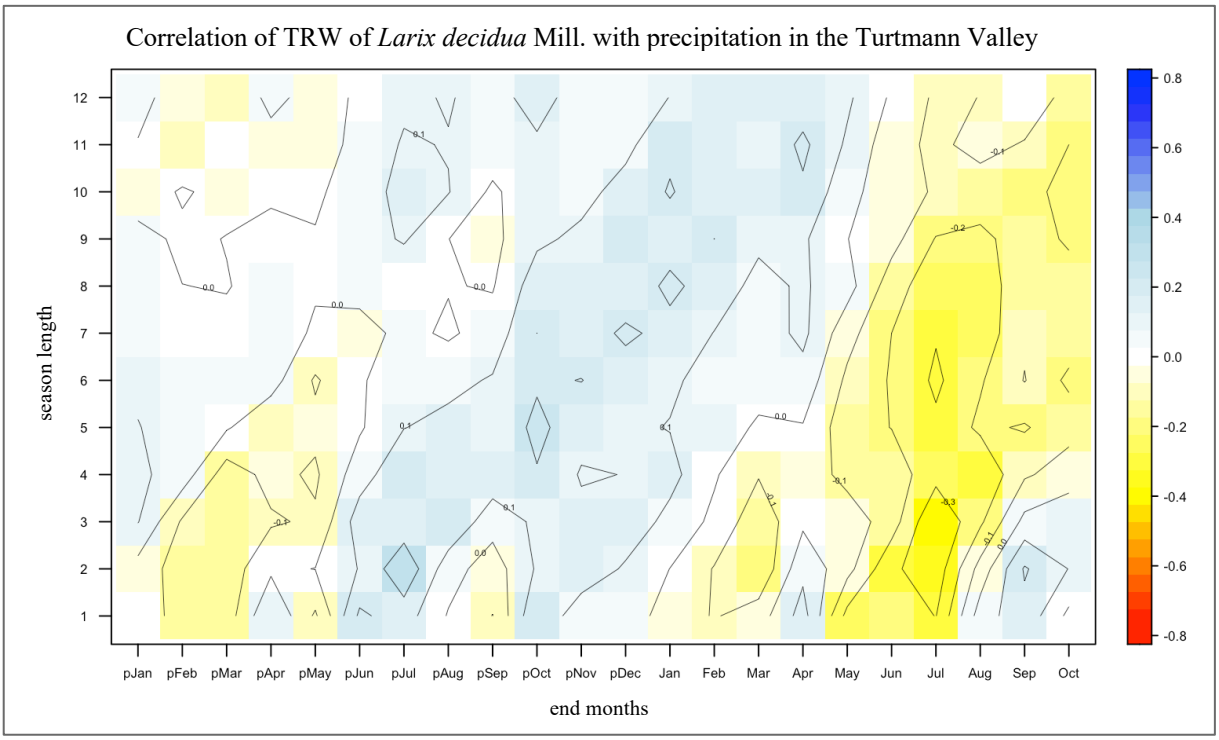

FIGURE 24 THE CORRELATION BETWEEN TREE-RING WIDTH GROWTH AND PRECIPITATION IN THE STUDY SITE OVER THE TIME PERIOD OF 1949 AND 2023 SHOWN IN A CONTOUR PLOT. THE Y-AXIS SHOWS THE SEASON LENGTH WHICH MEANS THE NUMBER OF MONTHS. THE X-AXIS SHOWS END MONTHS FOR THE CORRELATION OF TREE-RING WIDTH WITH PRECIPITATION IN THE TURTMANN VALLEY. EACH LABEL REPRESENTS A MONTH. THE LEFT SIDE (WITH "P" PREFIX) REPRESENTS PRECIPITATION IN DIFFERENT MONTHS PRIOR TO THE GROWING SEASON WHILE THE RIGHT SIDE SHOWS MONTHS WITHIN THE ACTUAL GROWTH PERIOD. THIS VISUALISATION ALLOWS TO SHOW HOW THE CORRELATION BETWEEN PRECIPITATION AND TREE-RING WIDTH VARIES ACROSS DIFFERENT MONTHS AND PERIODS LEADING UP TO AND DURING THE GROWING SEASON (ARIANE DIETH, 2024).

The temperature plot in **Figure 25** shows moderate to strong positive correlation in the summer months of May, June, July and August in blue. There is a strong positive correlation of with a value of +0.5 in the summer months July together with June and July (two months of season lengths) together with June and May (three months of season lengths). It shows that an increase tree-ring width might be correlated with an increase in temperature in these months. Another strong correlation with a value of +0.4 is visible in blue for the month July on its own, June, July and August (three months of season lengths) and May, June, July and August (four months of season lengths). In these months, the higher temperature might have a positive influence on tree growth.

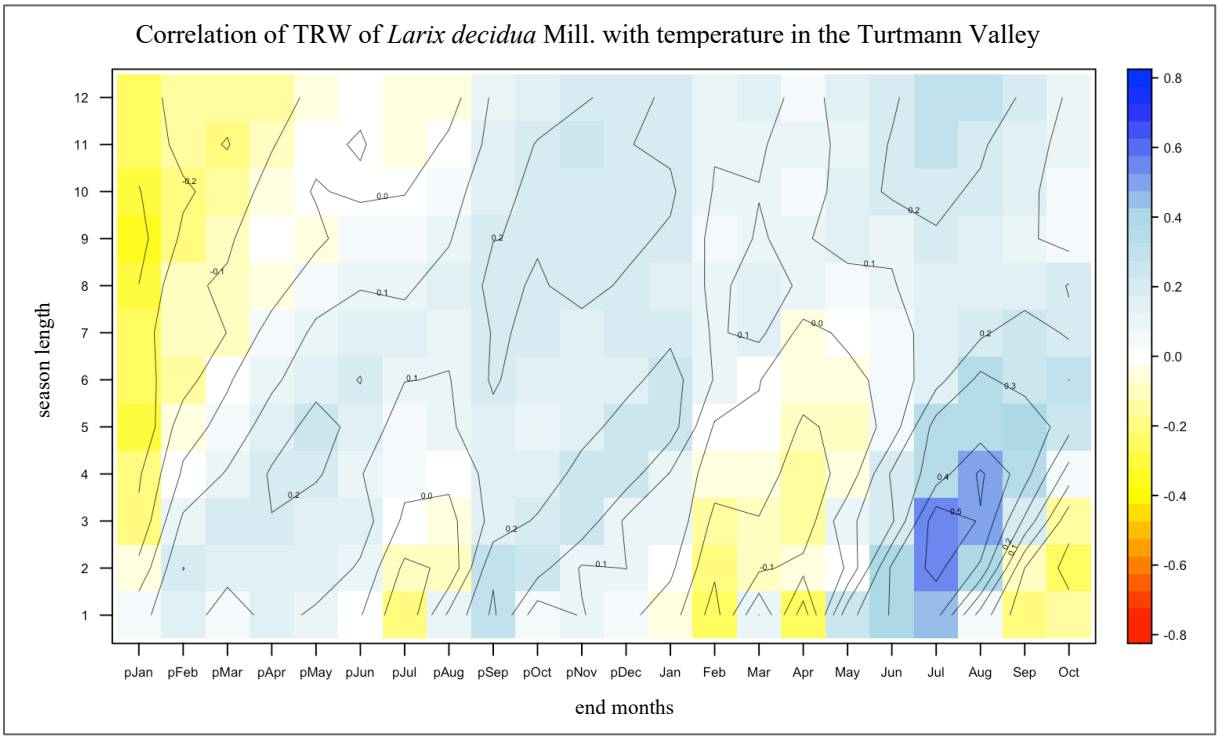

FIGURE 25 THE CORRELATION BETWEEN TREE-RING WIDTH GROWTH AND TEMPERATURE IN THE STUDY SITE OVER THE TIME PERIOD OF 1949 AND 2023 SHOWN IN A CONTOUR PLOT. THE Y-AXIS SHOWS THE SEASON LENGTH WHICH MEANS THE NUMBER OF MONTHS. THE X-AXIS SHOWS END MONTHS FOR THE CORRELATION OF TREE-RING WIDTH WITH TEMPERATURE IN THE TURTMANN VALLEY. EACH LABEL REPRESENTS A MONTH. THE LEFT SIDE (WITH "P" PREFIX) REPRESENTS TEMPERATURE IN DIFFERENT MONTHS PRIOR TO THE GROWING SEASON WHILE THE RIGHT SIDE SHOWS MONTHS WITHIN THE ACTUAL GROWTH PERIOD. THIS VISUALISATION ALLOWS TO SHOW HOW THE CORRELATION BETWEEN TEMPERATURE AND TREE-RING WIDTH VARIES ACROSS DIFFERENT MONTHS AND PERIODS LEADING UP TO AND DURING THE GROWING SEASON (ARIANE DIETH, 2024).

The time series is represented in **Figure 26** together with the mean annual precipitation. In contrast to **Figure 22** and the chronology used for the correlation calculations which resulted in **Figure 24** and **Figure 25**, the chronology is not detrended. Thus, the composition of the TRW might include different aged trees and the year-to-year comparison cannot be made entirely accurate with this graph. Although it is still useful to compare specific time periods with the climate data.

The annual mean precipitation shows a variability over the period of 1949 and 2023 with the highest 10% of precipitation in the years 1968, 1977, 1981, 1999, 2000, 2002 and 2008 and the lowest 10% in the years 1949, 1950, 1964, 1997, 2003, 2017 and 2022.

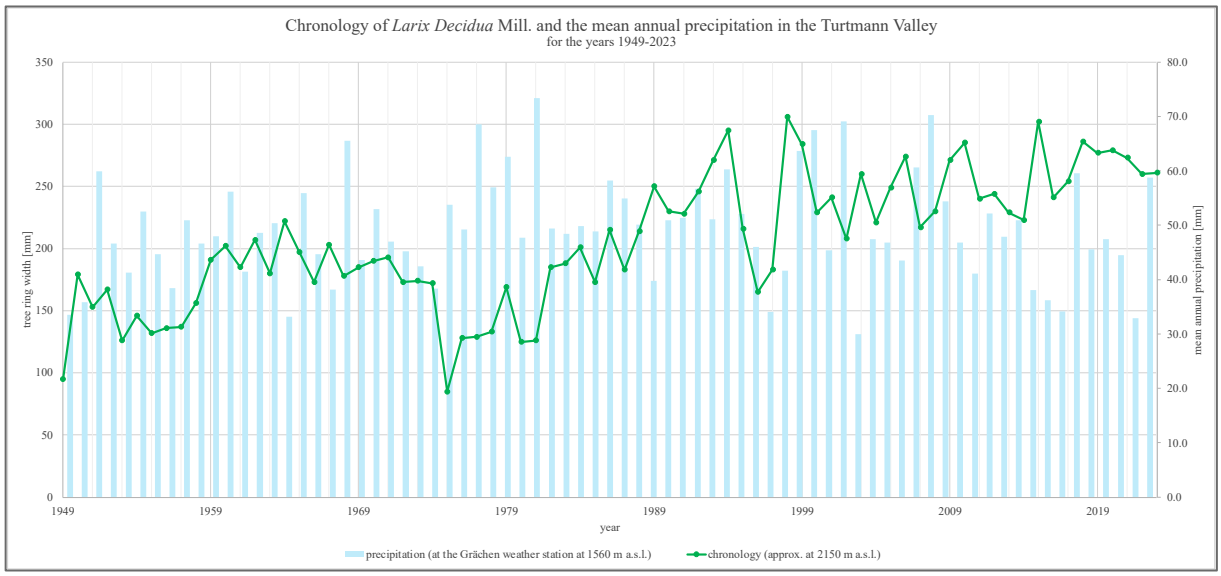

FIGURE 26 THE MEAN ANNUAL PRECIPITATION OVER THE TIME PERIOD OF 1949 AND 2023 (X-AXIS) IS PRESENTED AS BLUE BARS AND THE RAW TIME SERIES IS REPRESENTED AS A GREEN LINE. THE Y-AXIS ON THE LEFT SHOWS THE TREE-RING WIDTH FOR THE CHRONOLOGY AND THE Y-AXIS ON THE RIGHT SHOWS THE MEAN PRECIPITATION IN MM (ARIANE DIETH, 2024).

As a step following the correlation analysis with *L. decidua* Mill. , the mean precipitation of the months May, June and July is presented together with the raw chronology in **Figure 27**. Compared to the annual mean precipitation, there summer months have more absolute amount of precipitation and some years of low precipitation are more extreme.

The mean precipitation over the months May to July shows a variability over the period of 1949 and 2023 with the highest 10% of precipitation in the years 1957, 1969, 1977, 1985, 2002, 2007 and 2008. Additional years with high precipitation are found in 1965, 1978, 1981 and 2010.

The lowest 10% are found in the years 1950, 1952, 1954, 1962, 1966, 1976 and 1986. Other years with low precipitation are 1979, from 1988 to 1990, from 2003 to 2006, 2009, 2016 and 2017.

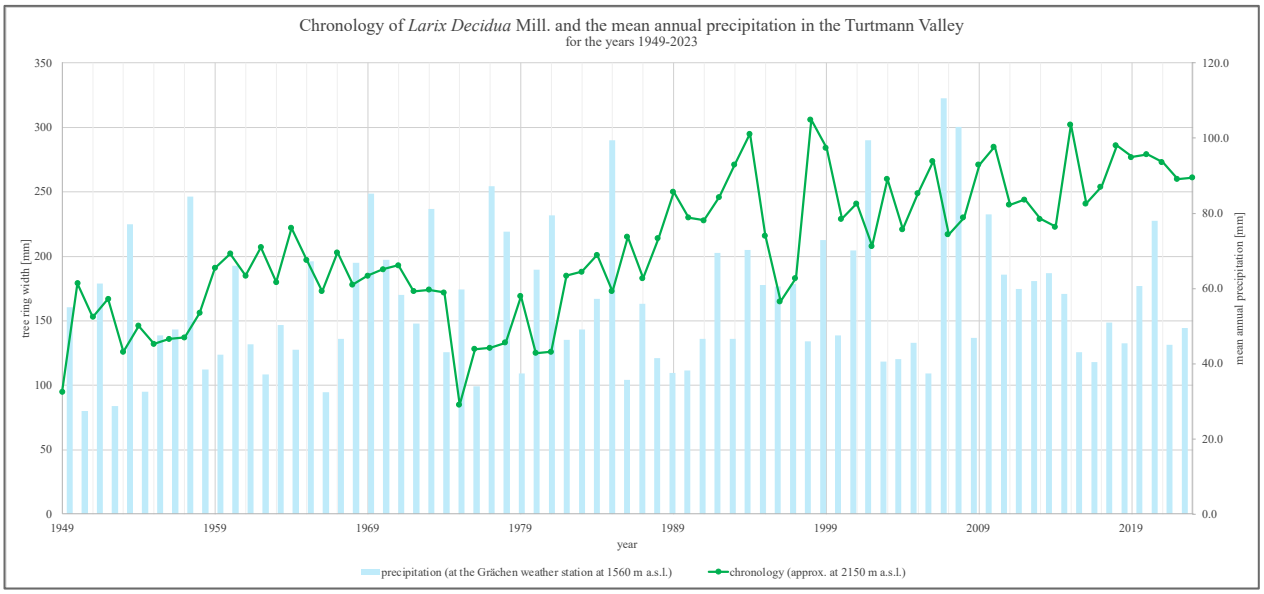

FIGURE 27 THE MEAN PRECIPITATION OF THE MONTHS MAY, JUNE AND JULY OVER THE TIME PERIOD OF 1949 AND 2023 (X-AXIS) IS PRESENTED AS BLUE BARS AND THE RAW TIME SERIES IS REPRESENTED AS A GREEN LINE. THE Y-AXIS ON THE LEFT SHOWS THE TREE-RING WIDTH FOR THE CHRONOLOGY AND THE Y-AXIS ON THE RIGHT SHOWS THE MEAN PRECIPITATION IN MM (ARIANE DIETH, 2024).

The raw chronology together with the mean annual temperature is illustrated in **Figure 28**. There is a variability of the mean annual temperature with an overall warming trend in the last 20 years compared to the middle of the 20th century. The highest 10% of mean annual temperature are found in the recent years 2003, 2006, 2007, 2011, 2020, 2022 and 2023. However, other noticeable peaks in comparison to the surrounding years are the peaks in the years 1961, 1964, 1983, 1989, 1994, 1997 and 2015.

The lowest 10% of mean annual temperatures are found in the years 1956, 1962, 1963, 1965, 1969, 1980 and 1984. Also worth mentioning are the troughs of the mean annual temperature of the years 1960, 1970, 1995, 1996, 2005, 2010, 2013, 2016 and 2021.

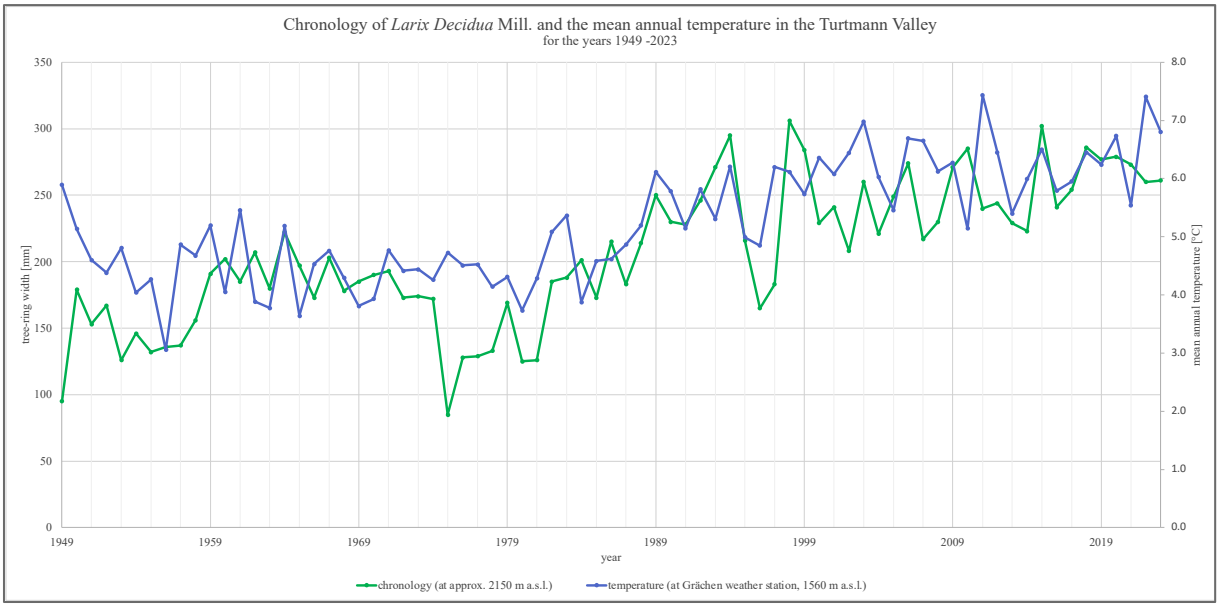

FIGURE 28 THE MEAN ANNUAL TEMPERATURE OVER THE TIME PERIOD OF 1949 AND 2023 (X-AXIS) IS PRESENTED AS A DARK BLUE CURVE AND THE RAW TIME SERIES IS REPRESENTED AS A GREEN LINE. THE Y-AXIS ON THE LEFT SHOWS THE TREE-RING WIDTH FOR THE CHRONOLOGY AND THE Y-AXIS ON THE RIGHT SHOWS THE MEAN ANNUAL TEMPERATURE IN °C (ARIANE DIETH, 2024).

Two additional graphs were made to analyse the relationship between the tree growth and temperature for the growing season of *L. decidua* Mill. which is from June to October (see **3.1** for information on growing season) in **Figure 29**, and the relationship between tree growth and mean temperature for the months of May, June, July and August in **Figure 30**. The months May to August in **Figure 30** were chosen because the tree growth in these months showed a positive correlation with the temperature as it is illustrated and described in the correlation analysis (see **Figure 25**).

The peaks of the highest 10% of mean temperatures of the growing season are the same as for the annual mean temperature except for the year 2007 and 2011, which are not within the 10% anymore and are exchanged by the years 2012 and 2018. There are high temperatures visible in the mean annual temperature (**Figure 25**) for the years 1983 and 1994. The high mean annual temperatures in 1961, 1964, 1989, 1997 and 2015 are not that significantly higher in the growing season. In addition to the mentioned high temperatures in the growing season, the years 1991, 2009 and 2019 are standing out as peaks.

The lowest 10% of mean temperatures of the growing season are the years 1955, 1956, 1960, 1972, 1974, 1978 and 1980 which is different to the mean annual temperature. However, the troughs of the years 1996, 2005, 2010, 2013 and 2021 of **Figure 25** are also visible during the growing season. Additionally, there were lower temperatures in the years 1993, 2004, 2007, 2014 and 2020 during the growing season.

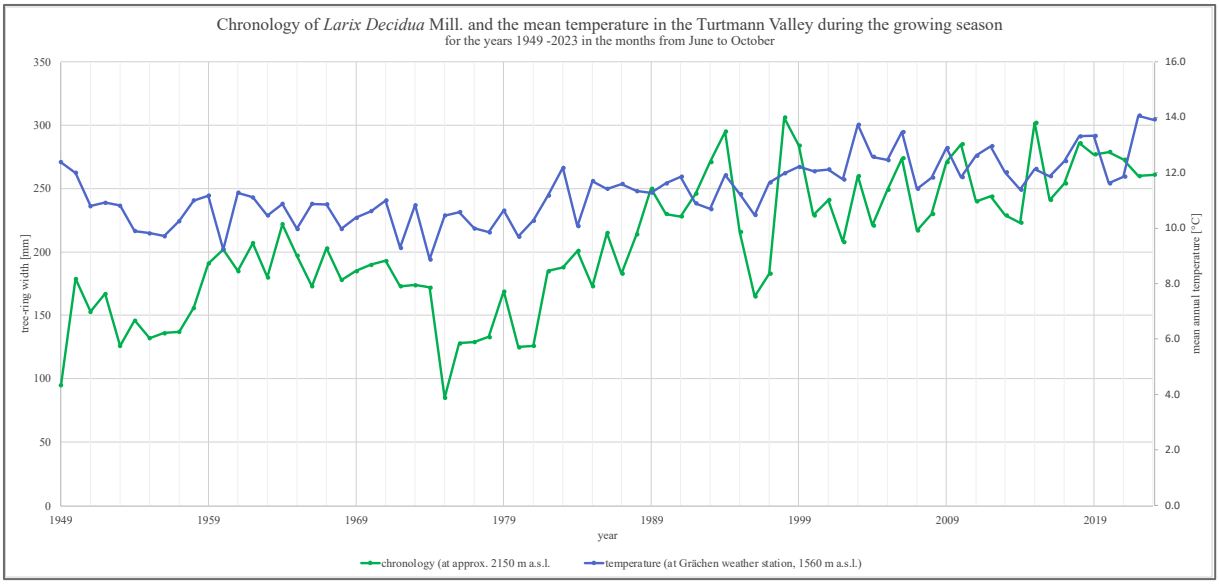

FIGURE 29 THE MEAN TEMPERATURE OF THE MONTHS OF THE GROWING SEASON OF *L. DECIDUA* MILL. (JUNE TO OCTOBER) FOR EACH YEAR OVER THE TIME PERIOD OF 1949 AND 2023 (X-AXIS) IS PRESENTED AS A DARK BLUE CURVE AND THE RAW TIME SERIES IS REPRESENTED AS A GREEN LINE. THE Y-AXIS ON THE LEFT SHOWS THE TREE-RING WIDTH FOR THE CHRONOLOGY AND THE Y-AXIS ON THE RIGHT SHOWS THE MEAN TEMPERATURE FOR THE GROWING SEASON IN °C.

The temperature pattern of the months May to August in **Figure 30** are most similar to the chronology out of the three figures with the temperature which is expected from the correlation analysis (**Figure 25**). The peaks of the highest 10% of mean temperatures of the months May to August are in the years 2003, 2009, 2012, 2017, 2018, 2022 and 2023 and other peaks mentioning are in the years 1964, 1982, 1983, 1986, 1994 and 2015.
The lowest 10% of mean temperatures of the months from May to August are the years 1968, 1972, 1977 to 1980, and 1984. The troughs of the years 1995 to 1997, 2010, 2013 and 2021 of **Figure 25** and **Figure 29** are also visible during these months. Additionally, there were lower temperatures in the years 1954 to 1957, 1987, 1993, 2004, 2007, 2014 and 2016 during the months May to August.

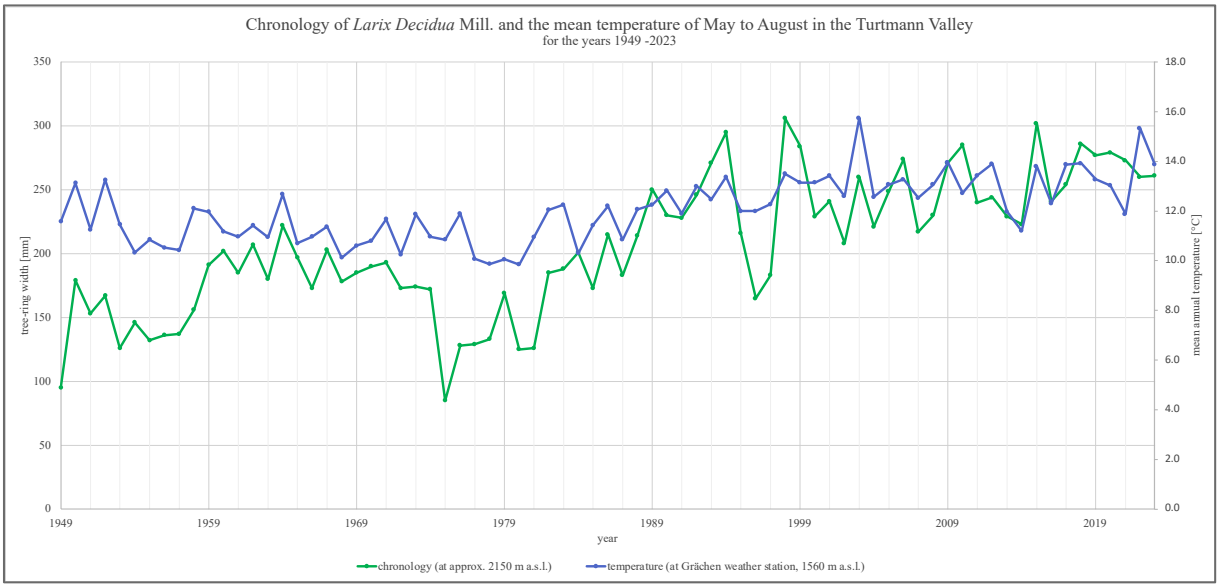

FIGURE 30 THE MEAN TEMPERATURE OF THE MONTHS MAY TO AUGUST FOR EACH YEAR OVER THE TIME PERIOD OF 1949 AND 2023 (X-AXIS) IS PRESENTED AS A DARK BLUE CURVE AND THE RAW TIME SERIES IS REPRESENTED AS A GREEN LINE. THE Y-AXIS ON THE LEFT SHOWS THE TREE-RING WIDTH FOR THE CHRONOLOGY AND THE Y-AXIS ON THE RIGHT SHOWS THE MEAN TEMPERATURE FOR THE MONTHS MAY, JUNE, JULY AND AUGUST IN °C.

Combination of tree growth together with temperature and precipitation

The chronology together with the mean temperature for the months May to August and mean precipitation for the months of May to July is illustrated in **Figure 31** and summarised in **Table 3**. The pointer years – years where there is distinctive low or high growth of TRW in all of the trees in the chronology – are illustrated in this section. These results are further discussed in **5.3.1**. The pointer years 1975, 1980 and 1981, 1995 to 1997 and 2004 are visible for low growth in both the detrended and raw data. For high growth, the pointer years 1979, 1986, 1994, 1998 and 2015 are emphasised in **Table 3**. Furthermore, the years 1982/1983 show clearly high temperatures but not that much of an increase in growth except if comparing to the very low growth of 1980 and 1981 (see **Figure 31**). The last five years (2018 to 2023) show visibly no pattern together with the climatic variations.

year	precipitation	temperature	
1950	low	high	
1952	low	high	
1955 to 1957	medium (high in '57)	low	
1962	low	high	
1964	low	high	
1967	medium	high	
1971	medium	high	
1975	medium	medium	*
1979	low	medium	*
1980 / 1981	medium to high	low to medium	*
1985	high	medium	
1986	low	high	*
1987	low/medium	low	
1989	low	medium	
1994	medium	high	*
1995 to 1997	medium	low	*
1998	low	high	*
2002	high	low	
2003	low	high	
2004	low	low	*
2006	low	high	
2007	high	low	
2009	low	high	
2010	high	low	
2013 / 2014	medium	low	
2015	medium	high	*
2016	low	low	

TABLE 3 AN OVERVIEW OF TREE GROWTH IN RELATION TO THE PATTERNS OF MEAN PRECIPITATION (MAY-JUL) AND MEAN TEMPERATURE (MAY-AUG). HIGH TREE-RING WIDTH (TRW) GROWTH IS INDICATED BY A GREEN RECTANGLE IN THE RIGHT-HAND COLUMN, WHILE LOW TRW GROWTH IS INDICATED BY A LIGHT-RED RECTANGLE. POINTER YEARS ARE MARKED WITH AN ASTERISK (*).

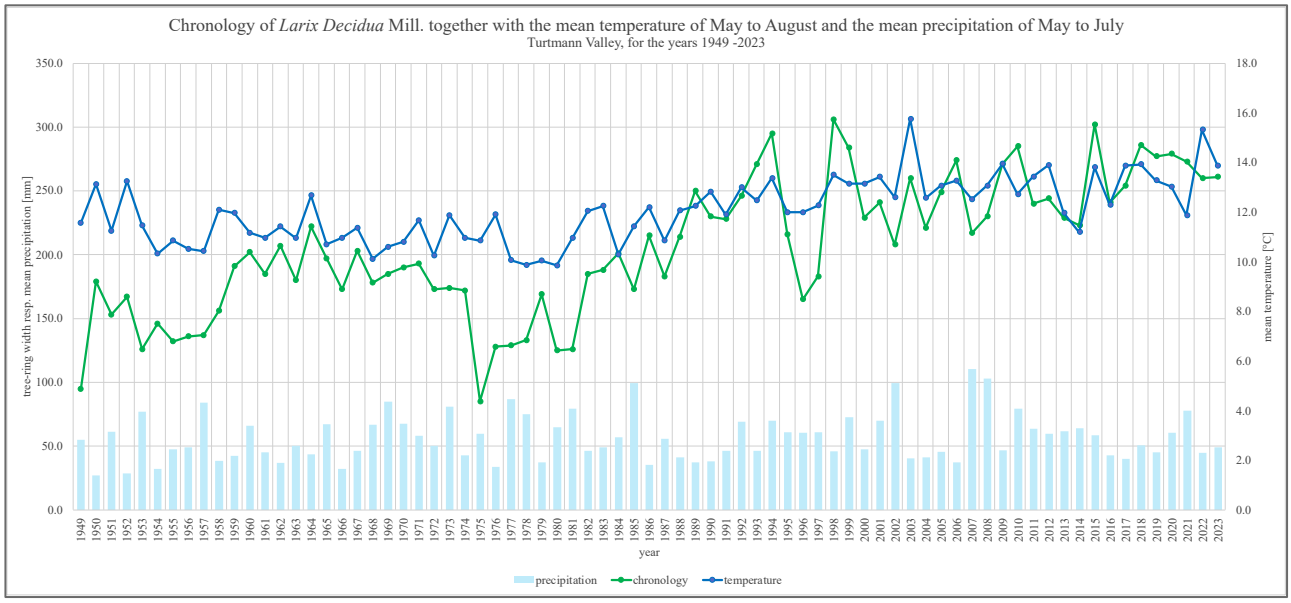

FIGURE 31 THE MEAN TEMPERATURE OF THE MONTHS MAY TO AUGUST FOR EACH YEAR AND THE MEAN PRECIPITATION OVER THE MONTHS OF MAY TO JULY OVER THE TIME PERIOD OF 1949 AND 2023 (X-AXIS) IS PRESENTED TOGETHER WITH THE TREE-RING WIDTH OVER THE SAME TIME PERIOD. THE DARK BLUE CURVE SHOWS THE TEMPERATURE AND THE GREEN CURVE THE RAW TIME SERIES. THE BLUE BARS SHOW THE AMOUNT OF PRECIPITATION IN MM. THE Y-AXIS ON THE LEFT SHOWS THE TREE-RING WIDTH AS WELL AS THE PRECIPITATION IN MM AND THE Y-AXIS ON THE RIGHT SHOWS THE MEAN TEMPERATURE FOR THE MONTHS MAY, JUNE, JULY AND AUGUST IN °C (ARIANE DIETH, 2024).

Outliers

The outliers included the trees L006, L022, L027 and L034 as it is described in **3.3.4**. However, of the tree L006 only sample L006A and L006X are considered to be outliers and of the tree L034 only the sample L034B. Hence, there are in total six samples that are included in the analysis of the outliers, as the samples -X were excluded for the analysis, parallel to the analysis of the chronology (see **Table 4**).

TABLE 4 THE OUTLIERS THAT WERE EXCLUDED FROM THE CHRONOLOGY AND ON WHICH A SEPARATE SHORT ANALYSIS WAS DONE.

sample name	dated year
L006A	1994
L022A	2000
L022B	2003
L027A	1991
L027B	1993
L034B	1988

The curves of the detrended TRW of the outliers together with the mean of themselves are visible in **Figure 32-A**. The single TRW are chaotic in the years from 2006 to 2024 which is visible in the smooth flattened mean curve and the high variability in the individual TRW curves. However, some peaks are visible for the years 1997, 1998 and 2005 and some not significant troughs of low growth in the years 1991, 1994, 1996 and 1999.

Comparing the mean curve of the outliers (red) with the mean curve of the chronology and the overall TRW curves making up the chronology (grey) in **Figure 32-B**, it gets clear that the growth pattern of the outliers is significantly different of the growth pattern of the chronology for the whole Turtmann Valley which is expected as the outliers could not be crossdated in a previous step (see **3.3.4**). The outliers are further discussed in **5.3.1**.

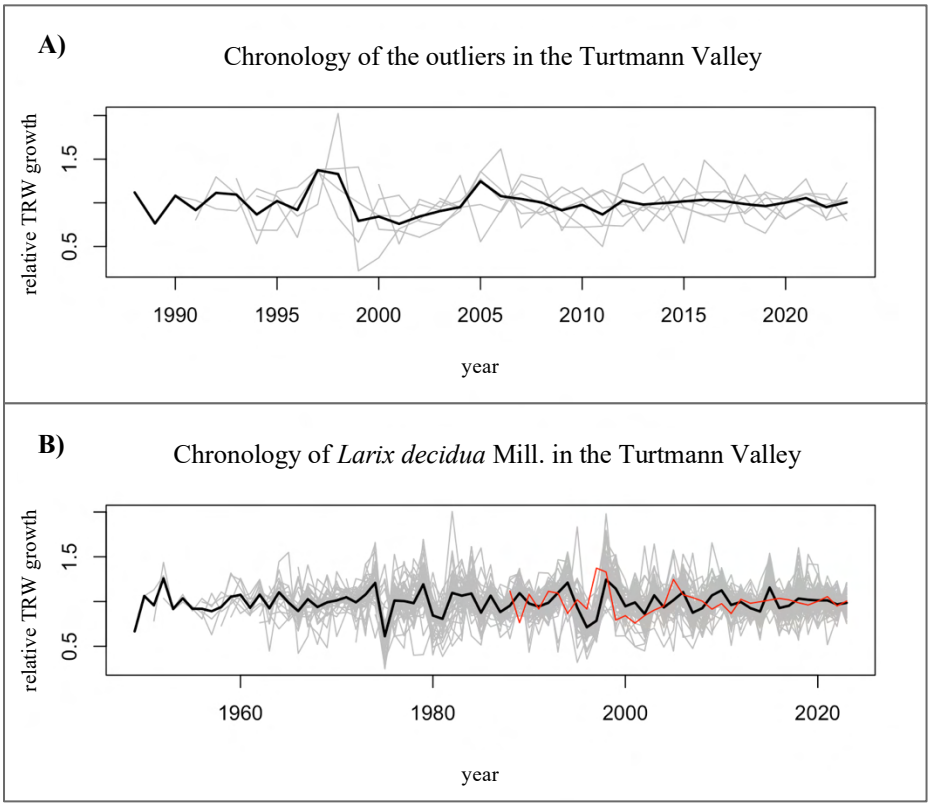

FIGURE 32 FOR BOTH GRAPHS THE Y-AXIS REPRESENTS THE DETRENDED TREE-RING WIDTH VALUES. **A)** THE TIME SERIES OF THE SAMPLES WITH THE SUFFIX -A AND -B OF THE OUTLIERS IS SHOWN. IN GREY THE SINGLE TREE-RING CURVES ARE VISIBLE AND IN BLACK THE MEAN CURVE OF THE OUTLIERS IS ILLUSTRATED. THE X-AXIS SPANS FROM 1988 TO 2023. **B)** THE DETRENDED SINGLE TREE-RING WIDTH CURVES OF THE SAMPLES WITH THE SUFFIX -A AND -B (IN GREY) TOGETHER WITH THE MEAN CHRONOLOGY FOR THE TURTMANN VALLEY (IN BLACK) AND THE MEAN CURVE OF THE OUTLIERS (IN RED) IS ILLUSTRATED. THE X-AXIS IS THE TIMELINE SPANNING FROM 1949 TO 2023 (ARIANE DIETH, 2024).

4.3.2 Age distribution *of L. decidua Mill.* in the Turtmann Valley

The minimum age of the 46 larch trees were determined with all three cross-dated samples per individual tree whereas often the sample named with the suffix -X was the oldest sample. **Table A 2** in the Appendix is a list of the age of each tree and as well what start of growth year the tree is dated to. The already mentioned outliers could not be crossdated to the chronology. However, as one sample of L006 and two of L034 could be crossdated, for the minimum age only the samples L022 and L027 are considered outliers (see **Table A 2**). The additional five trees from outside the study site in the forest further north in the valley as described in **3.3.1** are not shown here but they spanned from 301 years old (1722) to 181 years old (1826). The ages of the sampled trees were determined mostly by the samples with the suffix -X because this sample was taken at the lowest possible point to get the oldest tree rings (see **3.3.3**). The trees with their respective location and coloured in an age gradient are visible in **Figure 33**. The colour gradient shows the age from oldest in yellow (dated to 1946) to youngest tree in red (dated to 2004). The same colour gradient is visible in **Figure 34** but with bigger circles to be able to see patterns of the age distribution. In **Figure 34** the minimum age of each tree is represented. The four trees on the western side of the Turtmänna river are all not older than 52 years old. The four trees on the roche moutonnée in the south of the image are of different ages with three trees almost the same age (dated to the late 1960s) and one tree dated to 1991 (L006). There is a slight pattern that the trees on the more forested rampart (for instance L043) are older than the trees in the area where scree and blocks of rocks are located (for instance L017). The age distribution with possible patterns and their meaning are discussed in **5.3.2** and **5.4**.

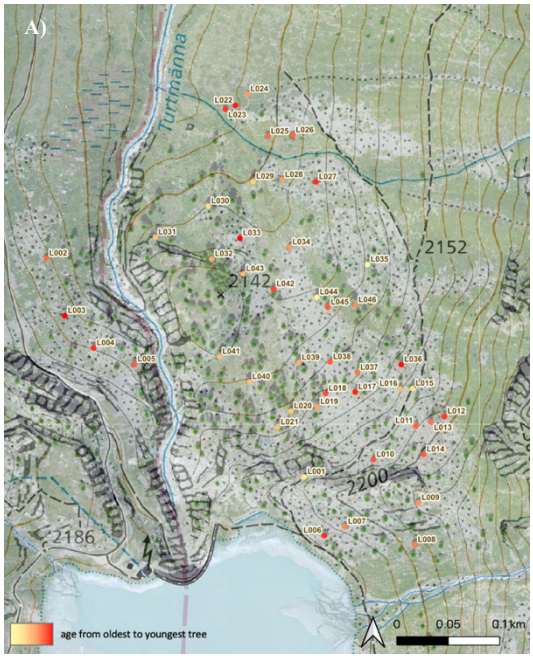

FIGURE 33 THE AGES OF TREES IN THE STUDY SITE. THE NAMES GIVEN IN THE FIELD TO THE TREES AS WELL AS THE AGE DISTRIBUTION LOOKING GAT THE COLOUR GRADIENT IS SHOWN (ARIANE DIETH, 2024).

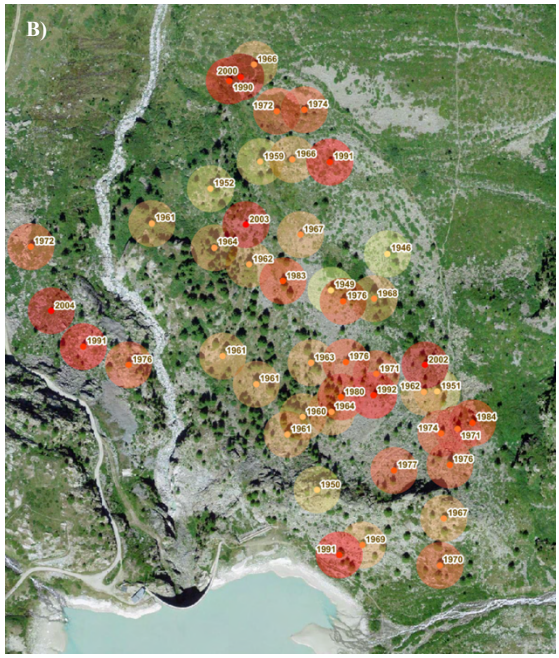

FIGURE 34 THE AGE DISTRIBUTION OF THE SAMPLED TREES IS CLEARER ILLUSTRATED WITH THE COLOURED CIRCLES AND THE DATED YEAR (ARIANE DIETH, 2024).

5. Discussion

The chapter provides a detailed analysis and discussion of the findings from the geomorphological mapping, glacier extents mapping and dendrochronological study done in the southern Turtmann Valley. It begins with an overview of the geomorphological analysis of the southern Turtmann Valley and critically analysing the mapping of the different process domains and the corresponding landforms. In a next part, the glacier history in the study site is analysed before, during and mostly after the maximum extent of the Turtmanngletscher during the the Little Ice Age (LIA) in the mid 19th century. This section explores the position of the terminus of the Turtmanngletscher in the proglacial area and uncertainties in the mapping of glacier extents over time. Next, the relationship between the growth of European larch tree (*L. decidua* Mill.) and climate is analysed through dendrochronological methods. In the focus site the age distribution of the sampled *L. decidua* Mill. is analysed. An assessment of the uncertainties related to the dendrochronological analysis follows this section. Thus, all three key topics of the thesis - geomorphology, glacier history and the succession of *L. decidua* Mill. - are discussed in their uncertainties in methodology. The chapter concludes with a synthesis of these three topics which provides an integrated understanding of how these processes have shaped the landscape of the southern Turtmann Valley especially in the context of climatic and geomorphological changes since the Little Ice Age.

5.1 Geomorphological analysis of the southern Turtmann Valley

5.1.1 Overview

The study site covering the southern Turtmann Valley consist of the main valley floor and three western hanging valleys and two eastern hanging valleys which are all most influenced by glacial, gravitational and some periglacial processes. The main valley has a typical U-shape that is made through linear-glacial erosion over the past glaciations (Dikau et al., 2019). However, there is a height difference between the northern and southern part of the study site with a transverse ridge of bedrock (riegel) at the location of the hydropower wall of the Turtmannsee. A gorge with the main river, the Turtmänna, breaks this riegel made out of gneiss (see **3.1.3**). The main valley floor, both north and south of the riegel, are mostly mapped as glacial process domain. These areas were glaciated during past glaciations (see **5.2.2**) and hence, glacial till was deposited. Some landslide deposits or alluvial fans are mapped which are clearly visible in the relief (Swisstopo, 2017). The overall study site is shown to be asymmetric in its geomorphic processes. The western hanging valleys such as Frilitälli, Wängertälli and Inners Wängertälli as well as the kars on Wängernhorn experience less periglacial processes than the eastern hanging valleys named Piipjitelli and the area around the Barrhorn and Brunegggletscher. The eastern side of the study site has still some ice or firn on their mountain flanks like the Pipijgletscher or on the flank of the Barrhorn. According to Kenner et al. (2019) the occurrence of permafrost on the western-exposed mountain flanks on Barrhorn or in the Piipjitelli is likely and thus, the periglacial process domain was mapped there if there were also periglacial landforms visible (see discussion in **5.1.3**). Other than periglacial processes, there are mostly gravitational processes happening in the hanging valleys as it is visible on the scree slopes (see discussion in **5.1.4**). Right in the proglacial area of the Turtmanngletscher a lot of change has happened in the last 20 year caused by paraglacial adjustment visible in the gullying of the lateral "LIA" moraine (see **5.2.2**). There is a lot of meltwater available from the decline of glacier which shapes the landscape in the main valley floor in the southern part of the study site. As the glaciers play a crucial role, the mapped domains and landforms are analysed and discussed first. After, the chapter includes the analysis and discussion of all process domains and landforms that were mapped in this thesis.

5.1.2 Glacial process domain and morphological landforms

The mapping of the glacial process domain was mostly based the orthophoto from 2020, historical maps and aerial images (Swisstopo, 2024a, 2024b, 2024c and 2024d) and the validation of the mapped landforms was made through the field campaigns and literature review (see **Table 2** and **Table A 1**). In this thesis, no field data was collected on the geology and sedimentology of the study site and thus, the given maps of the Geological Atlas of Switzerland and literature were the base on decisions on mapping ground of basal till as glacial process domain (Swisstopo, 2024g). The ground of the valley floor and some of slopes had been shaped by glaciation and thus, are considered to be basal till (Bearth, 1980; Bini et al., 2009; Marthaler et al., 2008; Swisstopo, 2024g).

The southern Turtmann Valley characterised by its typical U-shape is a product of extensive linear glacial erosion that occurred over multiple glaciations. The location of the hydropower lakes is not coincidental. In a situation where there would be not a gorge with its role as an outlet, the riegel might act as a natural dam to build up a lake, as it is visible in multiple glacial lakes in Switzerland (Haeberli et al., 2016; Steinemann et al., 2021). However, the gorge in this situation has probably acted as a natural outlet for the water of the glaciofluvial plain shortly after the Turtmanngletscher retreated in the 1940s and no natural lake has been formed in a overdeepened relief (Steinemann et al., 2021). An overdeepening is oftentimes apparent at locations where the surface slope increases, in a transition from a crevasse-rich area to a crevasse-free area and where lateral narrowing is happening (Haeberli et al., 2016; Magrani et al., 2020). A riegel is then influential as it can compress and stretch the glacier ice which builds up pressure on the ground surface with crevasses in the ice. The gorge could act as an outlet of the subglacial meltwater which then opens the possibility to build up more pressure on the ground by the glacier just behind the gorge as it is visible at the Trift glacier (Steinemann et al., 2021). The situation would have been optimal for overdeepening to occur except for the riegel being not too big in its height and therefore it might have not been a big obstacle for the ice to be blocked and for pressure on the ground to build up. The glacier ice extended during the maximum extent of the LIA higher up (see **Figure 18** in **4.2**) and this suggests that the glacier was mostly overriding this landscape without making a basin lower than the fluvial plain (Magrani et al., 2020). This conclusions are supported by the national map of 1947 (Swisstopo, 2024e), the stitched orthophoto of 1946 of the "US flight mission" (Swisstopo, 2024c) and a photo in Meyer (1923) (see **Figure 36-A** to **Figure 36-C**). It is not possible to further discuss an overdeepening or glacial erosional patterns of an older time span than today back to the maximum extent of the LIA with limited resources used in this thesis.

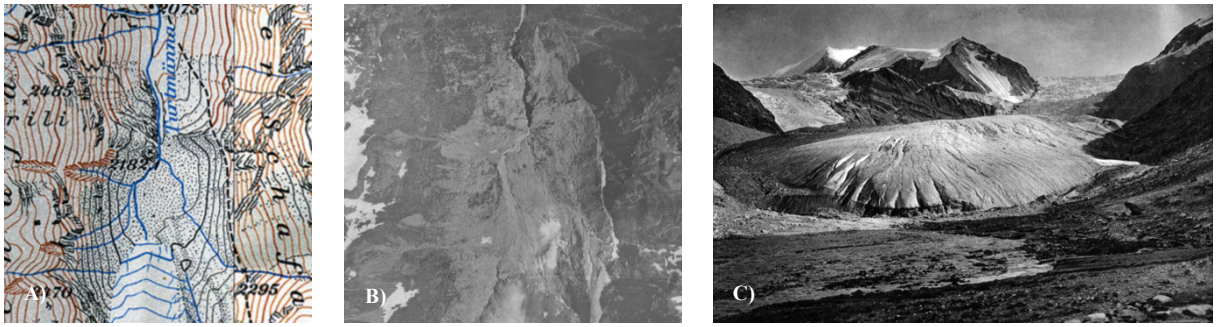

FIGURE 35 THESE DIFFERENT SOURCES WERE USED TO DECIDE ON IF THERE WAS AN OVERDEEPENING IN THE TURTMANN VALLEY AT THE LOCATION OF THE ARTIFICIAL TURTMANN LAKE. THE FIGURES SHOW **A)** THE SWISS NATIONAL MAP OF 1947 (SWISSTOPO, 2024D), **B)** THE AERIAL IMAGE OF THE "US FLIGHT MISSION" IN 1946 (SWISSTOPO, 2024C) AND **C)** A PHOTO TAKEN BY H. VOLLENWEIDER, UNKNOWN DATE BEFORE THE YEAR 1923 (MEYER, 1923).

In some cases of the geomorphological map, a mixture of the glacial with the fluvial resp. gravitational process domain is mapped. This is due to the surface material being mostly glacial till from the last and previous glaciations, although other processes are happening more recently which should be included in the geomorphological map as mentioned in **2.1.2**. The slopes in the Turtmann Valley are steep and thus, prone to gravitational processes (see **5.1.1** and **5.1.4**) Therefore, a mixture of the glacial and gravitational process domain is mapped on slopes that are suspected to be made of till and where only occasionally gravitational processes are occurring. This was determined by the existence of vegetation cover which is a sign of the slope being stabilised (Eichel, 2017). Thus, relatively stabilised surfaces with vegetation and which do not clearly show dominantly gravitational processes are mapped as glacio-gravitational. **Figure 36-A** and **-B** show a situation where the glacio-gravitational, the glacial and the gravitational process domain were mapped in the vicinity of each other. The gravitational process domain is clearly covering the landslide and its deposits, whereas the glacio-gravitational process domain covers the slope which is made of till but has some but not significant slope erosional processes happening such as small grass erosion described by Geitner et al. (2021). The slope with till material and a moraine without any gravitational processes is just mapped as a glacial process domain.

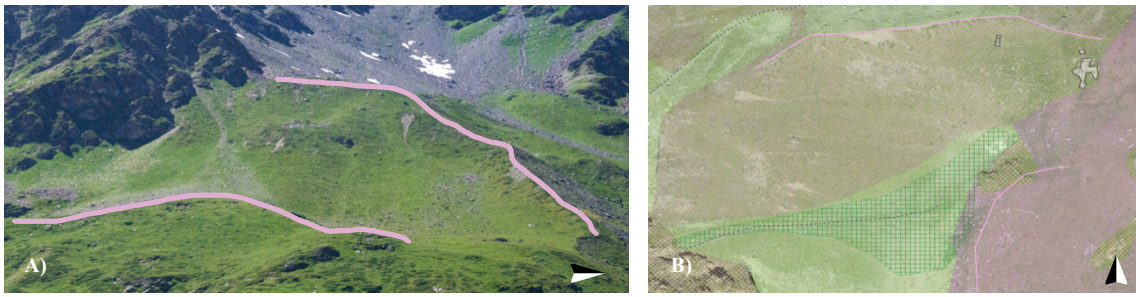

FIGURE 36 AN AREA WHERE GRAVITATIONAL, GLACIO-GRAVITATIONAL AND GLACIAL PROCESS DOMAINS ARE MAPPED. THE MORAINE RIDGES OF PAST GLACIATIONS ARE VISIBLE BY A PINK LINE IN **A)** AND **B)**. THERE IS A LANDSLIDE DEPOSIT VISIBLE AS GREEN-SQUARED AREA IN **B)** AS WELL AS THE RUINS IN THE NORTHEASTERN CORNER OF THE MAP (ARIANE DIETH, 2024).

In addition to the glacio-gravitational process domain, the glacio-fluvial process domain as a mixed process domain was mapped. The analysis of these mapped areas can be found in the discussion on the fluvial process domain in **5.1.5** as they are mostly influenced by fluvial erosion.

Glacial erosion through the movement of the Turtmanngletscher has not only shaped the main valley floor but also influenced the formation of smaller landforms such as roche moutonnées, glacier striations and other erosional features visible throughout the study site (see **Table 1** in the theory section in **2.1.3**). The roche moutonnée is an asymmetrical, streamlined relief form with a size that can range from a few metres up to several kilometres (Dikau et al., 2019). The mapped roche moutonnées in the proglacial area are not wider than 150 m. The lee side of the roche moutonnée is steep and often jagged whereas the luv side which is nearer to the glacier front is rounded and flatted. The whole landform is formed through abrasion and plucking processes when a glacier with rock fragments imbedded in the ice is overriding the landscape. The luv side is often polished and glacial scrapes such as chattermarks or linear striations might be visible through these abrasion processes (see **Figure 40**). The mapped roche moutonnées (examples in **Figure 37** to **Figure 40**) were observed in the field campaigns but also from the aerial image (Swisstopo, 2024a). More roche moutonnées were mapped than in literature (Eichel et al., 2013; Swisstopo 2024g) which can be explained that a more detailed map of the study site especially the main valley was aimed at in this master thesis.

FIGURE 37 OVERVIEW OF THE FLUVIAL PLAIN JUST SOUTH OF THE SMALLER HYDROPOWER LAKE WITH THREE ROCHE MOUTONNÉES (RED CIRCLES) AND ARROWS INDICATING THE DIRECTION OF GLACIAL FLOW (ARIANE DIETH, 2024).

FIGURE 38 A ROCHE MOUTONNÉE IN THE PROGLACIAL AREA (ALSO VISIBLE IN FIGURE 34) WITH MORAINES OF THE 1950S (PINK LINES) AND THE ARROW INDICATING THE DIRECTION OF GLACIAL FLOW (ARIANE DIETH, 2024).

FIGURE 39 JUST SOUTHWEST OF THE SMALLER HYDROPOWER LAKE IS A ROCHE MOUTONNÉE WITH A CLEAR POLISHED LUV SIDE ON THE RIGHT IN THE IMAGE AND A PLUCKED LEE SIDE ON THE LEFT (ARIANE DIETH, 2024).

FIGURE 40 THE POLISHED SURFACE OF THE LUV SIDE OF THE ROCHE MOUTONNÉE ON THE EASTERN RIEGEL AT THE LOCATION OF THE TREES L006 TO L009 IS VISIBLE BETWEEN THE DEBRIS ROCK FRAGMENTS (ARIANE DIETH, 2024).

Accumulative landforms shaped through glacial movement in this study site are moraines (see **Table 1** in the theory section in **2.1.3**). The oldest moraines visible in the relief are from the late Pleistocene, probably from the cooler period of the Younger Dryas and are approx. 11'700 years old (Marthaler et al., 2008; Swisstopo, 2024g). They were mapped according to the descriptions by Marthaler et al. (2008), the Geological Atlas of Switzerland resp. the data set GeoCover on map.geo.admin (Swisstopo, 2024g; Swisstopo, n.d.). Dikau and Otto (2004) however, did not map these ridges as moraines but rather as just a crest (DE: Kamm) in their geomorphological map in a scale of 1:25'000. As there is a consensus on the ice having reached the upper part of the hanging valleys during the LGM (Dikau et al., 2019 and authors of the Turtmann Valley as seen in **Table 2**) and there was a cold period during the Younger Dryas, these ridges could be moraines of the hanging glaciers or also of the main valley glacier. It is possible that Dikau and Otto (2004) did decide differently because of these moraine ridges not having a high relevance to their study over the whole Turtmann Valley. Additionally, they did not mention anything about old moraine ridges at all in their study. Thus, the decision was made to follow the mapping of Swisstopo (2024g) and Marthaler et al., (2008) for moraine ridges of the Late Pleistocene.

Other moraines from the Late Pleistocene and Holocene are making up some of the rock glaciers in the Turtmann Valley (Dikau et al., 2019). In the Piipjitelli, moraine ridges can build up inactive and active rock glaciers (Kenner, 2018). Although rock glaciers can be also built up by debris from gravitational processes (see **5.1.3**). These moraine

ridges integrated as rock glacier ridges are mostly moraines from the maximum extent of the LIA or younger if the rock glacier is still active (Messenzehl et al., 2018; Roer and Nyenhuis, 2007).

It is visible in **Figure 18** in **4.2** that the Turtmanngletscher reached the valley shoulders of the main U-valley during the LIA. The enormous lateral moraines on the eastern and western side near the current position of the glacier tongue as well as the eastern lateral moraine ridges studied by Eichel (2016) and Eichel et al. (2013) were probably shaped through the ice extent of the Turtmanngletscher and later on Brunegggletscher, before and during the LIA (see **Figure 42**). These moraines with a big height are not solely made through the glacier at its extent during the maximum extent of the LIA but also through various advances before, as seen in the schematic **Figure 41** from Le Roy et al. (2024). However, the frontal moraines of the Early and Middle Holocene are usually not that easily distinguishable in the valley floor because the glacier advances in the Late Holocene during the LIA often have overridden the previous deposits (Le Roy et al., 2024). Therefore, these moraine ridges are mapped as "LIA moraines" because this time period showed the maximum extent in the Turtmann Valley during the Little Ice Age (see **5.2.2**). Even though the composite lateral moraines are made of material from the Holocene and Pleistocene.

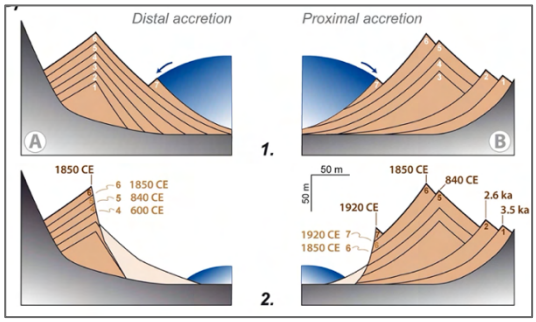

FIGURE 41 THE FORMATION OF LATERAL MORAINES HAPPENS OVER MANY GLACIER ADVANCES. (A) THE FORMATION OF A LATERAL MORAINE RIDGE MADE THROUGH DISTAL ACCRETION AND (B) PROXIMAL ACCRETION. FOR BOTH CASES THE FIRST IMAGE SHOWS THE SITUATION WHEN THE GLACIER ICE IS ADVANCING AND IN THE SECOND IMAGE WHEN THE GLACIER RETREATED. A MORAINE RIDGE OR A SEQUENCE OF MORAINE RIDGES CAN THUS BE MADE OF MATERIAL OF DIFFERENT YEARS (FROM LE ROY ET AL., 2024).

The location of the frontal "LIA" moraine, which is subject of the research objectives, is seen in **Figure 19** and **Figure 43**. The 1850 frontal and lateral "LIA" moraine ridges both act as hiking paths in that area. The moraines made of glacier retreat and advance since the maximum extent of the Turtmanngletscher during the LIA are discussed in the synthesis together with the findings from the dendrochronological data (see **5.4**). Younger moraines than the ones formed during the LIA extent around 1850 are mostly found in the valley floor in the Turtmann Valley and are presented and discussed in the sections on glacier extent and glaciation in the Turtmann Valley (see **4.2** and **5.2**). The mapping and determination of the time of the glacier advance was done mostly during the mapping process of the geomorphological mapping of the moraines. The orthophotos as well as the historic map were the first source combining the glacier data and the observable moraine ridges. Furthermore, the studies done in the Turtmann Valley (see **Table 2**) helped in the decision-making process. The proglacial area with the very visible frontal moraine of the 1980s (mapped as the 1984) has been described thoroughly by van der Meer (1997) and is analysed in **5.2.2**. An overview of the focus site can be found in **Figure 43** and **Figure 19**. The link between the glacier movement, dendrochronological data and the geomorphological map is further discussed in the synthesis in **5.4**.

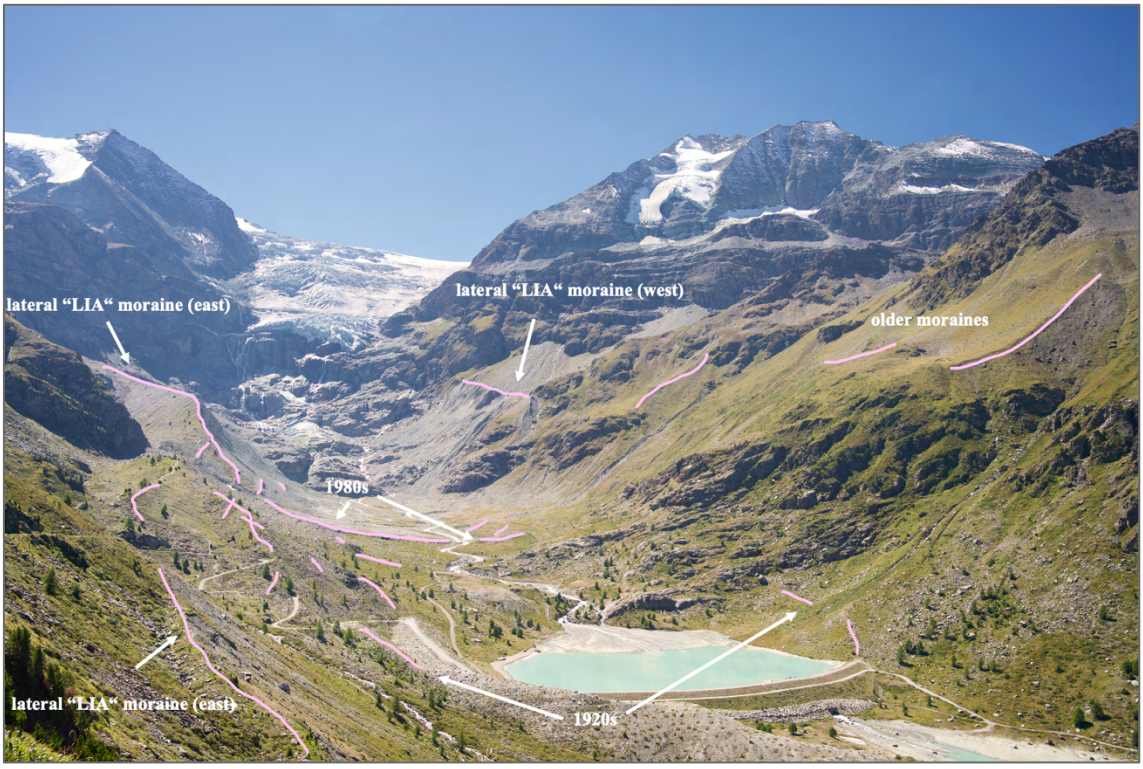

FIGURE 42 OVERVIEW OF THE FLUVIAL PLAIN JUST SOUTH OF THE SMALLER HYDROPOWER RESERVOIR AND NORTH OF THE POSITION OF THE GLACIER TONGUE OF THE TURTMANNGLETSCHER. DIFFERENT MORAINES ARE MAPPED IN THE IMAGE. (ARIANE DIETH, 2023).

FIGURE 43 OVERVIEW OF FOCUS SITE WITH THE MAPPED MORAINES AFTER THE LIA EXTENT (ARIANE DIETH, 2023).

5.1.3 Periglacial process domain and morphological landforms

The mapping of the periglacial process domain was mostly based on the permafrost and ground ice map (PGIM) by Kenner et al. (2019), the orthophoto from 2020 (Swisstopo, 2024a) and multiple studies done in the hanging valley of the Turtmann Valley (Dikau et al., 2019; Gärtner-Roer et al., 2013; Kenner, 2018; Messenzehl 2017 and 2018; Roer and Nyenhuis, 2007; van Tatenhove and Dikau, 1990). Areas influenced by periglacial processes are usually found on northern exposed slopes and in elevations up from c. 2'350 m a.s.l. A characteristic for the mapped areas is the ground temperature of ≤ 0° (Dikau et al., 2019) which is represented by the zone 1 of the PGIM (Kenner et al., 2019) as different morphological landforms made by periglacial processes are influenced by ground ice or a ground temperature of below zero degrees. The zone 2 of the PGIM is defined as the areas that might be categorised as permafrost because of the occurrence of excess ground ice but is outside of zone 1. These areas represent where ice or snow is buried and exists as ground ice such as ice-rich talus slopes or rock glaciers. Hence, zone 2 of the PGIM (Kenner et al., 2019) was also used to determine the periglacial process domain.

Classifications and characterisations of landforms in the periglacial process domain such as rock glaciers, solifluction and gelifluction lobes and others vary between scientists. In recent years more knowledge is known about rock glaciers and the conditions for them to exist. However, the distinguishment between different lobate landforms only from an orthophoto is difficult without knowledge on what process drives the shaping of the ground to a lobate landform. In this thesis multiple lobate landforms that belong to the periglacial process domains were observed through orthophotos (Swisstopo, 2024a and 2024b), the digital elevation model (Swisstopo, 2017) and during the second field campaign. Nevertheless, the mapping of these lobate landforms for the whole study area of the main valley floor and all the hanging valleys would extent the scope of this thesis in its detail and therefore, only periglacial landforms with widths bigger than 10 metres were mapped. Still, the differentiation between lobate landforms to make decisions on inclusion of landforms into the map had to be made.

Matsuoko et al. (2005) distinguishes the lobate landforms in alpine settings into four subgroups. They are differentiated according to their length, width, riser height and to their origin. The boulder rock glacier (BRG) has open work boulders in sizes up to 10 m in diameter and occur mostly below rock walls whereas the pebbly rock glacier (PRG) consists of pebbles and finer material and usually occurs as bulging of a talus slope. Solifluction lobes get differentiated between low and high solifluction lobes. They distinguish themselves morphologically by the hight of the rise due to diurnal frost action or only seasonal frost action, with a higher rise in seasonal movement. The main difference between solifluction lobes and PRGs is that they usually occur on slopes without the headwall-talus. However, there are some solifluction lobes that can form on upper talus slopes where fine debris dominates the surface. The biggest characteristic of solifluction lobes is that they are mostly affected by freeze-thaw action in the upper layers of the ground whereas rock glaciers are connected to permafrost (Matsuoko et al., 2005).

Solifluction lobes can also be differentiated between stone-banked and turf-banked solifluction lobes. Turf-banked solifluction lobes are characterised by the vegetation cover on the ridge whereas stone-banked solifluction lobes are occurring in scree slopes (Dikau et al., 2019: 448; Eichel, 2017; Kellerer-Pirklbauer, 2018). In previous studies on the Turtmann Valley, turf-banked solifluction lobes were mostly found in altitudes between 2'300 and 2'900 m a.s.l. and the stone-banked solifluction lobes in altitudes up to 3'400 m a.s.l. (Dikau et al. 2019). Stone-banked as well as turf-banked solifluction lobes together with vegetation growth were studied in detail by Eichel (2017) for the main valley floor at the location of the lateral "LIA" moraines.

In this thesis, stone-banked solifluction lobes together with the PRGs characterised by Matsuoko et al. (2005) characterised lobate landforms called pebbly rock glacier were put together in one category called "unbound lobe"

because the distinguishment cannot be made if there is no certain monitoring on freeze-thaw-cycles or certain knowledge about the presence of permafrost. Although the PGIM by Kenner et al. (2019) exists, it is just a model. The exact mapping in detail of lobes in the hanging valleys, where they mostly occur, is not that crucial for the study site and the research objectives. Hence, the multiple existing small solifluction and gelifluction lobes were not mapped but observations from the field campaign helped in deciding in categorising the relief into gravitational or periglacial process domain. Additionally, studies such as by Kellerer-Pirklbauer (2018) were used for comparison of landforms classified in the periglacial process domain in other site to the ones found in the southern Turtmann Valley. Areas that clearly showed lobate landforms and were in the zone 1 of the PGIM (Kenner et al., 2019), were usually mapped as periglacial process domain. In the zone 2 of the PGIM the areas were analysed on the occurrence of lobate landforms that could indicate ground ice or permafrost. Additionally, as described by Messenzehl et al. (2018) or van Tatenhove and Dikau (1990), north-exposed slopes and also northeast and northwest are more likely to have permafrost or ground ice due to less solar radiation. Hence, they are often mapped as periglacial process domain in this thesis. For instance, the small periglacial area on the upper Wängernalp is between a lot of gravitational slopes with talus scree but has lobate landforms categorised as "unbound lobes" visible in **Figure 44-A** and **-B**. Another example is shown in **Figure 45-A** and **-B** where "bound lobes" with vegetation cover have been identified which occur often in the southern Turtmann Valley. However, this area is mapped as glacio-gravitational because they are more stable and less likely to have permafrost or deep ice in the ground as it is visible by the vegetation cover (Dikau et al., 2019; Eichel, 2017; Messenzehl, 2018).

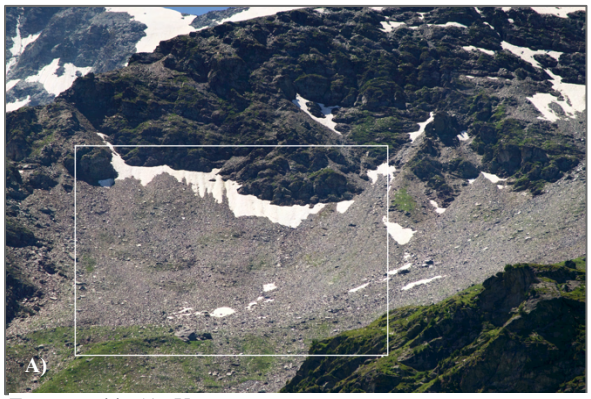

FIGURE 44 A) UNBOUND LOBATE LANDFORMS BETWEEN WÄNGERHORN AND WÄNGERALP ON A NORTHERN-EXPOSED SLOPE (ARIANE DIETH, 29.07.2024).

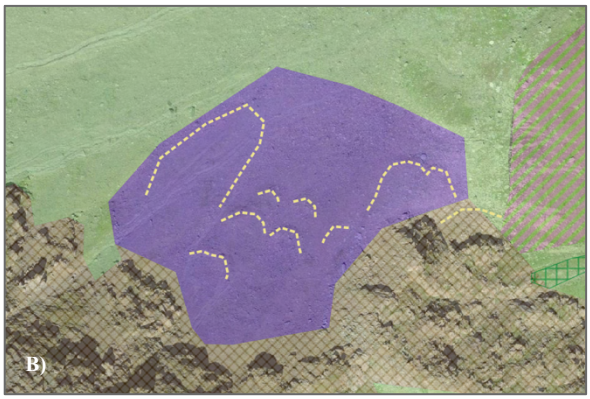

44 B) THE LOBATE LANDFORMS WERE MAPPED AS UNBOUND AND IN A PERIGLACIAL PROCESS DOMAIN.

FIGURE 45 A) BOUND LOBATE LANDFORMS COVERED WITH VEGETATION ON PIPIJALP (ARIANE DIETH, 30.07.2024).

45 B) THE BOUND LOBATE LANDFORMS ARE LOCATED IN A GLACIO-GRAVITATIONAL PROCESS DOMAIN.

Differentiation between relict, inactive and active rock glacier is difficult without knowledge of the kinematics (Roer and Nyenhuis, 2007). As this was not in the extent of the master thesis, previous studies and findings of the Turtmann Valley had to be taken as sources for the geomorphological mapping and categorising of the landforms considered to be rock glaciers. The study by Roer and Nyenhuis (2007) provided some insights into the differences of morphogeometry of rock glaciers in the eastern hanging valleys of the Turtmann Valley. Their approach with geomorphological mapping for the Piipjitelli was considered for this master thesis. As Messenzehl et al. (2018) also studied these eastern hanging valleys, their map of sediment storage landforms (modified map of Otto et al., 2009) was used to decide on the periglacial landform mapping in this master thesis. Furthermore, was the base map as usual GeoCover (Bearth, 1980; Marthaler et al., 2008; Swisstopo, 2024g). The geomorphological map in 1:25'000 by Otto and Dikau (2004) was used as a base for the geomorphological mapping and decisions as well. As the spatial resolution is smaller, it was only partially used whereas the other mentioned studies helped distinguish periglacial landforms in more detail. Therefore, most of the mapping of active, inactive as well as relic rock glaciers was a copying combined by critically thinking. For instance, the rock glacier in the Piipjitelli (see **Figure 46**) has had some discussions on which part is active, inactive or even relict (Roer and Nyenhuis, 2007). Often, vegetation cover is a sign for a relict rock glacier as well as a concave shape in the centre of the whole rock glacier which would be a sign of the middle has become devoid of ice. Thus, the part of the rock glacier with vegetation would be mapped as relict accordingly to the methodology in this thesis where the study site is mapped by visible signs in the orthophoto (see **3.2**). However, in the case of this particular rock glacier, there was a study done on the kinematics and thus, it was mapped accordingly to the findings (Roer and Nyenhuis, 2007). Hence, in the far-left corner of **Figure 46**, the part of the rock glacier with vegetation cover and a concave shape is mapped as inactive rather than relict. The PGIM shows that the whole rock glacier is mostly modelled in zone 2 (Kenner et al., 2019).

FIGURE 46 OVERVIEW OF THE ROCK GLACIERS IN THE PIIPJITELLI WITH SOME INACTIVE AND ACTIVE PARTS. THE FURTHER BACK INTO THE VALLEY, THE MORE ACTIVE THE ROCK GLACIER IS, AS IT WAS FORMED THROUGH MORAINES AND BURIED GROUND ICE FROM THE RETREATING PIIPJIGLETSCHER. THE ROCK GLACIER ON THE RIGHT IN THE IMAGE IS FED MOSTLY THROUGH ROCK FALLS FROM THE STEEP MOUNTAIN FLANK OF THE BARRWANG AND RETREATING GLACIER ICE OF THAT HAS NOT BEEN CONNECTED TO THE PIIPJIGLETSCHER SINCE APPROX. THE 1940S (SWISSTOPO, 2024D; ARIANE DIETH, 2024).

Some examples of mapped relict, inactive and active rock glaciers are shown in **Figure 47** to **Figure 49**. The inactive rock glaciers lobes in **Figure 47-A** and **-B** are at locations of PGIM zone 2 which means that there is a probability of local ground ice and conditions for ice to be in the blocks of this talus slope which is a precondition for rock glaciers to form (Kenner et al., 2019). However, the vegetation is a sign for no or little ice which would indicate that the rock glacier is inactive or might be even relict (Dikau et al., 2019; Roer and Nyenhuis, 2007). Also Otto and Dikau (2004) mapped these landforms as inactive rock glaciers. In the Geological Atlas of Switzerland (Swisstopo, 2024g) these landforms as well as the inactive part of the rock glacier in **Figure 46** or the protalus ramparts in **Figure 51** are mapped as "Schneehaldenmoräne" (DE) (Swisstopo, 2024g). It is not clear from the explanations by Marthaler et al. (2008) and Bearth (1980) what the distinction is based on. Therefore, the PGIM (Kenner et al., 2019) was used for decisions as well as the literature mentioned in **Table 2** in **3.2.2**. In **Figure 47-B** (not visible in the photo **Figure 47-B**), the relict rock glacier was not mapped by Otto and Dikau (2004) but is identified as such in the Geological Atlas of Switzerland (Swisstopo, 2024g) as well as in the orthophoto for this thesis (Swisstopo, 2024a). As these landforms in **Figure 47** are all exposed to the East, they might have a lot of sunlight contradictory to the categorisation by Messenzehl et al. (2018) or Dikau et al. (2019) that periglacial landforms are built on northern, north-eastern or north-western exposed slopes form. However, the shadow of the mountain in the afternoon might be keeping the ground conditions cool, especially in winter where also snow patches lead to the built up of ice in the ground (Colucci et al., 2016; Dikau et al., 2019).

Figure 48 shows multiple lobate landforms in the northern-exposed slopes. Snow patches that cool the ground are visible in **Figure 48-A** in late July during the second field campaign in the summer 2024. In multiple orthophotos the lobate landforms were visible, and the clear bulges indicate that these can be names small rock glaciers. The probability is high that there is ground ice or even permafrost (PGIM in the yellow zone 1 which means 1° - 0°C; Kenner et al., 2019).

The mapped rock glacier in **Figure 49** is clearly a relict rock glacier because there is a lot of vegetation cover and the concave shape of the centre of the rock glacier indicates the slump of the middle debris after ice has melted (Roer and Nyenhuis, 2007). It is also mapped in Otto and Dikau (2004) and in the GeoCover (Swisstopo, 2024g) as a relict rock glacier, hence, the identification of this landform as a relict rock glacier is confirmed.

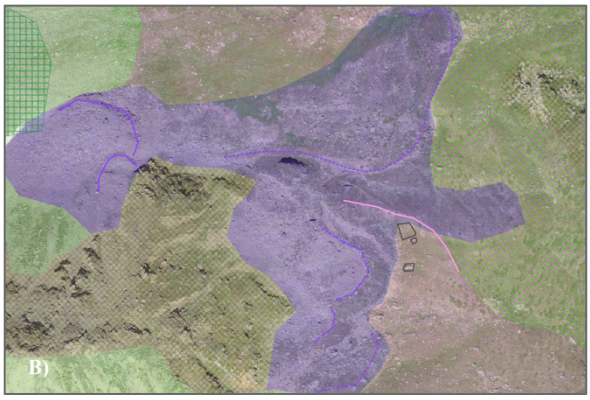

FIGURE 47 A) THE TWO HALF-MOON-SHAPED LANDFORMS ARE MAPPED AS INACTIVE ROCK GLACIERS (ARIANE DIETH, 30.07.2024).

47 B) AN OVERVIEW OF A RELICT (DOTTED LINE), INACTIVE (DASHED LINE) AND ACTIVE (NORMAL LINE) ROCK GLACIERS.

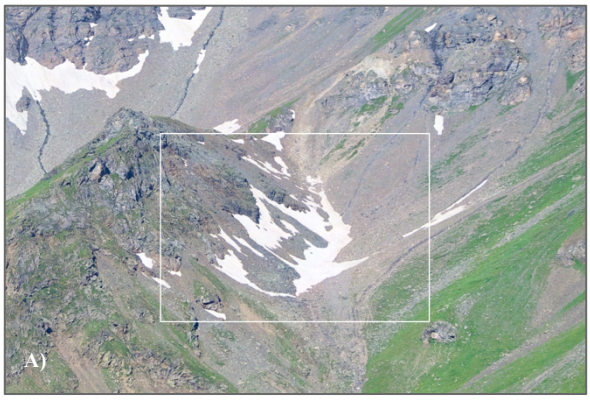

FIGURE 48 A) LANDFORMS OF LOBATE SHAPE CONSIDERED AS ROCK GLACIERS ARE COVERED BY SNOW (ARIANE DIETH, 30.07.2024).

48 B) PEBBLY LOBATE LANDFORMS WERE MAPPED AS ROCK GLACIERS IN THE SENSE OF PEBBLY ROCK GLACIERS (MATSUOKO ET AL., 2005).

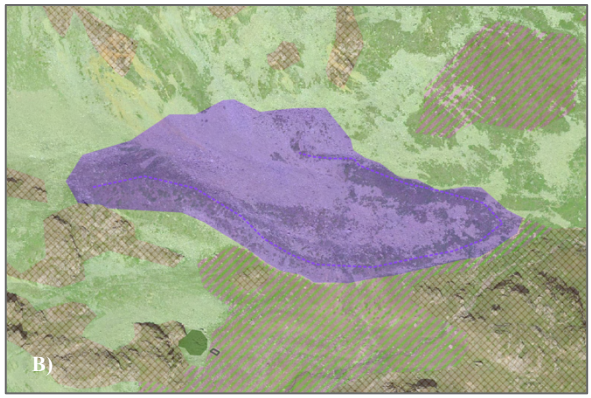

FIGURE 49 A) A RELICT ROCK GLACIER ON THE EAST-EXPOSED SLOPE ON THE WESTERN PART OF THE STUDY SITE (ARIANE DIETH, 29.07.2024).

49 B) THE RELICT ROCK GLACIER IS MAPPED AS PERIGLACIAL PROCESS DOMAIN

A protalus rampart is another morphological landform in the periglacial process domain that was mapped in this master thesis. Matsuoko et al. (2005) do not distinguish the morphological periglacial landform protalus rampart from a rock glacier and these landforms could be considered in their study to be a pebbly rock glacier. Also, in some countries and for some scientists, a protalus rampart is categorised as an embryonic rock glacier (Colucci et al., 2016; Dikau et al., 2019; Harrison et al., 2008). However, in this master thesis where the periglacial landforms are not the focus, the protalus rampart is defined simply as a ridge or rampart consisting of sediment such as pebbles and boulders underneath a slope with rock falls and with its direction crosswise to the slope direction (Dikau et al., 2019; Harrison et al., 2008). There is sometimes also the differentiation between pronival and protalus rampart in literature. The pronival rampart forms due to there being a snow patch in the slope, whereas the protalus rampart also might form if there is ground ice and not only snow (Colucci et al., 2016). In this master thesis, no monitoring of the winter and spring months and of snow patches was made, thus the differentiation is not made, and it is assumed that a protalus rampart also forms due to snow patches. Some of these mapped landforms in the Turtmann Valley are visible **Figure 50** and **Figure 51**. In both cases the protalus ramparts are on southern-exposed slopes. According to Roer and Nyenhui (2007), Dikau et al. (2019) and Harrison et al. (2008), the relict rock glaciers and thus, ground without continuous ice is usually found on these sun-exposed slopes. In the PGIM there is also no or almost no zone mapped and therefore, there is probably no to little ice content in the ground. However, the lobate landforms and the remaining snow patches visible in multiple orthophotos which are usually taken in June (Swisstopo, 2024a and 2024b) as well as observations during the field campaign, provide signs of periglacial lobate landforms. Hence, the probability might be high that the local ground temperature is around zero, and protalus ramparts form in these conditions as mapped in the geomorphological analysis.
Nevertheless, the differentiation between the landforms of the periglacial process domain can only be made as assumption. Without further knowledge and data on ground temperature, ground ice content and existence of permafrost, there is no certain way to categorise these landforms. Often, the border between periglacial and gravitational process domain remains unclear in these cases.

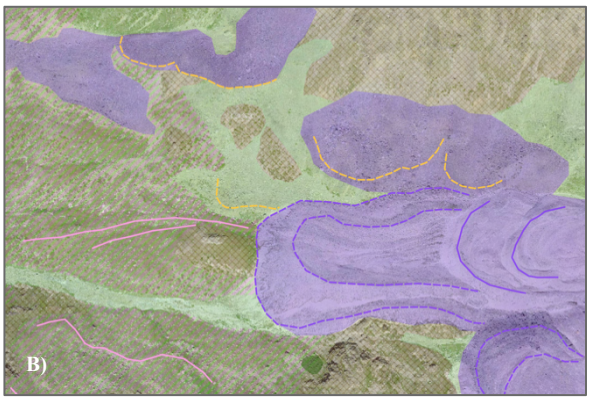

FIGURE 50 A) MULTIPLE PROTALUS RAMPARTS AROUND THE INACTIVE ROCK GLACIER IN PIIPJITELLI. (ARIANE DIETH, 30.07.2024).

50 B) THE PROTALUS RAMPARTS ARE MAPPED IN THE PERIGLACIAL PROCESS DOMAIN.

FIGURE 51 A) TWO PROTALUS RAMPARTS ON SOUTHERN-EXPOSED SLOPES IN THE FRILITÄLLI (ARIANE DIETH, 29.07.2024).

51 B) THE PROTALUS RAMPARTS ARE MAPPED IN THE PERIGLACIAL PROCESS DOMAIN AS SNOW STAYS LONGER THERE AND THERE COULD BE GROUND ICE.

5.1.4 Gravitational process domain and morphological landforms

In the main valley floor, the topography is predominantly shaped by glacial processes or glacio-gravitational interactions, particularly where gravitational deposits are present (explanations in **5.1.2**). The area north of the frontal "LIA" moraine in the focus site is largely devoid of trees likely due to frequent gravitational processes. Studies have shown that the entire Turtmann Valley is highly influenced by avalanches with a history of multiple events impacting the area (Dikau et al., 2019). This is particularly relevant for the tree-free area in the study site where avalanche activity is probably a significant geomorphological factor. The presence of landslide deposits and recurring gravitational processes in the Turtmann Valley has been studied by Otto et al. (2009) and Messenzehl et al. (2018).

A large landslide deposit is also evident in the relief (Swisstopo, 2017) as indicated by small streams and gullies that have developed around it (see **Figure 52**). A gully has formed on top of the landslide suggesting that the landslide is older, and the gully developed more recently. This chronological distinction between the features is important because it demonstrates the ongoing reshaping of the landscape by both older gravitational processes and newer fluvial activity (Swisstopo, 2024a and 2024g).

Just north of this deposit is an additional area mapped as a landslide that could also have originally been a debris flow which has since become an avalanche path (see **Figure 53**). Characteristics typical of a debris flow such as an onset point, a narrow path, and cone-shaped deposits at the valley floor are visible. The deposits may have temporarily blocked the Turtmänna river as it is observed by its current looping flow around the conical deposits (Swisstopo, 2017). Although no recent debris flows are clearly visible, the lighter coloured rocks in the deposit area suggests that new material continues to be delivered through the gully. The hypothesis that it might be an avalanche path in the current time is proven in the aerial images of 1980 and 1946 with snow patches visible in the deposit area (Swisstopo, 2024b and 2024c).

On the western side of the Turtmänna, a landslide of similar size to the one described above is visible (see **Figure 54**). While the Geological Atlas of Switzerland does not map this feature as a cone-shaped deposit, the relief reveals a distinct conical shape (Swisstopo, 2017 and 2024g). This feature was therefore mapped as a landslide in this thesis supported by both the morphology and field evidence. Up on the slope there is a distinctive rockfall deposit which was also mapped because it forms a prominent field of rocks in a previously glaciated area. Just south of this landslide another cone-shaped tree-free area suggests that frequent avalanches shape the landscape here and it is mapped as a landslide/avalanche zone. In the same area, alluvial fan deposits formed by streams are also visible. While these are influenced by gravitational processes, they are primarily classified under the fluvial process domain due to the active role of stream deposition in shaping the alluvial fans (see **5.1.5**).

The influence of the gravitational processes on the landscape as well as the establishment of vegetation such as *L. decidua* Mills. in the focus site will be discussed in the synthesis in **5.4**.

Small grass erosions such as studied by Geitner et al. (2021) are signs for gravitational process. As they are very small and do not shape the relief massively but rather the surface, the area with these erosional landforms were not mapped as gravitational but often as glacio-gravitational. However, these small erosional patches can still have an impact because they hinder stabilistation of the slope through preventing vegetation to grow. Additionally, the shallow erosion landslides and patches are highly influenced by rainwater which is slightly increasing with climate change and thus, there could be a higher importance of shallow erosion on mountain slopes in the future (Geitner et al., 2021).

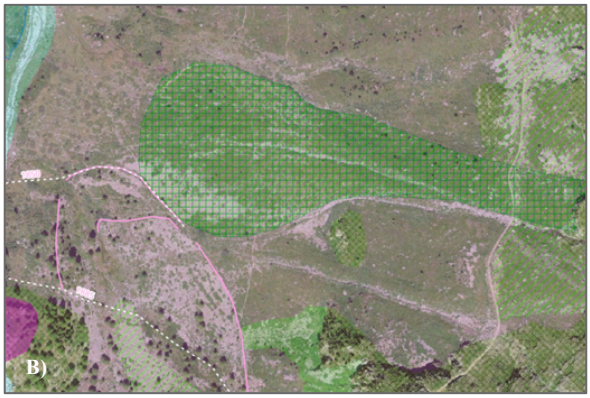

FIGURE 52 A) THE MOSTLY TREE-FREE ARE NORTH OF THE FRONTAL "LIA" MORAINE (ARIANE DIETH, 29.07.2024).

52 B) THE AREA WAS MAPPED AS A LANDSLIDE AS IT IS VISIBLE IN THE RELIEF.

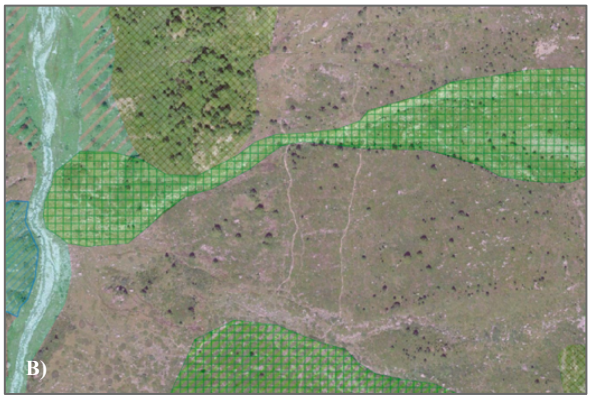

FIGURE 53 A) THE LANDSLIDE / DEBRIS FLOW IS VISIBLE WITH ITS ONSET POINTS, PATH AND THE DEPOSIT (ARIANE DIETH, 30.07.2024.

53 B) THE AREA WAS MAPPED AS A LANDSLIDE AS DEBRIS FLOWS ARE ALSO PARTS OF THE CATEGORY "LANDSLIDE" AND THE DEPOSITS ARE CLEARLY VISIBLE IN THE RELIEF.

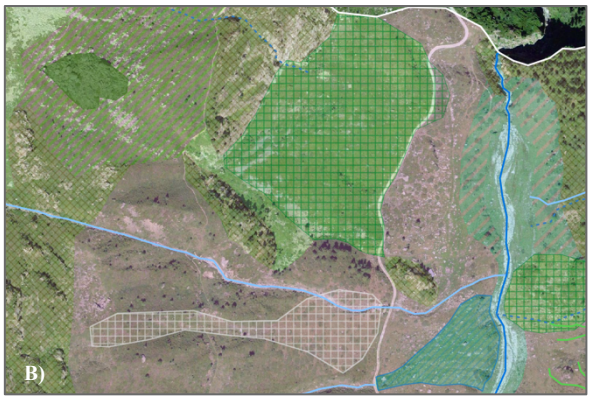

FIGURE 54 A) AN ALLUVIAL FAN, CONIC SHAPED TREE-FREE AREA AND A CONIC SHAPED LANDSLIDE RELIEF ARE VISIBLE (ARIANE DIETH, 29.07.2024).

54 B) THERE ARE MULTIPLE LANDFORMS OF THE GRAVITATIONAL AS WELL AS FLUVIAL PROCESS DOMAIN MAPPED.

Slopes with little to no vegetation cover where scree or other gravitational features such as debris flow onset points are present have been classified within the gravitational process domain provided there is no indication of permafrost or periglacial landforms. If evidence of periglacial processes is absent, these slopes are categorised based on gravitational activity alone. For instance, **Figure 55** shows a situation where the mostly eastern-exposed slope is mapped as gravitational process domain whereas the area with lobate landforms are mapped as periglacial process domain (see discussion about **Figure 44** in **5.1.3**). According to Messenzehl et al. (2018) and Harrison et al. (2008), slopes with a southern and eastern aspect are mostly free of ground ice and thus, these areas of talus scree are mostly mapped as gravitational process domain in this thesis. Most of the gravitational process domains are located in the hanging valleys (see **Figure 15** in **4.1**) where steep topography dominates. Conical-shaped deposits are typically formed through the accumulation of scree and were mapped as individual polygons and labeled "talus cones" (see **Figure 56**). In contrast, broader slopes covered with talus and rock deposits, referred to as "talus slopes", were not mapped as separate polygons as their distribution is widespread across the hanging valleys and below steep slopes. Instead, these areas were integrated directly into the gravitational process domain (**Figure 57**). Furthermore, periglacial processes such as frost creep or permafrost degradation may contribute to the ongoing movement of material downslope and thus, destabilising the landscape (Phillips et al., 2020). In this highly dynamic environment with previous and ongoing deglaciation occurring, scree and rocks falling off many slopes and mountain flanks present being hazards and slow down the establishment of vegetation (Dikau et al., 2019; Gärtner-Roer et al., 2022). The correlation between the periglacial and gravitational process domain is mostly discussed in the section of the periglacial process domain in **5.1.3**.

Next to periglacial processes, fluvial processes also influence the gravitational process domain. Seasonally dependent meltwater of snow or ice continue to reshape the gravitational deposits. High water content can destabilise debris masses and might cause debris flows or other mass movements (Phillips et al., 2020). In a bigger scale, the formation of gullies might lead to erosion further preventing the process of stabilisation. These gullies channel water flow around or through older landslide debris and thus, might also disturb the vegetation succession (Eichel, 2017; Geitner et al., 2021).

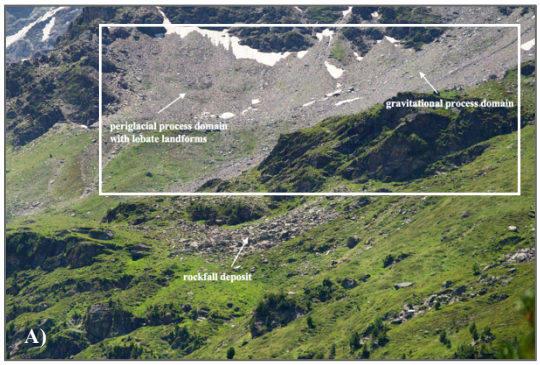

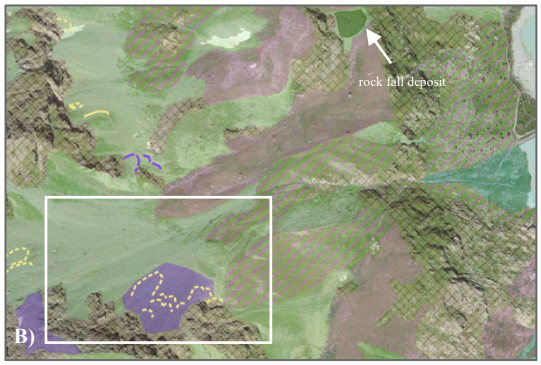

FIGURE 55 A) AN EXAMPLE OF PERIGLACIAL AND GRAVITATIONAL PROCESS DOMAIN ON THE SAME SLOPE. IN THE FOREGROUND THERE ARE SOME ROCKFALL DEPOSITS (ARIANE DIETH, 29.07.2024).

55 B) THE AREA WITH LOBES IS MAPPED AS PERIGLACIAL PROCESS DOMAIN NEXT TO AN OTHERWISE GRAVITATIONAL PROCESS DOMAIN.

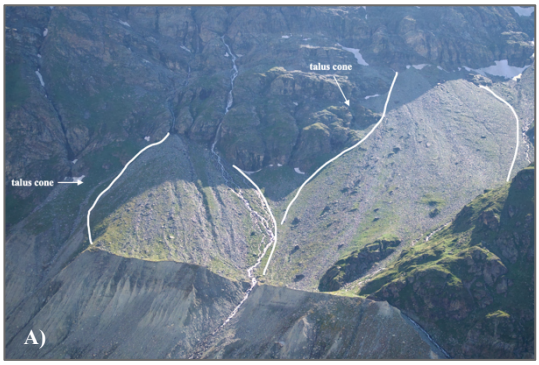

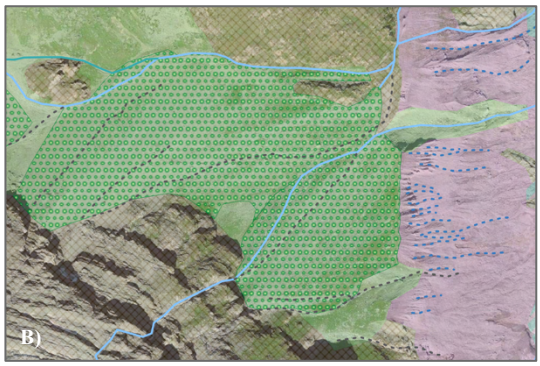

FIGURE 56 A) TWO TALUS CONES OUTSIDE OF THE LATERAL "LIA" MORAINE (ARIANE DIETH, 29.07.2024).

56 B) THERE ARE MULTIPLE LANDFORMS OF THE GRAVITATIONAL AS WELL AS FLUVIAL PROCESS DOMAIN MAPPED.

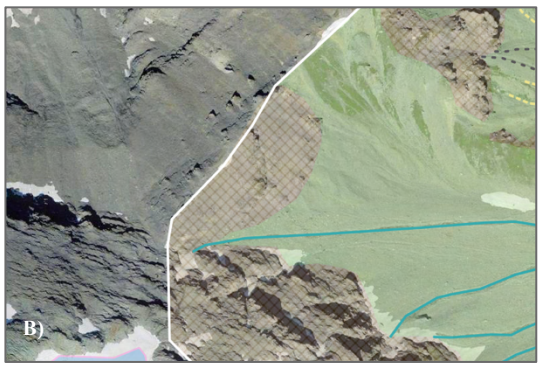

FIGURE 57 A) THE TALUS SLOPE COVERS A LOT OF AREA IN THE INNERS WÄNGERTÄLLI (ARIANE DIETH, 30.07.2024).

57 B) THE TALUS SLOPES ARE MAPPED AS JUST GRAVITATIONAL PROCESS DOMAIN.

5.1.5 Fluvial process domain and morphological landforms

The fluvial process domain in the study area is small compared to the other process domains. This is because in most cases other geomorphic processes have a greater influence on shaping the relief and the fluvial processer are often combined with other processes or occurring on top of other landforms such as landslides (see **5.1.4**). However, in key areas such as the immediate proglacial zone where the braided fluvial system lies, and around the main river, the Turtmänna, fluvial processes dominate and the surface is mapped as such. The Turtmänna is the primary fluvial stream of the Turtmann Valley having in its catchment meltwater from both the Brunegg- and Turtmannglетscher and streams and meltwater in various hanging valleys in the study site. This water first flows into the two hydropower reservoirs with the bigger northern lake called Turtmannsee. However, due to a pressure tunnel diverting water to the Val d'Anniviers for energy production, the natural discharge of the Turtmänna is reduced during electricity generation periods (Gougra AG, n.d.).

The Turtmänna's role as the lake's outlet and the presence of a dam influence the hydrological regime downstream. During heavy rainfall, the spillway is opened to prevent dam overflow, and in autumn, the lake is drained through the normal drainage into the gorge to clear sediment deposits (see **Figure 58** and **Figure 60**). Strong water flows after and during storms prevent vegetation growth at the spillway's outlet with water pressure and erosion inhibiting soil development and washing away young vegetation. Nevertheless, some larch trees have persisted in this otherwise barren area (see **Figure 59**). The gorge through which the Turtmänna flows is hypothesised to have formed through both fluvial erosion during interglacial periods and subglacial meltwater erosion during glaciations similar to other gorges in Switzerland. However, the erosion of these gorges is still discussed in literature (Dikau et al., 2019; Steinemann et al., 2021).

FIGURE 58 THE OPEN SPILLWAYS AT THE TURTMANNSEE AFTER HEAVY RAINFALLS ON THE 21ST OF AUGUST 2024 (THE SCREENSHOT OF THE WEBCAM WAS TAKEN AT 13:50).

FIGURE 59 THE BARREN ROCK WHERE THE WATER OF THE SPILLWAYS GOES THROUGH (ARIANE DIETH, 2024).

FIGURE 60 THE WATER-DRAINED LAKE IN OCTOBER 2023 (ARIANE DIETH, 03.10.2023).

Several deltas in the study area have been mapped as part of the fluvial process domain. The changing path of the streams and the paraglacial adjustment of lateral moraines influence the landscape. Sediments are deposited through these fluvial streams which receive their sediment input from the glacier tongue, hanging valley and slope debris caused by gravitational and fluvial processes (Dikau et al., 2019; Messenzehl et al., 2018). A prominent delta is located at the outlet of the Piipjitelli rock glacier, where the meltwater from both the Piipjigletscher and rock glacier contributes to the sedimentation (Eichel, 2017). This stream has been present already in the Dufour map covering the mid- to late-19th century (Swisstopo, 2024d). Other significant deltas can be found to the east of the Turtmannsee or between the lake and the smaller, southern hydropower reservoir. The largest delta forms a glaciofluvial outwash plain south of the southern reservoir (Dikau et al., 2019).

In the proglacial area near the glacier terminus the surface is characterised by a braided fluvial system that deposits glaciofluvial sediments. This area was mapped as fluvial rather than glaciofluvial process domain despite the till-dominated sedimentation. The ever-changing braided streams (see **Figure 61-A** to **Figure 61-C**) constantly re-shape the landscape creating new channels and pathways for water flow (van der Meer, 1997). Areas covered with vegetation in the orthophoto of 2020 (Swisstopo, 2024a) were mapped as glaciofluvial suggesting that these streams have not recently disturbed the landscape (Dikau et al., 2019). The change in this area is also documented by van der Meer (1997) and coincides with the glacier extents (see **5.2.2**). The ongoing fluvial erosion of glacial till and accumulation in a proglacial area cause the build-up of fluvial terraces (for instance in **Figure 62** and **Figure 63**). In the study of Marchese et al. (2017) it was found that rivers in a previously glaciated area experienced a narrowing after the LIA due to greater runoff and less sedimentation. Therefore, a widening of the river happens when a glacier is stagnant or advancing. This could have been the cause in the Early Holocene for the formation of the terraces north of the frontal "LIA" moraine in the focus site, mapped as fluvial and glacio-fluvial process domain in **Figure 15** in **4.1**. Some incisions in the plain of old river paths are visible in **Figure 62**. In contrast, the terrace in front of the Brunegggletscher has developed through incision of the river in the glacial basal till in the 1930s/1940s when the Brunegggletscher detached itself from the Turtmanngletscher and retreated (see the discussion on glacier extents in **5.2.2)**. The clear incision in the bed is visible in **Figure 63** for the proglacial area of the Brunegggletscher. Historic aerial images as well as the depth of the incision suggest that the erosion has already happened subglacially and later through a high amount of meltwaters during the glacier retreat. The glacial till must have been fine enough for an incision of this depth to occur (Dikau et al., 2019, Marchese et al., 2017).

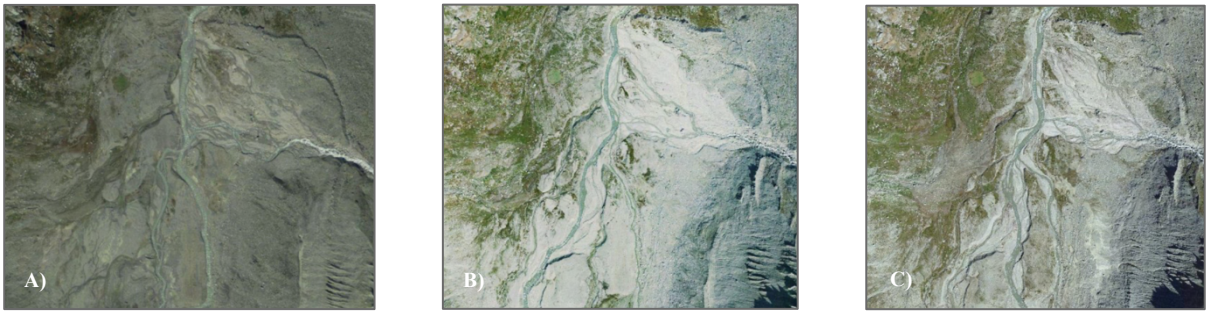

FIGURE 61 A) THE SITUATION OF THE FLUVIAL PLAIN IN THE YEAR 2008, **B)** IN THE YEAR 2017 AND **C)** IN THE YEAR 2024.

FIGURE 62 THE OLD PATHS OF THE TURTMÄNNA ARE VISIBLE AS INCISIONS IN THE FLUVIAL TERRACE. SOME TERRACE STEPS ARE ALSO VISIBLE (ARIANE DIETH, 04.10.2023).

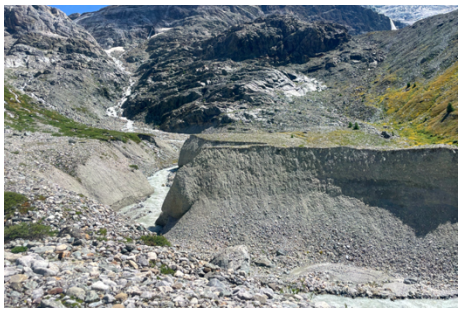

FIGURE 63 A HUGE OUTCROP OF THE GROUND BASAL TILL MADE BY A FLUVIAL INCISION AND EROSION AFTER THE RETREAT OF THE BRUNEGGGLETSCHER IN THE 1940S (ARIANE DIETH, 29.07.2024).

In this master thesis in the geomorphological map, streams are distinguished from rivers primarily based on their size and their connection to the reservoirs or glaciers. Major streams including the Turtmänna (mapped in dark blue in **Figure 14**) represent their significant role in transporting water between glaciers and lakes. The Turtmänna drains from the Turtmannsee northward toward the Rhône valley. Smaller streams (light blue line in **Figure 14**) are defined in this master thesis to have continuous channels within the aerial image of 2020 visible water flow (Swisstopo 2024a). Otto and Dikau (2004) and Eichel et al. (2013) have also mapped these streams to have a year-round activity. The hydrological map from swissTML3D further validated the presence and course of these streams (Swisstopo, 2024f).

Gullies are differentiated from streams in this master thesis and are categorised into three types: active gullies, dry gullies and moraine gullies. Per definition of Dikau et al. (2019: 234) a gully is a channel that is built through erosion with surface water (Deline et al., 2021). Surface soil is eroded into narrow linear hollow forms through strongly converged surface runoff. For the erosion to happen, water availability is crucial. "Active gullies" are characterised by seasonal water flow driven by snowmelt, ground ice melt or rainfall. Despite no visible water in the past and current aerial images (Swisstopo, 2024a and 2024b), active erosion is likely ongoing in these areas. Without having a possibility to have a monitoring system such as discharge measurement instruments at each gully, the only option to decide if active fluvial erosion is happening in the gully, is to check on past orthophotos. Thus, the identification of active gullies relied on a combination of orthophoto analysis and hydrological data from swissTML3D which classifies such features as "dry channels" (DE: Trockenrinne") that can occasionally carry water after rainfall or during melt seasons (Swisstopo, 2024f). However, Swisstopo (2024f) only distinguishes in this dataset between a dry channel (DE: "Trockenrinne") and a stream (DE: "Fliessgewässer") whereas the stream is defined to be at least 100 m long and has during most of the year a water flow. The dry channel in the swissTML3D is defined to be able to have a water flow after a heavy rain event or during melting season (Swisstopo, 2024f). Thus, in this master thesis the differentiation between a dry gully and an active gully is more detailed than by Swisstopo (2024f) but mostly based on past orthophotos (Swisstopo, 2024b).

Active gullies (turqoise lines in **Figure 14**) influenced by snowmelt are easier to detect than those formed by meltwater from ground ice or permafrost. In this thesis, the presence of snow patches was identified through the analysis of orthophotos spanning multiple years (Swisstopo, 20224b). Several assumptions were made about snowmelt availability based on the approximate number and thickness of snow patches by visual observation. More meltwater is likely to be available on north-facing slopes which receive less solar radiation as well as in shaded areas where snowmelt is slower (Dikau et al., 2019). Snow accumulation is also greater in hollows or flatter areas where thick snow cover is easier to develop. In higher elevations, colder temperatures further contribute to greater snow patches. Additionally, on permafrost ground snow tends to persist longer due to reduced ground heat flux from long-wave radiation (Kenner et al., 2019).

The mapped category "dry gully" (dotted dark grey lines in **Figure 14**) shows no signs of active water flow in either previous or current aerial images (Swisstopo, 2024a and 2024b). The absence of vegetation recovery suggests the gully may still be relatively young and occasionally has water flow capable of causing further gully erosion (Deline et al., 2021; Eichel, 2017). This justifies its classification as a dry gully rather than being disregarded.

"Moraine gully" (dotted dark blue lines in **Figure 14**) is a specific category mapped in the lateral moraines of the proglacial area. These gullies have been shaped by the deglaciation process and ongoing erosion. The process of gullying can occur due to frost weathering, surface wash, wind ablation, debris fall and avalanche with the most

probable cause in the lateral “LIA” moraine in the Turtmann Valley being a mix of frost weathering and surface wash (Deline et al., 2021). This erosion in the lateral moraines creates inter-gully walls which are very prominent ridge-like landforms in the moraines visible in **Figure 64** (Eichel, 2017: 39).

The mapped category “slope water” refers to small streams originating from moist grounds on the slopes. Although the exact sources of these streams are uncertain, they are hypothesised to originate from underground water given the moisture and vegetation present at these sites. No mapped water sources exist in the study area according to the online Geoportal of Canton Valais (Canton Valais, n.d.). However, one water source is mapped in the Geological Atlas of Switzerland (Swisstopo, 2024g) and has been used as a reference for identifying similar areas across the study site (Marthaler et al., 2008). This area is characterised as wet and with more vegetation making it a model for mapping other similar areas in this master thesis (see **Figure 65**). The geomorphological map of this master thesis excluded the supraglacial fluvial system on top of the Turtmanngletscher and Brunegggletscher. The exception are two small supraglacial streams mapped at the glacier terminus of the Turtmanngletscher on the dead ice that is disconnected from the glacier ice. Subglacial fluvial systems were also excluded due to a lack of monitoring data. Additionally, the waterfalls at the current glacier tongue are mapped and visible in the field (see **Figure 64**).

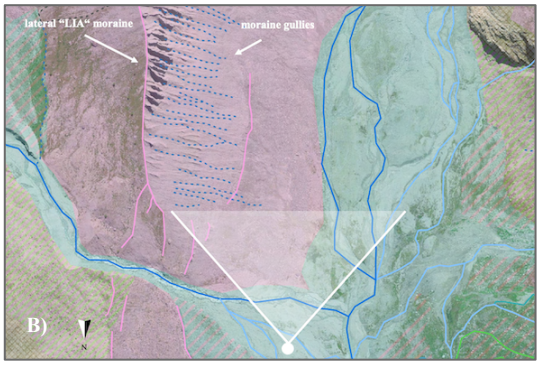

FIGURE 64 IN THE PROGLACIAL AREA THE LATERAL MORAINE OF THE LIA TOGETHER WITH THE “MORAINE GULLIES” ARE VISIBLE (ARIANE DIETH, 30.07.2024).

64 B) IN THE GEOMORPHOLOGICAL MAP, THE GLACIAL AND FLUVIAL PROCESS DOMAIN ARE MAPPED.

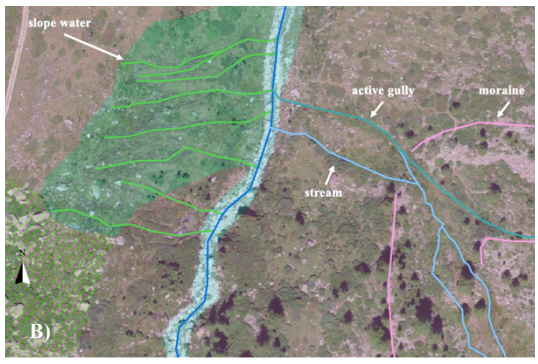

FIGURE 65 THE MAPPED “SLOPE WATER” LINEAR LANDFORM IN THE FLUVIAL DOMAIN IS SHOWN (ARIANE DIETH, 29.07.2024).

65 B) WEST OF THE TURTMÄNNA, THE WATER STREAMS ARE IN THE CATEGORY “SLOPE WATER”.

Lacustrine landforms are minimal in the study site limited to a few smaller lakes and the two big hydropower lakes. Notably one lake lies within the glacier forefield of the Turtmanngletscher while two others are located in the forefield of the Brunegggletscher. The surrounding landscape of these smaller lakes is mapped as lacustrine process domain. In contrast, the land surface around the two hydropower reservoirs was mapped as anthropogenic process domains because the lakes were constructed and therefore, the lake shores were not naturally made.

5.1.6 Anthropogenic process domain and morphological landforms

The most prominent anthropogenic landforms in the proglacial area of the Turtmann Valley are the two hydropower reservoirs. The Turtmannsee was constructed in 1958 while exact construction of the smaller reservoir could not be determined (Gougra, n.d.). Nevertheless, the lake must have been built between 1971 and 1978 as it is visible in the aerial images (Swisstopo, 2024b). The construction of these lakes offers an indication of when the Turtmanngletscher retreated from this area (see the discussion in **5.2** and in **5.4**). Other than the two reservoirs, the southern Turtmann Valley is relatively free from anthropogenic influence especially when compared to neighbouring valleys such as the Val d'Anniviers and the Matter valley, both of which feature more settlements and ski infrastructure. A reason for no ski infrastructure in the Turtmann Valley are especially the frequent avalanches that prevent people to venture into the valley during winter. Until the mid-19th century, the valley floor of the Turtmann Valley contained only sporadic wooden huts and barns. Later in the early 20th century small residential houses were built in nearby settlements such as Kleebodi, Gruben, Meiden, and Blumatt, though these lie outside the study site. These settlements have since developed modestly and are attracting some tourism for hiking and climbing (Meyer, 1923; CAS Section Prévôtoise, n.d.).

Smaller mapped anthropogenic features within the study area include the remains of alpine pasture settlements. These ruins were identified through orthophoto observations and fieldwork (see **Figure 14** in the resulted geomorphological map and some examples in **Figure 66** to **Figure 68**). Certain confirmation of their use as alpine pastures could only be made by consulting historical records and local knowledge. However, due to the scope of this thesis, no interviews were conducted, and interpretations rely on literature reviews such as Meyer (1923). This could be a source of making wrong assumptions as the names of past pastures are not existent in current maps or might have changed or have a different spelling. The ruins mapped in this thesis are interpreted as seasonal settlements used by shepherds during the summer months. The Alpine pasture use for sheep farming in the southern Turtmann Valley dates to the 1500s (Meyer, 1923). On the eastern side of the valley notable features include on the Emser sheep alp the ruins of the Piipjialp, visible in the aerial image of 2020 (Swisstopo, 2024a) and confirmed during fieldwork (see **Figure 66**). In addition, Holustei, once a shelter for shepherds, now hosts a chapel and two private huts. On the western slopes of the valley, further ruins were discovered including those attributed to the sheep alps Wengerstafel (**Figure 66** and **Figure 68**), Karlostafel, and Frilistafel (referred to as Frilys in **Figure 67**).

In the valley floor near the Turtmänna stream there is a former ore washing facility that once operated to process materials from the mines located on the ridge between Frilitälli and Blüomattälli. This facility was destroyed by an avalanche, leading to the abandonment of both the mines and the area in 1898 (Meyer, 1923). Another anthropogenic feature is the SAC Turtmannhut which was constructed in 1928 (CAS Section Prévôtoise, n.d.). The development of the cable car between Turtmann and Oberems along with the construction of the Turtmannsee dam and new roads in the 1950s has since made the area more accessible to tourists (Walliser Bote, 2003).

Meyer (1923) provides a detailed description of the anthropogenic history of the Turtmann Valley tracing human activity from the Middle Ages to the early 20th century. It is illustrated how humans have continuously ventured into this challenging environment despite harsh conditions marked by frequent avalanches, landslides and cold temperatures, and despite ice masses reaching into the main valley floor. Multiple hiking paths on moraine ridges and in areas with frequent rock falls in the area between the frontal "LIA" moraine and the Turtmanngletscher as well as fixed rope routes around the Brunegggletscher show how the southern Turtmann Valley is used by humans today (Swisstopo, 2024e).

FIGURE 66 THE RUINS OF THE PIIPJIALP ARE VISIBLE IN THE FOREGROUND OF THE IMAGE AND THE RUINS OF THE WENGERALP ON THE OTHER SIDE OF THE VALLEY (ARIANE DIETH, 30.07.2024).

66 B) THE RUINS OF PIPJIALP ARE VISIBLE IN THE ORTHOPHOTO OF 2020. THE NAME "PIIPJI" IN THE MAP LK25 OF THE AREA HELPS IDENTIFYING THE RUINS.

FIGURE 67 THE HYPOTHESIZED RUINS OF FRILYS WHICH WAS THE SUMMER SEAT OF A SHEEP PASTURE (ARIANE DIETH, 29.07.2024).

67 B) MULTIPLE SQUARE-SHAPED ROCK FORMATIONS WERE CONCLUDED TO BE REMNANTS OF THE FRILISTAFEL.

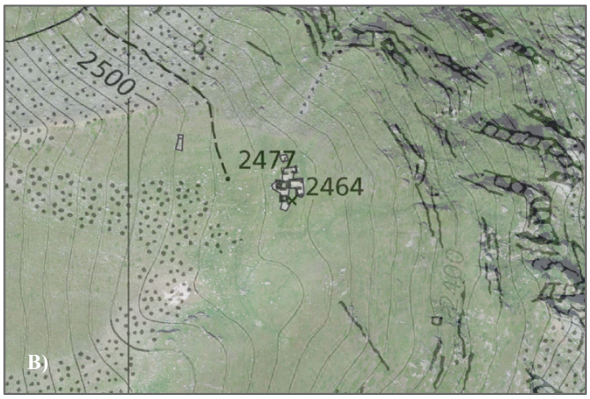

FIGURE 68 THE REMNANTS OF WENGERALP (ALSO CALLED WENGERSTAFEL) ARE VERY CLEARLY VISIBLE FROM A DISTANCE (ARIANE DIETH, 30.07.2024).

68 B) IN THE LK25 AS WELL AS THE ORTHOPHOTO OF 2020, THE WENGERSTAFEL IS MAPPED AND VISIBLE.

5.1.7 Bedrock as a process domain

The areas not mapped under any specific process domains primarily consist of exposed rock surfaces or mountain flanks. While Dikau and Otto (2004) classified these areas as “denudative”, in this master thesis it was not chosen to follow this approach. Their approach summarised some slope aquatic, gravitational, periglacial (e.g. solifluction) and some aeolian processes together in one undefined group. As the aim was to map multiple processes which are all important in a detailed geomorphologic analysis of the Southern Turtmann Valley, the new process domain “bedrock” was chosen. It emphasizes the exposed bedrock and outcrops of the ground rock without mixing them into the same category of the existing process domains. Roche moutonnées were mapped as bedrock even though their classification as glacial landforms are indicated in a separate landform polygon layer (see **Figure 17**).
The areas mapped as "bedrock" were selected based on their dominant relief and geological characteristics. These outcrops are subject to both chemical and physical weathering as well as processes associated with deglaciation. When glaciers retreat, the loss of their buttressing effect can increase instability along mountain flanks leading to more rockfalls and other mass movements (Deline et al., 2021; Dikau et al., 2019). However, this mapped domain exclusively accounts for processes of erosion and weathering as it represents areas without significant sediment accumulation or deposition. These are predominantly steep slopes or exposed bedrock outcrops in a previously glaciated valley mostly being devoid of glacial till deposits such as it was mapped extensively for the southern Turtmann Valley (Deline et al., 2021).
An alternative approach, as seen in the work of Eichel et al. (2013) could have been to leave these areas blank on the geomorphological map. However, to maintain a comprehensive representation of the landscape and its process domains, it was deemed crucial to map the exposed rock surfaces as bedrock and not leave it blank. This decision ensured the inclusion of all geomorphological features, preserving the intended mosaic of process domains across the study area.
The lithologies were purposely not taken into account while mapping to not overload the whole geomorphological map. However, the type of rocks can play a role in erosion and shaping the landscape (Theler et al., 2010).

While the geomorphological mapping of the Turtmann Valley has provided crucial insights into the landscape's evolution, several factors contribute to uncertainties in the mapping process. The complexity of this dynamic post-glacial environment combined with limitations in data resolution, seasonal variations and the challenges of interpreting geomorphological features from aerial imagery and historic maps introduces potential inaccuracies. The following section will explore these uncertainties, focusing on data sources, mapping techniques and the interpretation process.

5.1.8 Uncertainties of geomorphological mapping

Data Quality and Availability

Firstly, data quality and availability play a significant role in shaping the uncertainties in this study. One source of uncertainty is the timing of the aerial images used. The orthophotos are captured during the summer months and provide high-resolution and mostly snow-free imagery that is ideal for surface analysis (Swisstopo, 2024a). However, the seasonal aspect means that some geomorphological features such as seasonal streams may be missed leading to incomplete representations of certain processes. In addition, some past orthophotos show some snow cover which can obscure landforms and the surface that needs to be mapped (Swisstopo, 2024b). The data from the digital terrain model was not fully available in high resolution for the focus site which might have prevented observing some landforms (Swisstopo, 2017). Additionally, the lack of long-term monitoring data for the landscape and the geomorphology limits the study and thus, contributing to the overall uncertainties in mapping.

Mapping process and decision making

Secondly, the mapping process and decision-making also introduce uncertainties particularly because there are multiple ways to categorise and represent geomorphological features. In this thesis, a hierarchical approach was adopted following established mapping procedures like Eichel (2017), Otto and Dikau (2004) and Montgomery (1999). However, geomorphological mapping is interpretative and there is no singular, universally accepted method for classifying landforms. For example, the border where glacial processes end and fluvial processes begin can be subjective and influenced by the mapper's perspective. Additionally, process domains such as glacial, periglacial and fluvial are highly dynamic. Different categorisations could lead to different map outcomes and thus, potentially affecting the interpretation of the landscape (Couper, 2022; Otto and Dikau, 2004).

The decision to map a mosaic of process domains was made to create a comprehensive categorisation of the entire study area similar to the Geological atlas of Switzerland (Swisstopo, 2024g). By layering polygons and lines representing geomorphological landforms over the process domain mosaic, the analysis provided a thorough depiction of the proglacial area and its surrounding landscape including features that could influence the valley floor. However, due to the selected scale, mapping of some smaller landforms was discarded as capturing them in greater detail would have overreached the scope of this thesis.

Interpretation bias

Lastly, interpretation bias is another significant source of uncertainty. As discussed in section **2.1.2**, "reading the landscape" (Brierley et al., 2021) is influenced by prior knowledge, personal experience, and theoretical frameworks which can lead to confirmation bias. Through previous courses with the University of Zurich, the ETH Zürich and an exchange semester at the Norwegian University of Sciences and Technology (NTNU) a wide bandwidth of methods, techniques and concepts by different teachers could be obtained fostering critical thinking. Throughout the thesis, multiple hypotheses and drafts of the geomorphological map were developed to minimise bias (Alden, 2019; Couper, 2022). Field validation helped confirm or discard certain interpretations. But only a portion of the landscape could be directly assessed and thus, it had to be relayed on available remote sensing data (Swisstopo 2024a to 2024i). Despite a systematic approach and literature review, cognitive biases may have influenced the identification of features potentially leading to an overemphasis on certain processes. This highlights the need for validating interpretations and remaining open to alternative hypotheses during the mapping process (Couper, 2022).

5.2 Glaciation in the southern Turtmann Valley

5.2.1 Before the maximum extent of the LIA

During the Pleistocene, the Turtmann Valley was shaped by the Turtmanngletscher which converged into the Rhône Valley with the Rhônegletscher along with other glaciers. At the peak of the last glaciation, the Last Glacial Maximum (LGM), the ice surface reached elevations of up to 2'600 metres a.s.l. in the main valley and glaciers also occupied 15 hanging valleys (Dikau et al., 2019; Marthaler et al., 2008). According to glacier extent maps from the LGM (Bini et al., 2009), the ice covered nearly all of the mountain flanks, leaving only peaks above 2800 metres a.s.l. emerging as nunataks.

Following the LGM at approx. 18'000 years ago, a warming climate initiated widespread glacial retreat across Switzerland (Le Roy et al., 2024). Moraines mapped in the area attributed to the late Pleistocene/Early Holocene (see **Figure 69** and labeled moraine ridges in **Figure 42**) may belong to the Younger Dryas (Egesen stade) around the cold period with glacier advances in 11'700 to 10'300 years ago (Marthaler, 2008; Swisstopo, 2024g). Without precise dating of these landforms previous research as well as features in the landscape provide clues for interpretation. A key indicator is, that Early Holocene moraines are often found 150 to 200 metres downslope from "LIA moraines" (Le Roy et al., 2024). However, this trend may not fully apply to the hanging valleys as "LIA" moraines are often obscured by gravitational processes and the extent of glaciers in these valleys is unclear. Moraines identified by Marthaler et al., (2008) and Swisstopo (2024g) in the Augsttälli region in the northern Turtmann Valley outside of the study site suggest that in the hanging valley in the southern Turtmann Valley similar processes occurred due to the similarity in their morphology and position compared to the main valley. Therefore, the extent of the glaciers during the Younger Dryas could be derived from similar looking ridges as observed in the orthophoto (Swisstopo, 2024a).

During the Holocene, glacial advances in the Alps were mostly not greater than the maximum extent of the LIA. Thus, moraine ridges between the Younger Dryas and the maximum advance of LIA could be destroyed. However, as mentioned in **5.1.2**, the composite lateral "LIA" moraine are most likely older than just the maximum extent of the LIA in 1850. Relative age assumptions can be derived from examining the orientation of the ridges and determining which moraine cuts across another (see **Figure 70**). Since there are no direct dating data for these pre-LIA moraine ridges and no maps of this time period, these interpretations remain as assumptions (Dikau et al., 2019; Eichel, 2017; Le Roy et al., 2024).

As the glaciers continued to retreat into the Holocene, the landscape underwent significant transformations. These visible morphological landforms in the southern Turtmann Valley culminated in the LIA and shows a period marked by renewed glacier advances. The moraine ridges that dominate the current geomorphology in the proglacial area in the study site largely date from this era and assist in understanding the glacier dynamics during and after the LIA.

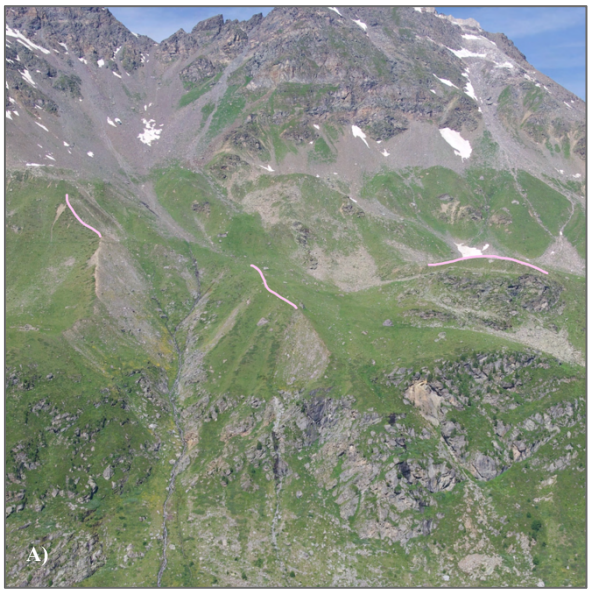

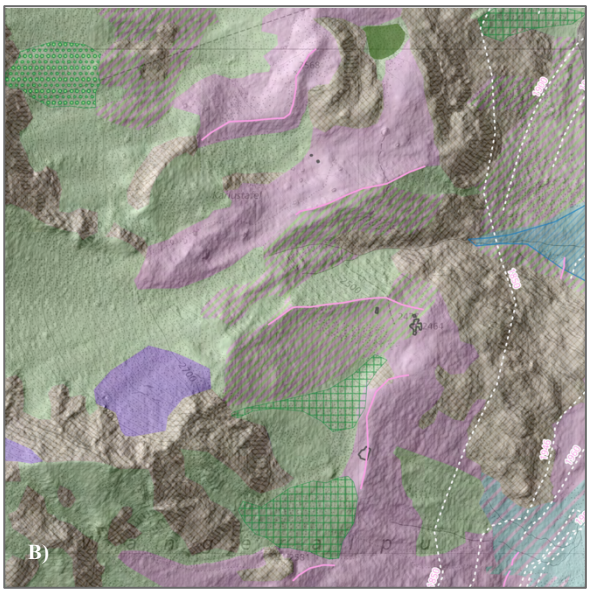

FIGURE 69 A) DIFFERENT RIDGES IN THE LANDSCAPE (COLOURED IN ROSE) ARE IDENTIFIED AS MORAINE RIDGES OF THE LATE PLEISTOCENE/ EARLY HOLOCENE (ARIANE DIETH, 30.07.2024).

69 B) THE MORAINE RIDGES OF THE LATE PLEISTOCENE/EARLY HOLOCENE ARE VISIBLE IN THE SHADED RELIEF AND WERE MOSTLY MAPPED IN THE GLACIAL OR GLACIO-GRAVITATIONAL PROCESS DOMAIN.

FIGURE 70 A) MORAINE RIDGES IN THE MAIN VALLEY FLOOR ARE MAPPED IN THE COLOUR ROSE AND MULTIPLE RIDGES CROSSING OTHER MORAINES ARE VISIBLE (ARIANE DIETH, 30.07.2024).

70 B) DIFFERENT AGED RIDGES CROSS THE MORAINE RIDGES WHICH GIVES A CLUE OF DIFFERENT GLACIER ADVANCES.

5.2.2 During the LIA and after the maximum extent of the LIA

During the Little Ice Age (LIA) the climatic conditions turned colder and in some parts of the Alps there was more precipitation, both causing glacial advances. These glacier advances of the LIA occurred during the Late Holocene between the mid-14th century and the mid-19th century (Le Roy et al., 2024). In the southern Turtmann Valley, the Turtmanngletscher like many other alpine glaciers reached its most prominent size during the LIA in the 19th century advancing down the valley and reshaping the landscape (Eichel, 2017; Reinthaler, 2024; Zemp et al., 2008). In some parts of the Alps, the glaciers have reached their maximum LIA extent around the 1820s and reached this extent again around the 1850s (Ivy-Ochs et al., 2009). This advance is seen in the evident frontal moraine and the huge lateral moraines in the Turtmann Valley in the field as well as the aerial images (Swisstopo, 2024a). They are mapped as frontal "LIA" moraine and lateral "LIA" moraines (see resulted map in **Figure 14** or a photo in **Figure 43**). The moraine ridges created during this time form some of the most prominent geomorphological features in the valley today. As temperatures rose after the LIA, glaciers began to shrink rapidly leading to a retreat that has continued save for some exceptions into the present day. This chapter examines the extent of the Turtmanngletscher during its LIA maximum, the moraine deposits formed and the following post-LIA retreat.

The frontal "LIA" moraine in the north of the focus site, where the tree samples were taken, is particularly distinct and described by several studies (Eichel, 2017; Marthaler, 2008; Otto and Dikau, 2004; Dikau et al., 2019; Swisstopo, 2024g). However, the Dufour map (Swisstopo, 2024h) shows the glacier tongue approx. 240 metres further south, indicating a possible discrepancy. This could result from the map being produced after the LIA glacier maximum or from inaccuracies due to the remote location and limited accessibility of the valley. With an error margin of 153 to 780 metres in the Dufour map (see **5.2.3**), this highlights the challenges of using historical maps compared to geomorphological evidence. The glacier retreat recorded and documented in GLAMOS data are supporting that the Dufour map shows an inaccurate extent (see **4.2**; GLAMOS, 1881-2023). Thus, mapping based on geomorphological interpretation is preferred in this study over the Dufour map (Swisstopo, 2024h).

Glacier extent mapping from other periods as shown in **Figure 19** and **Figure 20** largely draws from the works of Eichel et al. (2013), Eichel (2017), van der Meer (1997) and Dikau et al. (2019). Moraine positions reflect glacier advances, and both field mapping and aerial imagery analysis were essential for this study (Swisstopo, 2024a, 2024b). In periods without substantial literature or imagery, GLAMOS data provided validation for glacier extents (GLAMOS, 1881-2023). Following the LIA maximum, there were three advance periods in the Alps around 1890, in the 1920s and in the 1980s (Le Roy et al., 2024; Wanner et al., 2022; Zemp et al., 2008). In some regions, glaciers have advanced or stayed stagnate, in both cases of the 1920s and 1980s, moraines could build up (Le Roy et al., 2024). However, while GLAMOS data indicates a significant retreat of 290 metres from the first measurement of the Turtmanngletscher in 1887 to 1900, no notable advance occurred around 1890 for the Turtmanngletscher. Despite limited data from this period, a small moraine ridge observed in the field may correspond to this time (see **Figure 19** in the results and **Figure 69**). This small ridge could indicate the 1890s advance and therefore, the mapping of the glacial extents from 1850 and 1900 in this thesis can be trusted to some extent.

For the 1920s advance (see Eichel, 2017; Le Roy et al., 2024), while no precisely dated moraine exists in the study site, a lateral moraine ridge along the valley's east side might represent this advance. On the west side, two ridges could also correspond to this period. The moraine ridges on the East could be identified as the 1920s moraine when the Turtmanngletscher was mostly stagnate or slightly retreating (Eichel, 2017). **Figure 35-C** shows a photograph taken before 1923 with a lot of moraine material visible at the glacier tongue (Meyer, 1923). However, the exact dating for the moraines is not available together with historic maps or aerial images between the years 1892 of the

Siegfried map and 1946 of the "US flight mission" (Swisstopo, 2024c and 2024i) causing difficulties in glacial extent mapping. Therefore, the glacial extent mapping is more robust from the year 1946 on when the aerial image of the "US flight mission" (Swisstopo, 2024c) and the more regular updates of the topographic maps as well as aerial images by Swisstopo (2024b and 2024d) are available.

Until the 1980s cooling and glacier advance, there has mostly been no advances. In the early 20th century during deglaciation and glacier retreat, the Turtmanngletscher was probably covered by substantial debris due to paraglacial adjustments (Deline et al., 2021; Le Roy et al., 2023). Thus, complicating the mapping of glacier extents and the exact timing of the Turtmanngletscher and Brunegggletscher separation. Glacier extent measurements for the Brunegggletscher start in the year 1934 (GLAMOS, 1881-2023). However, in the aerial image of 1946, the glacier tongue is visible much further back than it would be expected when measuring the distance of the position where the glaciers divide in the relief is and the 185 metres of retreat of the Brunegggletscher. There is a possibility that in the aerial image of 1946 the real position of the tongue is not visible due to debris covering the ice and that it is much further to the north than it is visible in the image. Another possibility is, that the divide happened and the retreat of the glacier arm of the Brunegggletscher has occured earlier than 1934 but it is not in records of GLAMOS. Nevertheless, looking at the overall retreat of approx. 1'400 metres of the Brunegggletscher between the years 1934 and 2021, the distance is correct (GLAMOS, 1881-2023; Swisstopo, 2024a). Therefore, the conclusion is rather that the ice was covered by debris during the flight of 1946 and in this low-quality aerial image the correct position of the glacier tongue is not visible (Swisstopo, 2024c).

Between the 1920s advance and the 1980s advance, there are some ridges visible which could account for some cooler periods where the glacier was stagnant. For instance, the as 1953 labelled moraine rigdes in **Figure 20** shows the relatively stagnant position of the Turtmanngletscher (GLAMOS, 1881-2023).

The advance of the 1980s is visible by a large moraine ridge across the valley floor which marks a boundary between the vegetated landscape to the north and the fluvial-influenced terrain to the south (see **Figure 70**). This feature developed between the 1960s and 1980s, with the 1980s advances being particularly notable due to colder temperatures and higher-than-average precipitation in 1980, 1981, and 1984 (see climate data in **4.3.1**). According to van der Meer (1997), the landscape was very dynamic with changes in meltwater channels at the glacier tongue and irregular advances on only one side of the glacier tongue. In the aerial images between 1960 and 1984, the accumulation of debris at the position of the moraine ridge labelled as "1984" in **Figure 70** and **Figure 20** is observable over the years with the end result being a push moraine made of depositional debris of the glacier over multiple years (Dikau et al., 2019; Le Roy et al., 20204; van der Meer, 1997).

The above-mentioned gap of historical maps and aerial images in the early 20th century is not the only one making it difficult observe the glacier extents and positions of the glacier tongue. For the period between the years 1993 and 2004, another gap presents a source of inaccuracy in mapping glacier extents. In 1996 as well as 1998 glacier advances of more than 50 metres occurred (GLAMOS, 1881-2023). A lateral moraine ridge was probably built on the flank of the eastern lateral "LIA" moraine near to the ground as the glacier thickness was not as high anymore as during earlier stages, as seen in the geomorphological map (**Figure 14**). The 1990s advance is not visible in all valleys in the Alps (Le Roy et al., 2024), but in the Turtmann Valley a sequence of moraine ridges south of the 1984 moraine ridge is visible which can be accounted to the 1995 and 1998 advances monitored by GLAMOS (1881-2023). Since then, the Turtmanngletscher as well as the Brunegggletscher have retrated further. In 2018 and 2020, an icefall from the Turtmanngletscher left dead ice on the valley floor (Dikau et al., 2019; Eichel, 2016; Le Roy et al., 2024. Marthaler et al., 2008; Swisstopo, 2024a to 2024g).

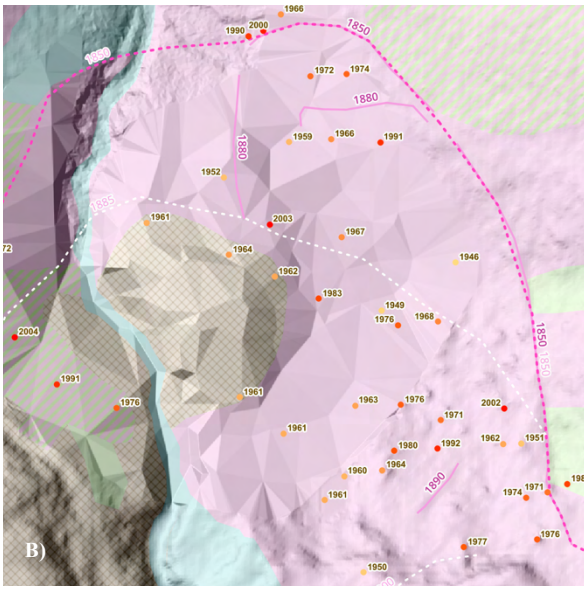

Figure 71 A) The focus site with different moraine rigdes and in the background the lateral "LIA" moraine and the moraine of the 1980s is visible (Ariane Dieth, 29.07.2024).

71 B) The glacier extent as well as the sampled trees and the moraine ridges are lain on top of the relief with the mapped process domains. It is clear that the resolution of the relief is low for the focus site.

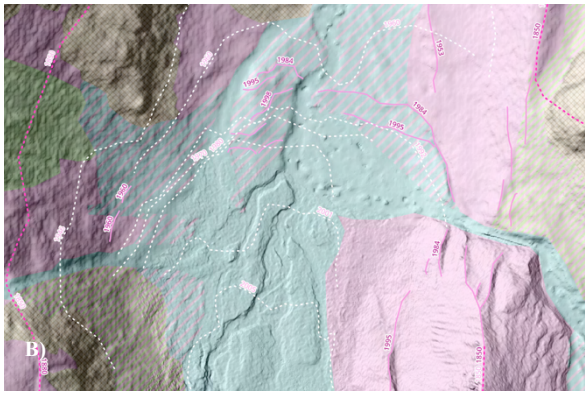

Figure 72 A) The main valley floor with the clearly visible 1980s moraine ridge (Ariane Dieth, 29.07.2024).

72 B) Different aged ridges cross the moraine ridges which gives a clue of different glacier advances.

5.2.3 Uncertainties in mapping of glacier extents

As discussed in **5.1.8,** the availability of high-quality data is crucial for accurate mapping. Historical maps and old aerial images are important for studying long-term landscape changes such as glacier changes but often suffer from lower spatial resolution and possible inaccuracies. These limitations in past datasets could affect the precision of the historical glacier extents. The earliest map available in the historic map inventory in the Geoportal of Swisstopo is the Dufour Map which was published between 1844 and 1864 (Swisstopo, n.d., 2024d and 2024h). There is no measure for the accuracy of the map because at that time the instructions just said to be "as accurate as possible". According to calculations by Swisstopo, the average positional error is approx. 153 metres, with a maximum error of 780 metres (Swisstopo, 2024h). Given that the southern Turtmann Valley is a remote and mountainous area, it is likely that the positional error exceeds the average. Consequently, the extent of the Turtmanngletscher on this map may be exaggerated due to the inaccessibility of the valley.

The Dufour Map covers the Turtmann Valley between 1854 and 1891 and is presented at a scale of 1:100'000. It was replaced by the Siegfried Map in 1892 which depicted the valley at a finer scale of 1:50'000. The intended positional accuracy of the Siegfried Map was 35 metres with a maximum allowable error of 75 metres (Swisstopo, 2024i). Thus, there might be still some inaccuracies presents.

By the 1930s, national topographic maps at a scale of 1:50'000 were introduced, followed by 1:25'000 maps in the 1950s (Swisstopo, 2024d). Over time, the accuracy of these maps improved with positional errors ranging from 1 to 15 metres for the 1:50'000 scale, and 2.5 to 7.5 metres for the 1:25'000 scale. For the Turtmann Valley, a new map at 1:25'000 became available in 1946. In the scale of 1:50'000 there are only minor changes in glacier front positions from 1892 to 1946 observable in the maps (Swisstopo, 2024d). However, this does not mean that the position of the glacier terminus did not move in these years. No maps were updated during the early 20th century in a key period of glacier retreat leaving gaps in the data since 1946 needed to track glacier extent during this time as mentioned above in **5.3.2**.

Aerial images which offer high resolution cover much of the past 70 years. However, there are gaps in coverage particularly between 1946 to 1959, 1960 to 1970, and 1993 to 2004 which could introduce inaccuracies in glacier extent mapping. While some additional topographic maps exist for the 1993 to 2004 period, the gaps in coverage may be due to the remote location of the study area and the reduced priority for regular updates (Swisstopo, 2024b and 2024d).

Although Glacier Monitoring Switzerland (GLAMOS) data are available for most of the period between the years1885 and 2018, they were used qualitatively in this thesis rather than for quantitative modelling. These data on glacier movements were useful for identifying periods when frontal and lateral moraines were formed, particularly in the absence of updated orthophotos (GLAMOS, 1881-2023). Nevertheless, more detailed temporal datasets such as historical aerial images or annual glacier movement data would have provided stronger evidence and validation for the interpretations made using orthophotos and topographic maps in this thesis.

5.3 *Dendrochronology*

5.3.1 Relationship between the growth of *L. decidua* Mill. and climate

The time series analysis of the tree-ring width (TRW) as seen in **Figure 22** in section **4.3** shows a general trend of relative stability in growth rates over the long term despite short-term variations. Theses variations in growth of *L. decidua* Mill. were analysed by comparing the raw chronology with the climatic variations visually (see **Figure 26** to **Figure 31**) and by correlation calculation of the detrended chronology with the climatic parameters R (results in **Figure 24** and **Figure 25**).

Precipitation

The correlation analysis between tree growth and precipitation reveals a generally weak relationship with a maximum negative correlation of -0.3 observed for July, as well as for the combined months of July and June, and July, June and May. This suggests that increased precipitation during these months may slightly inhibit tree growth and a decreased precipitation might lead to an increase in tree growth. Based on Moser et al. (2009) who studied the onset of growing season of *L. decidua* Mill. in the nearby Lötschental, the growing season for the Turtmann Valley has been defined to the period from June to October (see **3.1.2**). Similar to the findings on growing season of larch trees in high mountain sites of Saderi et al. (2019). The effective growing season might vary depending on temporal environmental factors that influence the onset of growth such as temperature, frost damage, assimilation of carbon, new snow (Saderi et al., 2019). Therefore, in the discussion and analysis of the relationship between tree growth and precipitation, the months June and July are especially taken into, while the month May might also influence the onset of growth as seen in the correlation analysis (**Figure 24**), and thus, May is included.

The lowest and the highest precipitation means of the months May to July are extremer than the mean annual precipitation as seen in the graphs depicted in **Figure 26** and **Figure 27** in the results in **4.3.1**. This could be a reason why some extreme measurements of precipitation might correlate negatively with tree growth for these months. Late spring and early summer precipitations combined with cooler temperatures could lead to cold soils causing physiological stress in *L. decidua* Mill. ultimately leading to a reduced tree growth, especially if there is really high amount of precipitation (Schweingruber, 1996). Additionally, precipitation during these months could fall as snow. This would potentially delay the onset of the growing season or causing frost damage to newly developing roots and shoots (Schweingruber, 1996). Furthermore, *L. decidua* Mill. is known to thrive in well-drained soils and does not require excessive water (see **3.1.4**). Excessive precipitation could lead to waterlogged soil conditions causing less oxygen content in the soil. A lack of oxygen can inhibit root respiration and thus, slowing the uptake of essential nutrients and hindering overall tree growth (Schweingruber, 1996). Considering that heavy precipitation is often accompanied by cloud cover, the reduced solar radiation during this crucial early growth period may also limit tree growth as *L. decidua* Mill. is a species that requires a lot of sunlight for optimal growth (Da Ronch et al., 2016). In addition, increased rainfall might trigger more mass movements such as landslides and debris flows which can damage or disturb trees (Gärtner and Heinrich, 2013; Schweingruber, 1996).

The precipitation peaks illustrated in **Figure 27** frequently overlap with periods of low tree growth as observed in the years 1953, 1975, 1980 and 1981, 1985, 2002, 2007 and 2008. In the other way, there might also be a weak correlation between low precipitation and high tree growth for the months May to July (**Figure 27**). There are multiple years where this is visible, namely in the 1950s in 1950, 1952 and 1954, in the 1960s in 1962 and 1964, the year 1979, in the 1980s in 1986 and 1989, in the 1990s in 1993 and 1998 and in the last twenty years in 2003, 2006 and 2009. Most of these years are however also linked to higher temperature which has a bigger influence

on tree growth as seen in the correlation analysis between temperature and tree-ring width (see **Figure 31** or section about temperature below). Because of the *L. decidua* Mill. not needing that much water availability, low precipitation might not be a too limiting factor (Da Ronch et al., 2017; Schweingruber, 1996).

The correlation between precipitation and tree growth at the study site remains weak and further research is necessary to determine whether a stronger relationship exists. Utilising more precise climate data such as that from the weather station at Turtmann Lake (MeteoSchweiz, 2024) or doing an interpolation with data of overall climate data would provide more accurate insights into the interaction between climate and tree growth in the region. However, the station at the Turtmann Lake has only had precipitation data since 2011 and was thus, not chosen for the correlation analysis with the TRW data (MeteosSchweiz, 2024). Additionally, the tree growth in the sampled forest area was observed to be more influenced by temperature than by precipitation as the correlation analysis in R showed (see **4.3.1**) and is confirmed in other studies and sites (Eichel, 2017; Körner and Hoch, 2023).

Temperature

Positive correlations were found for the summer months of May to August with values reaching as high as 0.5 for the combination of June and July together and May, June and July together (see **Figure 25**). This indicates that higher temperatures during these months enhance tree-ring growth of *L. decidua* Mill. The temperature of the early summer months is crucial for the onset of the growth of larch trees (Moser et al., 2009; Saderi et al., 2019). A higher temperature, especially in an alpine environment, leads to an earlier onset of growth which leads to a longer growing season and thus, the tree ring growth is increased (Schweingruber, 1996). At temperatures below 0°C the cambium activity slows down to protect the tree and its roots, therefore the air temperature is influential especially in the early spring where the tree is mostly growing (Saderi et al., 2019). Hence, temperature has an effect on the effective growing season and also cellular activity. Not considered in this thesis is the differences between soil temperature and mean air temperature. However, for a study of biological processes in the tree, more than just air temperature would be needed to monitor the reaction of tree-ring width growth on climate variations (Körner and Hoch, 2023).

The relationship of the mean annual temperature and TRW (**Figure 28**) is less accurate than only comparing the months that resulted out of the correlation analysis. Although, a graph for the growing season (June to October) was also analysed, the correlation analysis in R determined the air temperature of the months May to August to be positively correlated to TRW growth. Thus, figure **Figure 30** is the most representative when comparing the growth of the sampled trees and temperature and is discussed in the synthesis in **5.4**. Wider tree rings and therefore better growth is clearly coupled with a higher temperature as it is visible for the years 1964, in the 1980s in 1982, 1983 and 1986, in the 1990s in 1994, and 1998, in the last twenty years 2003, 2006, 2009 and 2015.

Narrow tree rings and thus low growth is coupled with especially colder temperatures (troughs in the chronology curve) are found in the period of 1954 to 1957, in the year 1975, around 1980 and 1981, 1987, 1996 and 1997, 2002, 2004, 2007, 2013 and 2014, and 2016. The low temperature in the beginning of the growing period probably inhibited the growth of the trees. In these early summer months, colder temperature might lead to frost damage to the trees and would not offer optimum conditions for growth to start (Schweingruber, 1996; Moser et al., 2009).

Combination of temperature and precipitation influencing tree growth

The expected increase in tree growth with high temperatures for the months of May to August combined with the low precipitation for the months of May to July is visible for the years marked green in **Table 3** in the results in **4.3.1**. The positive pointer years are 1979, 1986, 1998 and 2015. Although the temperature was not that high in 1979, 1986 and 1998, compared to the warmer temperatures in the last 20 years, the tree ring width increased significantly compared to the surrounding years. The rising temperature over the whole period is due to climate change (Le Roy et al., 2024; Zemp et al., 2008). The negative pointer years in 1975, 1980 and 1981, 1995 to 1997 and 2004 show that the cold temperature is more influential than the precipitation which is different for these pointer years.

In 1984, the tree growth is different than it would be expected. The temperature is low and precipitation is in an average range for the months of May to July resp. August. With these low conditions of temperature, less growth would be expected, but the TRW data shows a peak (see **Figure 31**). As the climate data is not from the study site, the microclimatic conditions might vary and in the study site it might have been warmer than expected. There might have also been good light availability for the larch trees to experience high growth (Schweingruber, 1996). As *L. decidua* Mill. is relatively resistant to cold temperature, it could also mean that it did not play such a big role for that specific year because there were fewer young trees starting to growth (see **Figure 23**).

The year 2010 also shows an unexpected tree growth because temperature in the months May to August was low and precipitation for the months May to July was high which both correlated with low tree-ring growth in other years observed in the study site. The sample size for the year 2010 is big with many trees already having an established age of more than 20 years old (**Figure 23**). Older trees are less sensitive to climatic changes and *L. decidua* Mill. is relatively adapted to cold temperature, thus, making the cold temperature in spring not that influential (Da Ronch et al., 2016). Older trees might have also adapted to frost accompanied by cold temperatures in the study site (Schweingruber, 1996).

The smooth chronology curve for the years 2018 to 2023 shows that there has been not a clear trend in tree-ring growth in these particular years (see **Figure 31**). No anthropogenic changes to the open forest have happened in the last twenty years as answered by the forestry department Forst Region Leuk upon request (Forst Region Leuk, 2023). Therefore, the tree-ring growth in these years as well as the age of the trees should show the natural processes of the last twenty years. With the warming of the recent years and the more extreme weather, it is possible that these trees might have reacted individually to microclimatic changes and therefore, no pattern can be observed. However, the effect of climate change on tree-ring width growth as well as on small glaciers is still an ongoing topic in studies.

Outliers

The outliers that could not be crossdated are visible in **Figure 73** to **Figure 76**. The comparison between the mean curve of the outliers and the overall chronology (**Figure 32** in **4.3.1**) shows that the outliers consistently diverged from the general trend except for some individual years (e.g. low growth in the year 1996). This suggests that these trees are not representative of the broader forest stands and further validating their exclusion from the overall chronology.

All samples of the tree L022 could not be crossdated. L022 is positioned just outside the frontal moraine which marks the glacier extent during the LIA (see **4.2**). As L023 and L024 are also at the same location but they could be crossdated to the chronology, there might not be an explanation concerning the site location. In the second field campaign all outlier trees were observed and for L022 a slight curved stem was observed (see **Figure 73**). L022 is in the ditch just outside of the moraine where water could flow through during snow melt or heavy rainfalls. It is also a ditch full of debris and rocks and it is probable that the tree is disturbed by rockfalls and ground movement which would explain the curved stem. Reaction wood can be built up when the ground is unstable and thus, the tree ring width pattern would be different (see **2.2.2**). However, there was no analysis on reaction wood and other wood anatomical characteristics done because it would go over the limit of this thesis.

In **Figure 74**, it is visible that the tree L027 shows two stems coming out of the ground at the same location. This is also the case for L006 in **Figure 76** where there are multiple stems. It could just be that there are two seeds that grew on the same spot and are now grown. Another reason which would also explain the special growth patterns could be that the trees were disturbed by an avalanche, rock avalanche or a debris flow. Thus, leading to multiple stems after injuries on the stem or the roots (Schweingruber, 1996). For L027 this is a very possible as the tree is positioned on the west and would be one of the first trees to be disturbed through a mass movement event. The ground also shows multiple rocks and in the geomorphological map (see **Figure 14**) in the region, the surrounding area is mapped as glacial-gravitational or gravitational process domain if it is not the default of glacial process domain.

However, for L006 there is more difficulties explaining the different growth pattern of the sample with the suffix -A or why there are multiple stems coming out of the same ground. The roots were not analysed in the field and therefore, there cannot be any certain conclusions. L006 might be influenced by the ground being mostly blocks of rocks and debris and by the water level of the lake. However, the lake has a spillway that helps in preventing flooding of the area (see **5.1.5**). Therefore, no further conclusions could be made from the observations that were done.

L034 has probably experienced an avalanche or other mass movement event which is visible in the sabre growth with the broken-off primary crown (see **Figure 75**). There are vertical sprouts growing from the branches that now act as the crown. This shape is sometimes also called “candelabra”-form (Schweingruber, 1996: 188). In the TRW curves it is visible that the damage to the crown happened between the growing season of 1998 and 1999 because there is a dip in the TRW curve and the sample tree L034 shows very thin tree rings in the growing season of the year 1999.

FIGURE 73 L022 IS JUST OUTSIDE OF THE FRONTAL "LIA" MORAINE IN A DITCH AND SHOWS A CURVED STEM (ARIANE DIETH, 2024).

FIGURE 74 THERE ARE TWO STEMS VISIBLE RIGHT NEXT TO EACH OTHER AND OF ONE OF THEM THE SAMPLES OF L027 WERE TAKEN (ARIANE DIETH, 2024).

FIGURE 75 THE TREE L034 LOST ITS CROWN AT SOME POINT AND HAS MULTIPLE BRANCHES ACTING AS CROWNS AND STEMS (ARIANE DIETH, 2023).

FIGURE 76 L006 HAS MULTIPLE STEMS CLOSE TO EACH OTHER SHOOTING OUT OF THE GROUND (ARIANE DIETH, 2024).

5.3.2 Age distribution *of Larix Decidua* Mill. in the Turtmann Valley

The age distribution of *Larix Decidua* Mill. (*L. decidua* Mill.) in the Turtmann Valley provides important insights into the post-glacial landscape development and ecological succession. Understanding the distribution and variation of tree ages can help interpret the timing of glacier retreat and other environmental processes at the study site. Tree growth in the focus site is influenced by several factors, including the development of soil and the time between glacier retreat and seed germination, known as the ecesis interval (Zhu et al., 2019). These factors along with geomorphic processes and local disturbances create a complex pattern of tree ages across the focus site. While this section focuses on the specific age distribution patterns of the sampled trees, the broader implications for glacier retreat and landscape evolution will be addressed in the synthesis (see the synthesis in **5.4**).

The sampled trees cover a time span from 19 to 77 years old with germination dates ranging from 2004 to 1946. The sampling method aimed to capture the oldest trees in each quadrant of the study site which resulted in few young trees being included (see the sampling strategy in **3.3.1**). Although there is some variation in ages, there is no clear chronosequence related to proximity to the glacier terminus in different periods. This lack of a simple age gradient suggests that multiple factors such as local conditions (e.g. soil, topography, disturbances) and the associated ecological succession influence establishment of a forest (see **2.2.3**; Wojcik et al., 2021).

Localised patterns of tree age do emerge with certain cohorts being found in different locations. For instance, the trees on the rampart (L019 to L021, L030 to L032, L039 to L041 and L043) are shown to have almost the same germination dates from the years 1960 to 1963. As they are located on a higher rampart (mapped as roche moutonnée in the geomorphological map in **4.1.3**), the local conditions might be different than the surrounding area. Being more exposed to sunlight, with fewer shadows cast by the topography, the rampart may provide an advantage for *L. decidua* Mill. which thrives in light-demanding environments (Saderi et al., 2019). Additionally, the trees on the rampart are likely more protected from gravitational processes such as avalanches, landslides, and rockfalls which affect the whole study site. Disturbances to the soil during its development stage can disrupt vegetation succession making it harder for trees to establish (Egli et al., 2011; D'Amico et al., 2014). The relative stability of the rampart might explain why these trees have experienced less disturbance in contrast to the younger trees on the western side of the gorge (samples L002 to L005), which germinated in 1972, 1976, 1991 and 2004. These younger trees particularly the two most recent ones are located beneath a rock wall where rockfall debris is visible in both the orthophoto of 2020 (Swisstopo, 2024a) and in the field (see **Figure 19**).

The oldest trees in the focus area are scattered throughout the focus site (for instance samples L001, L015, L029, L030, L035, L044) with no clear pattern indicating soil age differences from north to south or between the frontal "LIA" moraine and the riegel (see **Figure 33** and **Figure 34**). For example, trees L029 and L030 are located at the northern edge of the focus site, near the frontal "LIA" moraine, while trees L001 and L015 are positioned farther south near the riegel, which is also identified as a roche moutonnée (see **Figure 19**). Meanwhile, L035 and L044 are centrally located on the slope. This lack of clear pattern might be a sign that at least the overall ground conditions and climatic conditions are too similar over the whole focus site for the trees to be able to grow (D'Amico et al., 2014; Wojcik et al., 2021).

However, a distinct pattern emerges in the central section of the focus site where trees growing on debris-covered ground with large rock blocks are significantly younger with germination dates ranging from the 1980s to 2003 as seen in **Figure 33** and **Figure 34**). This suggests that the instability of this terrain likely due to paraglacial adjustments, seasonal periglacial process such as freeze-thaw cycles or gravitational processes that may have delayed

the successful establishment of *L. decidua* Mill. For a later succession stage to occur, stabilisation of the ground is important (Eichel, 2017).

The variability in tree age across the site suggests that a combination of geomorphic processes, local disturbances and ecological factors influence tree establishment, making it difficult to draw straightforward conclusions from the age data alone. Additionally, the methodological choices made during sampling and analysis, as well as the limitations of the data introduce uncertainties that must be carefully considered. The following section will discuss these uncertainties in detail, addressing both fieldwork and laboratory procedures, as well as the challenges posed by the environmental conditions and the data used for analysis.

5.3.3 Uncertainties in dendrochronological analysis

Sampling strategy

The sampling strategy used in this study presented several opportunities for improvement that could have reduced uncertainties in the interpreation (see sampling strategy in **3.3.1**). The grid used to guide the sampling process was not as precise or systematically laid out as it could have been. Some trees were taken in almost the same square in the grid due to the uneven distribution of the trees in the focus site. A more consistent grid would have allowed for a more even distribution of tree samples capturing a wider variety of growth patterns and environmental influences. Also, the photo documentation of the sampled trees and surrounding environment was not as thorough as it could have been in the first field campaign which led to difficulties analysing growth patterns of specific trees that did not fit well into the chronology. A documentation is crucial for ensuring accurate records of the sampling locations and contextual factors such as slope, exposition, water availability and special growth for example reaction wood. Better photographic records would have made a clearer understanding of each sample's environment and its potential influence on tree growth patterns together with overall more documentation during the field campaign as described by Wilford et al. (2005).

Additionally, the selection of trees for sampling also contributed to the uncertainties in the analysis. In hindsight, the choice of trees could have been more carefully controlled. Some of the trees sampled had multiple stems or roots which can lead to different growth patterns that complicate the interpretation of tree rings (see discussion above). Furthermore, some trees exhibited reaction wood which could possibly bring difficulties in crossdating (for instance the outliers in **4.3.1**). However, choosing trees without any signs of gravitational disturbances showed to be difficult in this study site. After the glacial retreat, the ground takes time to stabilise and as described in **5.1.4**, there are multiple landslides and gravitational processes influencing the southern Turtmann Valley, especially visible in the forested area of the sampled trees where rock and debris are evident (see synthesis in **5.4**).

While the number of samples taken was sufficient for the purposes of this thesis, taking more samples could have improved the statistical robustness of the data. A larger sample size would have helped in reducing the influence of individual tree anomalies and thus, providing a more representative picture of past climatic conditions and glacier activity (Wilford et al., 2005). In some cases, the pith was not captured in the samples. The absence of the pith introduces a degree of uncertainty because the exact age of the tree cannot be determined without it. This issue is particularly important in young trees or those with narrow growth rings where missing the pith could significantly affect age estimations. Careful coring to ensure the inclusion of the pith would have minimized this uncertainty (Gärtner et al., 2023). However, this problem was not significant in the context of this master thesis as it was only the case in a small amount of samples.

Lab work

As it was a pilot to use the GSC-holders some disadvantages next to the in section **3.3.2** previously mentioned advantages that arise without having to glue them emerged while using the core microtome. By assembling the long 20 cm GSC-holder with the smaller 10 cm GSC-holder, a height discrepancy of the tree core in the sample holder of the core microtome can occur. Nevertheless, this can also happen in the classical method. For further steps in the measurements, it is important that the entire core is cut (Gärtner et al., 2024).

Another critical aspect of cutting a tree core with a core-microtome is the freshness of the tree sample. The cell walls of the tree cores should be sufficiently soft to prevent breakage of the core during cutting. Therefore, cutting the tree cores as soon as they arrive in the laboratory is advisable. In this thesis it took several days to weeks for the lab work to start but it was no problem when the samples were put in water before cutting them (Gärtner and Nievergelt, 2010; Gärtner et al., 2024).

Analysis

The climate data used for analysis comes from Grächen (1560 m a.s.l.) while the study site in the Turtmann Valley is at a significantly higher elevation (2150 m a.s.l.). This altitude difference introduces a discrepancy in the recorded temperature and precipitation values potentially misrepresenting the actual climatic conditions experienced by the sampled trees. The Turtmann Valley likely experiences cooler temperatures and differing precipitation patterns including snowfall that are not captured in the Grächen data (Meteoschweiz, 2023). This mismatch could lead to errors in correlating tree ring growth with climate variables. However, this discrepancy was considered in the interpretation of the correlation and discussion of this master thesis.

Some important environmental factors such as soil conditions were not recorded in the dataset which introduces uncertainty (Egli et al., 2011). Tree growth is influenced by a combination of climatic and allogenic factors and the absence of data on soil characteristics limit the ability to accurately assess the growth response to their environment (Burga et al., 2010; Egli et al., 2011; Wojcik et al., 2021)

Furthermore, the lack of snow height data in the valley adds to the uncertainties. Snow height significantly affects soil temperature and moisture availability in the growing season which are critical to tree growth (Burga et al., 2010; Saderi et al., 2019). With climate change, the days with snow cover will change so it is important to take it into account in studies on vegetation growth (Rist et al., 2020). Also, as there is no monitoring of the southern Turtmann Valley data on gravitational processes such as avalanches or landslides which could influence tree growth, the interpretation of growth patterns are made only on previous literature and assumptions .

The statistical crossdating process in TSAP could be prone to errors particularly when dealing with reaction wood or trees affected by gravitational processes (Gärtner et al., 2024). However, by using the digital measurements in CooRecorder, measurements could be looked at a second time and errors in measurement could be fixed. Although the sample size was sufficient for the analysis, a larger sample would have increased the robustness of the statistical models in R Studio.

5.4 Synthesis of geomorphological mapping, glacier extents, and growth of *Larix decidua* Mill.

This chapter brings together the core findings of this thesis to answer the three central research questions. First, it integrates geomorphological mapping, glacier extent analysis since the Little Ice Age (LIA) and dendrochronological insights to reconstruct the landscape development and glacial history of the southern Turtmann Valley. The second question focuses on the position of the glacier terminus during the LIA. This section will draw from findings of the mapped geomorphic processes and landforms and from the sampled trees, offering insights into the dynamic processes shaping the landscape in the focus site. The third section investigates how the proglacial area outside of the focus site has evolved and the potential of using dendrochronology to validate the determination of glacier advances and retreats. Lastly, a short paragraph brings together if dendrochronology can be used for minimum age determination of frontal moraines formed during the LIA in the southern Turtmann Valley. By combining the geomorphological, glaciological, and dendrochronological data, this chapter highlights the connection of these processes and provides an extended understanding of the valley's landscape evolution.

Landscape development and glacial history of the southern Turtmann Valley

The southern Turtmann Valley is shaped by dynamic geomorphic processes that have continuously evolved through glaciation and deglaciation (see **5.2**). The overall geomorphological analysis gives insight into the landscape history of the highly dynamic southern with its hanging valleys (see resulted geomorphological map in **4.1.1** and the extensive discussion in **5.1**). These landforms provide evidence of past glacier extents, erosional and depositional processes, and the ongoing influence of periglacial conditions in this montane study site. The holistic approach to not only analyse the focus site but also the surrounding area and the processes occurring in the whole southern Turtmann Valley provides a comprehensive view of how geomorphic processes interact and influence each other. As almost the whole Turtmann Valley was glaciated during the LGM (see **5.2.1**) and since then, temperatures are increasing which makes deglaciation the main driver in the whole study site (Dikau et al., 2019). Following the deglaciation, ice might still be present in the ground, and thus, periglacial processes and landforms are found in especially higher elevations on north-faced slopes where glacier ice, permafrost, or ground ice might prevail longer due to less exposure to solar radiation (Dikau et al., 2019; Kenner et al., 2019). Periglacial landforms and processes such as freeze-thaw cycles and permafrost degradation influence the main valley floor and the focus site in different ways. Through changes in permafrost or ice content in rock glaciers, fluvial gullies might gain more water if the ice melts, which influences erosion, sediment deposition, and even vegetation in the main valley floor (as discussed in **5.1.3** and **5.1.5**). The mapped lobate landforms in the study site show where freeze-thaw cycles, as well as permafrost, are influential in the shaping of the relief. Ice content in the slope might stabilise the ground during cold temperatures as ice near the ground surface, such as permafrost, prevent water to infiltrate and to destabilise the ground and rock masses (Phillips et al., 2020). However, ground ice restricts vegetation growth causing slope instabilities. When water infiltrates the ground during warmer temperatures and ice melt, the loose rock fragments and debris in the highly permeable ground might be further loosened or washed away (Geitner et al., 2021; Phillips et al., 2020). Permafrost degradation is shown to lead to instabilities in the slope surface and to gravitational processes such as landslides to occur (Cavalli et al., 2019; Deline et al., 2021; Phillips et al., 2020). Having landslides such as debris flows or rock avalanches, as well as snow avalanches coming down from the main valley's slopes, influences the relief. Hence, vegetation growth of a higher successional stage such as shrubs

and trees are prevented. For instance this is the case in the tree-free area north of the frontal "LIA" moraine as discussed in **5.1.4** (Eichel, 2017). Other than gravitational, periglacial and fluvial processes, the glacial process domain was mapped to cover the areas influenced by the glacier's movement. The glacial process domain is clearly showing the glacial history of the Turtmanngletscher in the proglacial area since the LIA by the mapped moraine ridges and roche moutonnées (discussed in **5.1.2**). The direction of the glacier movement is visible in the landforms of the roche moutonné and coincides with literature from the Turtmann Valley as well as aerial images and maps (Swisstopo, 2024b and 2024d). Through different parameters concerning the moraine ridges, such as the location, the level of erosion, and the succession of vegetation, conclusions of the relative changes in glacier extent and the glacier retreat could been made (Eichel, 2017; Swisstopo, 2024a to 2024d). These combined findings are discussed in the following paragraphs in the main valley floor from the focus site with the frontal "LIA" moraine to the position of the glacier tongue for the year 2020 as it is the orthophoto used for the resulted maps (Swisstopo, 2024a).

Position of the glacier terminus during the LIA and dendrochronological determination of the frontal "LIA" moraine in the focus site

The terminus of the Turtmanngletscher during the LIA is marked by a distinct moraine ridge, frontal "LIA" moraine, identified in the field campaigns and confirmed through comparisons with historical maps and aerial imagery (see **5.1.2**). Moraine ridges in the valley floor provide information on the position of the glacier tongue while the Turtmanngletscher was retreating and advancing throughout the 19th and 20th centuries. Dendrochronological evidence from *L. decidua* Mill. was further used to provide a comparison of the mapped glacier extents and geomorphological landforms to gain information on the landscape development in the focus site of the terminus of the Turtmanngletscher during the LIA (**Figure 19** in **4.2**) The lack of a clear pattern of the germination years of the sampled trees might be evidence that the Turtmanngletscher retreated fast in that area (see **5.3.2**). From a glacier retreat to the onset of germination, some period of time occurs called ecesis interval (Garbarino et al., 2010). In the European Alps, the ecesis interval for *L. decidua* Mill. was named differently by multiple authors: 14 to 34 years (Garbarino et al., 2010), 12 to 15 years (Egli et al., 2010; Burga et al., 2010), 10 to 20 years (Le Roy et al., 2023) or 20 to 30 years (D'Amico et al., 2014). With an average ecesis interval of 20 years, it would mean the glacier has only retreated after 1926, according to the oldest sampled tree with the germination year of 1946. This would not coincide with the mapped glacier extents in section **4.2**. Choosing an ecesis interval of ≥ 30 years, as described by D'Amico et al. (2014) and Garbarino et al. (2010), would still be too small for the trees established near the mapped frontal "LIA" moraine. The oldest tree in between the mapped glacier extent of 1850 and 1885 is dated to 1952, which would mean with an ecesis of approx. 30 years that the glacier retreated in around 1920, which is a difference of 70 years in the determination of the glacier extent by dendrochronology and geomorphological mapping through the field and literature such as Eichel et al. (2013) or Swisstopo (2024g). Therefore, there need to be other explanations for why it took more than 50 years up to 100 years for the larch trees to grow in this area where the glacier was supposed to have retreated earlier, as seen in **Figure 19** in the results in **4.2**.

According to multiple authors, it takes between 40 to 80 years for larch trees to establish as a cluster (Burga et al., 2010; D'Amico et al., 2014; Egli et al., 2010; Garbarino et al., 2010) and more than 150 years for a *Larici-Pinetum cembrae* forest establishment near to a state of stability (Burga et al., 2010; D'Amico et al., 2014; Egli et al., 2011). However, in a montane setting, there is never a state of complete stability as processes concerning deglaciation occur constantly, as analysed in the discussion of the different process domains in **5.1** (Wojcik et al., 2021). The

establishment of the cluster or open forest of *L. decidua* Mill. in the focus site coincides with the values for later establishment such as for 77 years of glacier retreat and of vegetation of late succession stages (Egli et al., 2011; Eichel et al., 2013). There are many different possible explanations for such a late establishment of the *L. decidua* Mill. cluster and the high ecesis interval. A simple reason could be that not the oldest trees in the study site were taken samples of. However, as explained in section **3.3.1**, a strategy to the find old trees in the study site was made. There might have been earlier grown individual trees that have been buried by gravitational processes as discussed in **5.1.4** and **5.3.2**. Gravitational processes such as landslides, debris flows, rock avalanches and slope movement prevent vegetation to establish (Schweingruber, 1996). Nevertheless, *L. decidua* Mill. is a tree species that can thrive on recently disturbed forests and soils as it is not highly depended on water availability, is light-demanding, and can easily grow on young substrate with high proportion of soil skeleton or even between boulders (Burga et al., 2010; Da Ronch et al., 2016; Egli et al., 2011). Still, for the pioneer tree species, soil with organic matter and some stability for the roots to grow needs to have established to some degree (Eichel et al., 2013).

Soil development in recently glaciated areas is usually fast (Conen et al., 2007) and a clear chronosequence of soil development to the glacier retreat is visible in different sites in the Alps (Egli et al., 2010 and 2011; Eichel et al., 2013; Rydgren et al., 2014; Wojcik et al., 2021). In the beginning of soil formation and succession, the autogenic development through chemical weathering, physical weathering and autogenic plant colonisation is most influential (see Theory in **2.2.3**). The built up of organic matter in the soil is caused by the early pioneer plants and chemical weathering (Wojcik et al., 201). Hence, the faster the early succession occurs, the faster trees like *L. decidua* Mill. of the later succession stage might be able to grow. More soil organic matter is found further away from a current glacier tongue with a considerable amount after about 150 to 180 years of glacier retreat for a cluster or a forest of *L. decidua* Mill. to form (Burga et al., 2010; Mavris et al., 2013). This time to have a considerable amount of soil organic matter would coincide with the establishment of *L. decidua* Mill. in the focus site of this thesis.

Additionally, for germination of *L. decidua* Mill. to occur, seeding dispersal is important. Other larches need to be in the area for seeds to be able to disperse (Geitner et al., 2021). The ages of the oldest tree taken samples of, that are dated but not further analysed in this thesis (see **4.3.2),** span from 301 years old (1722) to 181 years old (1826). This shows that the forest just north of the study site is older and thus, there was a source of seeds of *L. decidua* Mill. available during the retreat of the glacier after the maximum extent of the LIA. Seed establishment of primary plants need developed soil and enough water, showing that the development of soil and the autogenic processes are both important for the whole vegetation succession (Eichel, 2017; Geitner et al., 2021).

Nevertheless, in the Turtmann Valley allogenic factors have a high influence on vegetation succession (Wojcik et al., 2021) which is studied thoroughly by Eichel (2017) for the lateral "LIA" moraines. The lateral "LIA" moraines are highly disturbed through fluvial erosion for instance through gullying (mapped "moraine gullies in the geomorphological map, see **Figure 16** in **4.1.3**), debris flows, sliding scree, and other processes concerning paraglacial adjustments (Eichel, 2017). A disturbance in the area of early succession resets the succession which could have happened here in the Turtmann Valley and the focus site (see **2.2.3**; Wojcik et al., 2021). The scree in the centre of the focus site devoid of trees is a sign of slope instability and repeated events of gravitational processes (see discussion of age distribution of the trees in **5.3.2**). The "candelabra"-form of the outlier L034 as discussed in **5.3.1** is evidence of a disturbance between the growing season of 1998 and 1999 because there is a dip in the tree-ring width (TWR) curve. As there is a gap between the aerial images of 1994 and 2004 (see **5.2.3**), there is no clear evidence of what happened. Nevertheless, there a change in the crown of the tree L034 is visible and other

surrounding trees visible in the orthophoto 1994 are missing. An avalanche or single rock falls are the most plausible explanations because there are no signs for a landslide or a debris flow visible in the site (Swisstopo, 2024g). Furthermore, the younger trees in the centre of the focus site in the scree are shown to be younger which is another sign for disturbances (see **5.3.2**). The lack of a significant difference between tree age except for when disturbances occur, the lack of trees older than 77 years old and the high amount of time it took for the establishment of *L. decidua* Mill, is therefore left on hypotheses about what happened after glacier retreat as it is mapped in **Figure 18** in **4.2**. The map of glacier extents (**Figure 18**) has been carefully verified by literature review (Dikau et al., 2019; Eichel et al., 2013 and 2017; GLAMOS, 1881-2023; Swisstopo, 2024g) and by mapping of geomorphological landforms such as moraine ridges visible in the field and aerial image (see **Figure 14** and discussion in **5.2**). Therefore, there might be other explanations aside of disturbances.

The rocky riegel mapped as roche moutonnée in the geomorphological map, where the glacier extent of 1900 has been mapped (**Figure 18** in **4.2**), has a steep rock face to the north. A glacier in a steep area such as that particular site, is usually under a lot of pressure due to gravity and crevasses might form (Dikau et al., 2019). In warming temperatures, the temperate glacier retreats back from that area and a hypothesis could be that glacier ice might have detached at some point in the retreat and the remnant of the glacier tongue might have stayed in the focus site as dead ice. If the ice does not melt immediately for instance through debris cover, periglacial conditions prevail for a longer time than if the glacier has retreated entirely. Thus, leading to a longer time until soil starts to develop and succession can start (Dikau et al., 2019; Haugland and Beatty, 2005; Wojcik et al., 2021).

A more plausible explanation than the ice-fall hypothesis would be that meltwaters have influenced the concave-shaped focus site together with mass movements. In the aerial image of 1946 (Swisstopo, 2024c), as well as later aerial images (Swisstopo, 2024b), streams flowing through the focus site are visible (near tree L040 and L042, see **Figure 19** in the results in **4.2**). With a high intensity and frequency of fluvial disturbances through the focus site, the area, the soil development and succession might have been disrupted repeatedly through the meltwaters of the retreating Turtmanngletscher. However, the gorge with the Turtmänna must have been used as the main outlet after the glacier has retreated further around the year 1900 (similar to the situation at Triftgletscher studied by Steinemann et al., 2021). Still, repeated fluvial erosion would wash away minerals and organic soil components and slow down succession which would explain the slow development of the *L. decidua* Mill. forest cluster (Wojcik et al., 2021).

In the early retreat between the years1850 and 1900, aeolian processes might have played a role in addition to disturbances through fluvial, periglacial and gravitational processes. As the focus site was in proximal distance to the ice margin, cold glacier wind might have been disadvantageous for plant growth (Garbarino et al., 2010; Wojcik et al., 2021).

The observable anthropogenic influence on the focus site is little (see discussion in **5.1.6**). Only hiking path on the frontal “LIA” moraine as well on the lateral moraine ridge in the focus site are visible. According to the forestry department Forst Region Leuk, no changes have been done on the forest in the last twenty years answered upon request (Forst Region Leuk, 2023). Also no anthropogenic changes in earlier years are visible through aerial images or described in literature (Meyer, 1923; Swisstopo, 2024b). However, grazing by animals might have influenced succession of vegetation in the southern Turtmann Valley. As the focus area is covered by rocks and the glacier was at the location of the frontal “LIA” moraine in the late Holocene, the probability of the usage of the focus site for grazing is low. However, the north of the frontal “LIA” moraine as well as the hanging valley have

been used and are still used as alpine pastures (see **5.1.6**; Meyer, 1923). Therefore, the focus site was likely to develop without anthropogenic influence.

Although there are various factors discussed and hypothesised to have influenced the tree establishment in the focus site, the most plausible explanation for the lack of a distinct age pattern in *L. decidua* Mill., based on the proximity to the glacier terminus at the study site, is the impact of gravitational processes. The instability of the ground following the glacier's retreat likely prevented succession of later stages and tree growth with frequent disturbances disrupting soil formation and vegetation succession (Wojcik et al., 2021). These disturbances might have reset the succession process causing a delayed tree establishment despite the potential for suitable conditions in other respects This is evident through the rock and debris covered area in the centre of the focus site. There are some local pattern which suggest some influence of geomorphological features and local microclimates as discussed in **5.3.2**. For example, on the rampart trees germinated between the years 1960 and 1963. This relatively uniform cohort could be explained by the rampart's stability and favourable conditions such as more solar radiation and protection from gravitational processes like rockfalls, avalanches or landslides (Eichel, 2017; Wojcik et al., 2021). In contrast, trees in other areas, particularly those near rock walls such as the roche moutonnée or the eastern rock wall where debris is visible, germinated much later. Therefore, the late overall establishment of the *L. decidua* Mill. cluster can be primarily connected to the gravitational instability of the landscape and the local climatic conditions after the retreat of the Turtmanngletscher. Thus, while the broad trend does not indicate a direct chronosequence, these localised differences suggest that small variations in topography and exposure to disturbances significantly affect tree establishment (Eichel et al., 2013; Garbarino et al., 2010; Wojcik et al., 2021).

An additional possible source of the discrepancy between glacier retreat and tree establishment mentioned above might be the choice of the maximum LIA extent being the year 1850 (Carrivick et al., 2022). The maximum advances of glaciers in the Alps are ranging from 1850 to 1860 (Ivy-Ochs et al., 2009; Nicolussi et al., 2022). The moraines have not been dated by exposure dating or radiocarbon dating. Thus, the choice of the year 1850 for the maximum extent of the Turtmanngletscher rather than the year 1860 was based on previous studies done in the Turtmann Valley (see **Table 2**). These studies can be trusted as a difference of ten years for the maximum extent for the Turtmanngletscher would not make a huge difference in the study on the establishment of the larch trees because the geomorphological reasons mentioned above would outweigh the autogenic development (Wojcik et al., 2021). The gravitational processes, instabilities and cold conditions would have affected the focus site in either case for the onset of growth of *L. decidua* Mill.

Position of the glacier terminus outside the focus site compared with growth of *L. decidua* Mill.

For the proglacial area outside of the focus site, the dendrochronological analyses can be compared to the glacier extents of the last 70 years as the oldest sampled trees is dated to 1946. From that year on, the study of the reaction of tree-ring width growth on climatic conditions and therefore the comparison with glacier fluctuations is possible. Three advance periods in the Alps were found after the last maximum LIA advance in the years 1890, in the 1920s and 1980s which reflect cold conditions for the Turtmann Valley (Le Roy et al., 2024). For the year 1890 as well as 1920, no dated tree in the study site is old enough to compare the tree growth with the geomorphological mapped moraines and the glacier extents. Although, the moraine of the 1920s (mapped as 1924 in **Figure 20** in **4.2**) is shown to represent the relatively small advance or stagnant period of the Turtmanngletscher (GLAMOS, 1881-2023; Le Roy et al., 2024).

The moraines mapped as 1953 in in **Figure 20** in **4.2** are discussed in **5.2.2** and can be compared to the dendrochronological data from the sampled trees. Only three sampled trees make up the tree-ring curve of the chronology for the year 1953 (as seen in **Figure 23** in **4.3.1**), but for all of them low growth is visible in the TRW curve. It coincides with more precipitation (see discussion in **5.3.1**) but not particular low temperatures. Therefore, the Turtmanngletscher must have been in a stagnant or slightly advancing position for the frontal moraine to form. There could have been a higher amount of sediment deposition because of the high precipitation but this cannot be known with the methods employed in this thesis.

For the 1980s glacier advances, a comparison of the geomorphological and glacier extent mapping with the dendrochronological data obtained in this thesis can be made. There was a cold period in the analysed summer months as it is visible in the Grächen climate data for the year 1980 (Meteoschweiz, 2023), as well as lower growth of the sampled trees for 1980 and 1981 (see **Figure 30**). Summer precipitation as well as the yearly precipitation was medium or even a bit higher compared to other years (see **Figure 31**). This is evidence for a period of accumulation for the glacier in 1980 and 1981. The cold temperatures in 1984 (Meteoschweiz, 2023) and the visible advance in the orthophoto of 1984 (Swisstopo, 2024b) are emphasising the glacier advances of the 1980s. Although, the advance of 1984 was not visible in the dendrochronological data as low growth in TRW (as discussed in **5.3.1**). Still, the 1980s moraine is one of the most visible moraine in the proglacial area of the Turtmanngletscher (see **Figure 18** in **4.2**, **Figure 42** in **5.1.2**, and **Figure 72** in **5.2.2**), and thus concludes that the multiple 1980s advances are visible through geomorphological mapping and supported by some of the dendrochronological analysis.

Smaller advances in 1996 and 1998 were observed through the analysis of the aerial images together with the GLAMOS data as discussed in **5.2.2** and visible in **Figure 20** (in **4.2)** and **Figure 72** (in **5.2.2**) (GLAMOS, 1881-2023; Swisstopo, 2024b). The time period of 1995 to 1997 is considered to be pointer years for the sampled *L. decidua* Mill. because TRW decreased massively for all larch trees due to the cold temperatures. Especially the cold spring temperatures but also mean annual temperatures showed to have inhibited TRW growth (see **5.3.1**). The spring and summer precipitation was not very high or low but the mean annual precipitation was low compared to other years measured at the Grächen weather station (Meteoschweiz, 2023). Hence, the glacier advances of the mid-1990s that was observed in some sites in the Alps is observed in the southern Turtmann Valley by the moraine ridges mapped in **Figure 20** in **4.2** and validated by the climatic conditions influencing *L. decidua* Mill. in the study site (Deline et al., 2022; Dikau et al., 2019; Le Roy et al., 2024).

Use of dendrochronological analysis for landscape development

One of the key goals of this thesis was to assess whether dendrochronological analysis could reliably determine the age of the frontal "LIA" moraine in the Turtmann Valley. The results are mixed. Although dendrochronology provides valuable insights into tree establishment and the timing of vegetation recovery, the absence of older trees in the study area and the high variability in ecesis intervals complicates precise minimum age determination of the moraine. The oldest sampled tree in the focus site, with a germination year of 1946, implies that glacier retreat occurred no earlier than 1916 based on an ecesis interval of 30 years. However, this conflicts with the mapped glacier extents from historical data and literature which place the glacier terminus much farther upstream by the early 20th century. Possible explanations for this delay include disturbances from gravitational processes such as avalanches or debris flows, that may have buried earlier generations of trees, or the presence of periglacial conditions that slowed soil development and delayed tree growth. Fluvial disturbances from meltwater streams also may have played a role in soil development and vegetation growth, contributing to the extended ecesis interval observed in this study (see discussion above in this chapter; Dikau et al., 2019; Wojcik et al., 2021).

Given the irregularity in the ages of the trees and the ongoing disturbances from gravitational processes, it is clear that dendrochronological data alone cannot provide a reliable estimate for the timing of glacier retreat or the determination of the frontal “LIA” moraine (Garbarino et al., 2010). The influence of these allogenic factors combined with the observed tree ages highlights the need for alternative dating methods such as cosmogenic nuclide exposure dating or lichenometry to complement the tree-ring analysis (Carrivick et al., 2020; Zhu et al., 2013). These methods would allow for a more accurate reconstruction of the movement of the Turtmanngletscher and the position of the “LIA” moraines especially in areas where tree growth has been delayed or interrupted by environmental factors (Dikau et al., 2019; Eichel, 2017; Wojcik et al., 2021).

In conclusion, the synthesis of geomorphological mapping, glacier extent analysis and dendrochronological analysis has provided a comprehensive understanding of the landscape evolution of the southern Turtmann Valley. The integration of these methods reveals the dynamic relationship between different processes in a valley with deglaciation occurring such as glacial, periglacial, gravitational, fluvial and some anthropogenic processes and the role of *L. decidua* Mill. in the post-glacial development of the area. This thesis highlights how the surfaces, landforms and vegetation has been shaped through these different processes instead of only following an autogenic succession of soil and vegetation development after glacier retreat (Wojcik et al., 2021). Although dendrochronological data provided key insights into the timing of tree establishment, limitations remain in using it for precise glacier extent dating and the dating of glacier extent in the 19th and early 20th century. The observed discrepancies between geomorphological evidence and tree age distribution suggest the influence of complex processes such as delayed soil development, repeated disturbances and late succession of vegetation. Therefore, the approach of chronosequence alone without any other dating methods might be not optimal in the case for the focus site (Garbarino et al., 2010). However, this interdisciplinary approach not only reconstructs the glacier's history since the LIA but also highlights the broader landscape dynamics in this alpine environment.

6. Conclusion

This thesis examined the landscape evolution of the southern Turtmann Valley and the glacial history of the Turtmanngletscher through detailed geomorphological mapping, glacier extent reconstruction since the Little Ice Age (LIA), and dendrochronological analysis of *Larix decidua* Mill. The research was guided by three research questions, each of which has been addressed to provide insights into the glacier's behaviour and the valley's post-glacial evolution.

The first question "What can geomorphological mapping, glacier extents since the Little Ice Age, and a dendrochronological analysis of *Larix decidua* Mill. tell about the landscape development of the southern Turtmann Valley and the glacial history of the Turtmanngletscher?" was answered through detailed mapping of the valley's landforms and processes (see section **4** and **5.4**). The geomorphological map (in section **4.1**) captured the processes shaping the landscape in the southern Turtmann Valley and key features such as terminal moraines, rock glaciers and roche moutonnées. These features show a complex interaction between the glaciers that occupied the whole southern Turtmann Valley and the surrounding environment. Glacier reconstructions since the LIA confirmed the glacier reached its maximum extent in the mid-19th century. A phase of glacier retreats with smaller readvances followed the LIA (see section **4.2** and **5.2**). Several of these smaller advances were observed through moraines geomorphological mapping (for instance the moraine ridge of the 1980s) and it was showed that the behaviour of the Turtmanngletscher aligned with regional patterns of alpine glaciers as a response to climatic conditions. Dendrochronological analysis of *L. decidua* Mill. offered further insights into the valley's post-glacial development. The establishment of trees in the proglacial area was found to correlate with the retreat of the glacier although the age distribution of the trees did not follow a clear chronosequence based on proximity to the glacier front (see section **5.3.2**). However, localised tree cohorts emerged indicating that factors such as substrate stability, gravitational disturbances and microclimatic conditions may have strongly influenced tree establishment.

The second research question "Where was the terminus of Turtmanngletscher in the Little Ice Age and how did the landscape in the proglacial area develop afterwards?" was addressed by geomorphological mapping and by the glacier extent reconstructions (see **5.4**). The maximum LIA extent of the Turtmanngletscher was placed at its terminal moraine located in the northern section of the valley which was clearly visible as a moraine ridge (see **5.2.2**). Following the glacier's maximum extent, it began to retreat in response to warming temperature. Therefore, the period of proglacial landscape development started with mostly glacier retreats that were disturbed by small readvances which are documented by minor moraines and could be observed in historic maps and aerial images (see **4.2**). These moraines reflect the temporary stagnant phases or advances of the Turtmanngletscher during cooler climatic phases. The landscape in the proglacial area evolved significantly during this period which is characterised by many geomorphological landforms, for instance the proglacial fluvial plain, slope instabilities, the gullying of the lateral moraines and the succession of vegetation.

The dendrochronological analysis revealed that tree growth responded to both temperature and precipitation similar to the glacier's response to climatic changes. The generally weak correlation between precipitation and tree growth that was observed was found to have less of an impact on tree-ring width growth than temperature. However, the most negative correlation for the months of June and July with higher levels of precipitation showed to might inhibit growth likely due to water-logged soils or delayed growing seasons caused through less favourable conditions which mostly are accompanied by cold temperatures or frost damage. On the other hand, low

precipitation had a limited effect as *L. decidua* Mill. is adapted to drier conditions. Temperature emerged as a more significant factor in tree growth particularly during the early summer months and the months contributing to the onset of tree growth (May to August). Positive correlations were found with higher temperatures during this period leading to wider tree rings. This can be explained that the trees experienced longer growing seasons. The most pronounced effect of temperature was observed in specific pointer years like 1979, 1986, 1994, 1998 and 2015 where warmer conditions significantly increased tree-ring width. Meanwhile, colder temperatures in certain years such as 1975, 1980/1981, 1995 to 1997 and 2004 resulted in narrow rings due to frost damage or delayed onset of growth. Thus, it was shown that the interaction of temperature and precipitation where high temperatures combined with low precipitation led to optimal tree growth in specific years while the opposite with cooler conditions and high precipitation restricted growth (see **5.3.1**). This analysis provided a timeline of tree-ring growth from the year 1946 on that aligned with documented glacier retreat phases and geomorphological evidence. Therefore, climate fluctuations were shown to be a key driver of both glacial and vegetation changes in the valley.

The third question "Can the frontal moraines from the Little Ice Age be identified and dated using dendrochronological methods (minimum age determination)?" revealed the limitations of using tree-ring data alone for moraine dating. Although geomorphological mapping clearly identified the frontal moraines, using dendrochronological methods provided mixed results. The oldest sampled tree dated back to 1946 and the youngest to 2004 with in total 46 trees sampled. This suggested that tree establishment in the area occurred only after the glacier had retreated significantly from its LIA extent (see **5.3.2** and **5.4**). Several factors were hypothesised in the synthesis in **5.4** to delay tree establishment including the instability of the ground following glacier retreat as evidenced by the mapped rockfalls and landslides, and other gravitational processes that might have disrupted soil development. A sign for this was the observed pattern of the germination date of the trees on the rampart being similar which highlighted how isolated areas of stability might have allowed earlier establishment compared to more unstable regions. Disturbances might have created conditions unfavourable for immediate tree growth, meaning that the minimum age of the trees does not necessarily reflect the age of the moraine. Additionally, local micro-environments and substrate conditions played a crucial role in determining where and when trees could establish. While dendrochronological methods provided valuable insights into post-glacial vegetation dynamics, they were insufficient for directly dating the frontal moraines with high precision. This suggests that geomorphic processes such as gravitational and periglacial disturbances might have been crucial in delaying tree establishment in parts of the proglacial area when the Turtmanngletscher retreated after the maximum extent during the LIA around the year 1850. For more accurate dating of LIA moraines, complementary methods such as cosmogenic nuclide exposure dating or lichenometry would be necessary. These methods could provide direct evidence of when the moraine surfaces were last exposed and, thus, a more accurate timeline of glacier retreat.

In conclusion, the combination of geomorphological mapping, glacier extent analysis and dendrochronology provided valuable insights into the post-glacial evolution of the southern Turtmann Valley. While dendrochronology alone could not accurately date the terminus of the Turtmanngletscher during the maximum extent of the LIA, it has provided a valuable understanding of how geomorphic processes and climatic factors influence tree growth patterns in the proglacial area. The new chronology of *L. decidua* Mill. for the southern Turtmann Valley contributes to the archive of dendrochronological data in the Alps. The detailed geomorphological map lead to an addition to a wide variety of studies done in the Turtmann Valley. Overall, this thesis adds new knowledge to the field by highlighting the complex interactions between glacial dynamics and vegetation development. Future research could integrate more precise dating techniques and expand dendrochronological sampling to better understand the interplay of geomorphology, glacier behaviour and succession of *L. decidua* Mill after deglaciation. Additionally, long-term climate change impacts on proglacial environments should be further examined to gain information on the landscape evolution of previously glaciated valleys.

Literature

Agassiz, L. and Bettannier, J. (1840). Etudes sur les glaciers. Jent et Gassmann, Neuchatel.

Alden, A. (2019). Geological Thinking: Method of Multiple Working Hypotheses. ThoughtCo, Apr. 3, 2019. URL: https://www.thoughtco.com/geological-thinking-1440872 [last access: 23.09.2024].

Bearth, P. (1980). Blatt 1308 St. Niklaus. In: Bundesamt für Landestopografie swisstopo (Eds.), Geologischer Atlas der Schweiz 1:25000, Erläuterungen. [in German].

Bini, A., Buoncristiani, J.-F., Couterrand, S., Ellwanger, D., Felber, M., Florineth, D., Graf, H. R., Keller, O., Kelly, M., Schlüchter, C. and Schoeneich, P. (2009). Die Schweiz während des letzteiszeitlichen Maximums (LGM), Karte 1:500'000 [Switzerland during the last glacial maximum (LGM), map 1:5000’000]. Bundesamt für Landestopografie swisstopo. Viewable on the Geoportal of Swisstopo (n.d.). [in German].

Brardinoni, F. and Hassan, M. A. (2006). Glacial erosion, evolution of river long profiles, and the organization of process domains in mountain drainage basins of coastal British Columbia. *Journal of Geophysical Research*, 111, F01013. DOI: https://doi.org/10.1029/2005JF000358.

Brierley, G., Fryirs, K., Reid, H. and Williams, R. (2021). The dark art of interpretation in geomorphology. *Geomorphology*, 390. DOI: https://doi.org/10.1016/j.geomorph.2021.107870.

Burga, C. A., Krüsi, B., Egli, M., Wernli, M., Elsener, S., Ziefle, M., Fischer, T. and Mavris C. (2010). Plant succession and soil development on the foreland of the Morteratsch glacier (Pontresina, Switzerland): Straight forward or chaotic?. *Flora - Morphology, Distribution, Functional Ecology of Plants*, 205(9), 561-576. DOI: https://doi.org/10.1016/j.flora.2009.10.001.

Canton Valais (n.d.). Cantonal Geoportal. URL: https://www.vs.ch/de/web/egeo [last access: 13.09.2024].

CAS Section Prévôtoise (n.d.). Turtmannhütte. URL: https://www.cas-prevotoise.ch/cabanes/Turtmannhtte.php [last access: 02.09.2024].

Carrivick, J. L., Andreassen, L. M., Nesje, A. and Yde, J. C. (2022). A reconstruction of Jostedalsbreen during the Little Ice Age and geometric changes to outlet glaciers since then. *Quaternary Science Reviews*, 284, 107501. DOI: https://doi.org/10.1016/j.quascirev.2022.107501.

Cavalli, M., Heckmann, T. and Marchi L. (2019). Sediment Connectivity in Proglacial Areas. In: Heckmann, T. and Morche, D., *Geomorphology of Proglacial Systems. Landform and Sediment Dynamics in Recently Deglaciated Alpine Landscapes*, 1, Springer Charm. DOI: https://doi.org/10.1007/978-3-319-94184-4.

Chandler, B. M. P., Lovell, H., Boston, C. M., Lukas, S., Barr, I. D., Benediktsson, , Í. Ö., Benn, D. I., Clark, C. D., Darvill, C. M., Evans, D. J. A., Ewertowski, M. W., Loibl, D., Margold, M., Otto, J.-C., Roberts, D. H., Stokes, C. R., Storrar, R. D. and Stroeven, A. P. (2018). Glacial geomorphological mapping: A review of approaches and frameworks for best practice. *Earth-Science Reviews*, 185, 806-846. DOI: https://doi.org/10.1016/j.earscirev.2018.07.015.

Cherubini, P., Gargano, A., Grob, M., Nievergelt, D. and Passardi, S. (2020). Dendrochronologia's tutoring recipes: How to take samples for small basic dendroecological studies. *Dendrochronologia*, 64, 125774. DOI: https://doi.org/10.1016/j.dendro.2020.125774.

Colucci, R. R., Boccali, C., Žebre, M. and Guglielmin, M. (2016). Rock glaciers, protalus ramparts and pronival ramparts in the south-eastern Alps. *Geomorphology*, 269, 112-121. DOI: https://doi.org/10.1016/j.geomorph.2016.06.039.

Conen, F., Yakutin, M.V., Zumbrunn, T. and Leifeld, J. (2007). Organic carbon and microbial biomass in two soil development chronosequences following glacial retreat. *European Journal of Soil Science*, 58, 758-762. DOI: https://doi.org/10.1111/j.1365-2389.2006.00864.x.

Couper P. R. (2022): Interpretative field geomorphology as cognitive, social, embodied and affective epistemic practice. *Canadian Geographies*. DOI: https://doi.org/10.1111/cag.12821.

Crang, R., Lyons-Sobaski, S. and Wise, R. (2018). Plant Anatomy. A Concept-Based Approach to the Structure of Seed Plants. *Springer Nature Switzerland AG*, 2018. DOI: https://doi.org/10.1007/978-3-319-77315-5.

Cybis Elektronik & Data AB (2023). CooRecorder on www.cybis.se. URL: http://www.cybis.se./forfun/dendro/helpcoorecorder7/index.htm [last access: 09.09.2024].

D'Amico, M., Freppaz, M., Filippa, G. and Zanini, E. (2014). Vegetation influence on soil formation rate in proglacial chronosequence (Lys Glacier, NW Italian Alps). *Catena*, 113, 122 – 137. DOI: https://doi.org/10.1016/j.catena.2013.10.001.

Da Ronch, F., Caudullo, G., Tinner, W. and de Rigo, D. (2016). L. decidua Mill. and other larches in Europe: distribution, habitat, usage and threats. In: San-Miguel-Ayanz, J., de Rigo, D., Caudullo, G., Houston Durrant, T., Mauri, A. (Eds.), *European atlas of Forest Tree Species*. Publ. Off. EU, Luxembourg, 108-110.

Davis, W. M. (1900). Glacial erosion in France, Switzerland and Norway. *Proceedings of the Boston Society of Natural History*, 29, 273–322.

Deline, P., Gruber, S. Amann, F., Bodin, X., Delaloye, R., Failletaz, J., Fischer, L., Geertsema, M., Giardino, M., Hasler, A., Kirkbride, M., Krautblatter, M., Magnin, F., McColl, S., Ravanel, L., Schoeneich, P. and Weber, S. (2021). Chapter 15 - Ice loss from glaciers and permafrost and related slope instability in high-mountain regions. In: Haeberli, W. and Whiteman, C. (Eds.), *Hazards and Disasters Series, Snow and Ice-Related Hazards, Risks, and Disasters (Second Edition),* Elsevier, 501-540. DOI: https://doi.org/10.1016/B978-0-12-817129-5.00015-9.

Dikau, R., Eibisch, K., Eichel, J., Messenzehl, K. and Schlummer-Held, M. (2019). Geomorphologie. Springer Spektrum Berlin, Heidelberg. DOI: https://doi.org/10.1007/978-3-662-59402-5. [in German].

Egli, M., Mavris, C., Mirabella, A. and Giaccai, D. (2010). Soil organic matter formation along a chronose-quence in the Morteratsch proglacial area (Upper Engadine, Switzerland). *CATENA*, 82(2), 61-69. DOI: https://doi.org/10.1016/j.catena.2010.05.001.

Egli, M., Wernli, M., Burga, C., Kneisel, C., Mavris, C., Valboa, G., Mirabella, A., Plötze, M. and Haeberli, W. (2011). Fast but spatially scattered smectite-formation in the proglacial area Morteratsch: An evaluation using GIS. *Geoderma*, 164(1–2), 11-21. DOI: https://doi.org/10.1016/j.geoderma.2011.05.001.

Eichel, J. (2017). Biogeomorphological dynamics in the Turtmann glacier forefield, Switzerland. Dissertation, Rheinische Friedrich-Wilhelms-Universität Bonn. URL: https://nbn-resolving.org/urn:nbn:de:hbz:5n-46884 [last asccess: 24.09.2024].

Eichel, J., Krautblatter, M., Schmidtlein, S. and Dikau, R. (2013). Biogeomorphological interactions in the Turtmann glacier forefield, Switzerland. *Geomorphology*, 201, 98-110. DOI: https://doi.org/10.1016/j.geomorph.2013.06.012.

Forst Region Leuk (2023). E-Mail correspondence between Ariane Dieth and Rinaldo Hug (operations man-ager/district forester) resp. Dominic Gruber (section leader for forest). [available on request].

Frank, D., Fang, K. and Fonti, P. (2022). Dendrochronology: Fundamentals and Innovations. In: Siegwolf, R.T.W., Brooks, J.R., Roden, J., Saurer, M. (eds) Stable Isotopes in Tree Rings. Tree Physiology, 8, Springer, Cham. DOI: https://doi.org/10.1007/978-3-030-92698-4_2.

Garbarino, M., Lingua, E., Nagel, T. A., Godone, D. and Motta, R. (2010). Patterns of larch establishment fol-lowing deglaciation of Ventina glacier, central Italian Alps. *Forest Ecology and Management*, 259(3), 583-590. DOI: https://doi.org/10.1016/j.foreco.2009.11.016.

Gärtner, H. and Schneider, L. (n.d.). Skippy. URL: https://www.wsl.ch/de/services-produkte/skippy/ [last access: 24.09.2024].

Gärtner, H. and Nievergelt, D. (2010). The core-microtome: A new tool for surface preparation on cores and time series analysis of varying cell parameters. *Dendrochronologia,* 28, 2, 85–92. DOI: 10.1016/j.dendro.2009.09.002.

Gärtner, H. and Heinrich, I. (2013). Dendrogeomorphology. *Encyclopedia of Quaternary Science: Second Edition*, 2, 91-103. DOI: 10.1016/B978-0-444-53643-3.00356-3.

Gärtner-Roer, I., Heinrich, I. and Gärtner, H. (2013). Wood anatomical analysis of Swiss willow (Salix helvetica) shrubs growing on creeping mountain permafrost. *Dendrochronologia*, 31(2), 97-104. DOI: https://doi.org/10.1016/j.dendro.2012.09.003.

Gärtner, H., Cherubini, P., Fonti, P., von Arx, G., Schneider, L., Nievergelt, D., Verstege, A., Bast, A., Schweingruber, F.H. and Büntgen, U. A. (2015). Technical Perspective in Modern Tree-ring Research - How to Overcome Dendroecological and Wood Anatomical Challenges. *Journal of Visualized Experiments*, 97, e52337. DOI: 10.3791/52337.

Gärtner, H., Schneider, L., Lucchinetti, S., Cherubini, P. (2023). Advanced Workflow for Taking High-Quality Increment Cores - New Techniques and Devices. *Journal of Visualized Experiments*, 193, e64747. DOI: 10.3791/64747.

Gärtner, H., Schneider, L. and Cherubini, P. (2024): A new workflow for sampling and digitizing increment cores. *Journal of Visualized Experiments*, 211, e67098, URL: https://www.jove.com/t/67098/a-new-workflow-for-sampling-and-digitizing-increment-cores [last access: 28.09.2024].

Geitner, C., Mayr, A., Rutzinger, M., Löbmann, M. T., Tonin, R., Zerbe, S., Wellstein, C., Markart, G. and Kohl, B. (2021). Shallow erosion on grassland slopes in the European Alps – Geomorphological classification, spatio-temporal analysis, and understanding snow and vegetation impacts. *Geomorphology*, 373, 107446. DOI: https://doi.org/10.1016/j.geomorph.2020.107446.

GLAMOS (1881-2023). The Swiss Glaciers 1880-2022/23, Glaciological Reports No 1-142, Yearbooks of the Cryospheric Commission of the Swiss Academy of Sciences (SCNAT), published since 1964 by VAW / ETH Zurich. URL: https://www.glamos.ch/ [last access: 27.09.2024]

Gougra AG (n.d.). Eine Kraftwerkanlage im hinteren Val d'Anniviers und Turtmanntal [A power plant in the rear Val d'Anniviers and Turtmann valley]. Alpiq. URL: https://www.alpiq.ch/energieerzeugung/wasserkraftwerke/speicherkraftwerke/gougra [last access: 28.08.2024]. [in German].

Haeberli, W., Linsbauer, A., Cochachin, A., Salazar, C., and Fischer, U. H. (2016). On the morphological characteristics of overdeepenings in high-mountain glacier beds. *Earth Surface Processes and Landforms*, 41, 1980–1990. DOI: https://doi.org/10.1002/esp.3966.

Haritashya, U. K., Harbor, J. and French, H. (2022). 4.01 - The Development, History and Future of Cryospheric Geomorphology, Editor(s): John (Jack) F. Shroder, *Treatise on Geomorphology (Second Edition),* Academic Press, 1-19. DOI: https://doi.org/10.1016/B978-0-12-818234-5.00181-4.

Harrison, S., Whalley, B. and Anderson, E. (2008). Relict rock glaciers and protalus lobes in the British Isles: implications for Late Pleistocene mountain geomorphology and palaeoclimate. *Journal of Quaternary Science*, 23, 287-304. DOI: https://doi.org/10.1002/jqs.1148.

Haugland, J. and Beatty, S. (2005). Vegetation establishment, succession and microsite frost disturbance on glacier forelands within patterned ground chronosequences. *Journal of Biogeography*, 32, 145 - 153. DOI: 10.1111/j.1365-2699.2004.01175.x.

Heckmann, T., Morche, D. and Becht, M. (2019): Introduction. In: Heckmann, T. and Morche, D., *Geomorphology of Proglacial Systems. Landform and Sediment Dynamics in Recently Deglaciated Alpine Landscapes*, 1, Springer Charm, 1-19. DOI: https://doi.org/10.1007/978-3-319-94184-4.

Hutton, J. (1788). Theory of the Earth or an Investigation of the Laws observable in the Composition, Dissolution, and Restoration of Land upon the Globe. *Earth and Environmental Science Transactions of The Royal Society of Edinburgh*, 1(2), 1788 , 209-304. DOI: https://doi.org/10.1017/S0080456800029227.

Iten, W. B. (1948). Zur Stratigraphie und Tektonik der Zone du Combin zwischen Mettelhorn und Turtmanntal (Wallis). *Eclogae Geologicae Helvetiae*, 41 (1948), Heft 2.

Ivy-Ochs, S., Kerschner, H., Maisch, M., Christl, M., Kubik, P. W. and Schlüchter, C. (2009). Latest Pleistocene and Holocene glacier variations in the European Alps. *Quaternary Science Reviews*, 28(21–22), 2137-2149. DOI: https://doi.org/10.1016/j.quascirev.2009.03.009.

Kellerer-Pirklbauer, A. (2018). Solifluction rates and environmental controls at local and regional scales in central Austria. *Norsk Geografisk Tidsskrift - Norwegian Journal of Geography*, 72(1), 37-56. DOI: https://doi.org/10.1080/00291951.2017.1399164.

Kenner, R. (2018). Geomorphological analysis on the interaction of Alpine glaciers and rock glaciers since the Little Ice Age. *Land Degradation & Development*, 30, 580–591. DOI: https://doi.org/10.1002/ldr.3238.

Kenner, R., Noetzli, J., Hoelzle, M., Raetzo, H. and Phillips, M. (2019) Distinguishing ice-rich and ice-poor permafrost to map ground temperatures and ground ice occurrence in the Swiss Alps. *Cryosphere*, 13(7), 1925-1941. DOI: https://doi.org/10.5194/tc-13-1925-2019.

Körner, C. and Hoch, G. (2023). Not every high-latitude or high-elevation forest edge is a treeline. *Journal of Biogeography*, 50, 838 – 845. DOI: 50. 10.1111/jbi.14593.

Lyell, C. (1830). Principles of Geology, An Attempt to Explain the Former Changes of the Earth's Surface by Reference to Causes Now in Operation. John Murray, London.

Le Roy, M., Nicolussi, K. and Schlüchter, C. (2023). Tree-ring Dating of the Little Ice Age Maxima of Arolla Glaciers (Valais, Switzerland). *Journal of Alpine Research*. DOI: https://doi.org/10.4000/rga.12170.

Le Roy, M., Ivy-Ochs, S., Nicolussi, K., Monegato, G., Reitner, J. M., Colucci, R. R., Ribolini, A., Spagnolo M. and Stoffel, M. (2024). Holocene glacier variations in the Alps. In: Palacios, D., Hughes, P. D., Jomelli, V., Tanarro, L.M. (Eds.). *European Glacial Landscapes The Holocene*. Chennai: Elsevier, 2024, 367-418. DOI: https://doi.org/10.1016/B978-0-323-99712-6.00018-0.

Magrani, F., Valla, P. G., Gribenski, N. and Serra, E. (2020). Glacial overdeepenings in the Swiss Alps and foreland: Spatial distribution and morphometrics. *Quaternary Science Reviews*, 243, 106483. DOI: https://doi.org/10.1016/j.quascirev.2020.106483.

Marthaler, M., Sartori, M., Escher, A. and Meisser, N. (2008). Feuille 1307 Vissoie. In : atlas géologique de la Suisse 1:25000, Notice explicative. 122. Bundesamt für Landestopografie swisstopo (Ed.). [in French].

Marchese, E., Scorpio, V., Fuller, I., McColl, S. and Comiti, F. (2017). Morphological changes in Alpine rivers following the end of the Little Ice Age. *Geomorphology*, 295, 811-826. DOI: https://doi.org/10.1016/j.geomorph.2017.07.018.

Matsuoka, N., Ikeda, A. and Date, T. (2005). Morphometric analysis of solifluction lobes and rock glaciers in the Swiss Alps. *Permafrost and Periglacial Processes*, 16, 99-113. DOI: https://doi.org/10.1002/ppp.517.

Matthews, J. A. and Whittaker, R. J. (1987). Vegetation succession on the Storbreen glacier foreland, Jotunheimen, Norway: a review. *Arctic and Alpine Research*, 19(4), Restoration and Vegetation Succession in Circumpolar Lands: Seventh Conference of the Comité Arctique International (Nov., 1987), 385-395. DOI: https://doi.org/10.2307/1551403.

Mavris, C., Egli, M., Plötze, M., Blum, J. D., Mirabella, A., Giaccai, D., and Haeberli, W. (2010). Initial stages of weathering and soil formation in the Morteratsch proglacial area (Upper Engadine, Switzerland). *Geoderma,* 155(3-4), 359-371. DOI: https://doi.org/10.1016/j.geoderma.2009.12.019.

Messenzehl, K., Viles, H., Otto, J.-Ch., Ewald, A. and Dikau, R. (2018). Linking rock weathering, rockwall instability and rockfall supply on talus slopes in glaciated hanging valleys (Swiss Alps). *Permafrost and Periglac Process*,1-17. DOI: https://doi.org/10.1002/ppp.1976.

MeteoSchweiz (2023). Temperature and Precipitation Data at Grächen Station. URL: www.//meteoschweiz.admin/services/Graechen [last access: 24.09.2024]

MeteoSchweiz (2024). Weather station Turtmann. URL: https://www.meteoschweiz.admin.ch/service-und-publikationen/applikationen/messwerte-und-messnetze.html#param=messnetz-automatisch&table=false&station=VSTUR [last access: 25.09.2024].

Meyer, L. (1923). Das Turtmanntal. In: Zentralkommittee des Schweizer Alpenclubs (Eds.). *Jahrbuch des Schweizer Alpenclub*, Verlag des Schweizer Alpenclubs, Bern, 279 – 322. URL: https://www.sac-cas.ch/de/die-alpen/ausgaben/1923/ [last access: 25.09.2024] [in German; only accessible with membership to SAC].

Montgomery, D. R. (1999). Process domains and the river continuum. *Journal of the American Water Resources Association*, 35(2), 397-410. DOI: https://doi.org/10.1111/j.1752-1688.1999.tb03598.x.

Moris, J. V., Vacchiano, G., Ascoli, D. and Motta, R. (2017). Alternative stable states in mountain forest ecosystems: the case of European larch (L. decidua Mill.) forests in the western Alps. *Journal of Mountain Science,* 14(5), 811-822. DOI: 10.1007/s11629-016-4328-1.

Moser, L., Fonti, P., Büntgen, U., Esper, J., Luterbacher, J., Franzen, J. and Frank, D. (2009). Timing and duration of European larch growing season along altitudinal gradients in the Swiss Alps. *Tree Physiology*, 30 (2), 225–233. DOI: https://doi.org/10.1093/treephys/tpp108.

New House Internet Services BV (n.d.). PTGui. Rotterdam, The Netherlands, URL: https://ptgui.com [last access 09.09.2024].

Newsom, L. A. (2022a). Woody Plants. Wood in Archaeology, Cambridge: Cambridge University Press (Cambridge Manuals in Archaeology), 73–92. DOI: https://doi.org/10.1017/9781107280335.004.

Newsom, L. A. (2022b). Wood Anatomy Basics. Wood in Archaeology, Cambridge: Cambridge University Press (Cambridge Manuals in Archaeology), 93–152. DOI: https://doi.org/10.1017/9781107280335.005.

Nicolussi, K., Le Roy, M., Schlüchter, C., Stoffel, M., and Wacker, L. (2022). The glacier advance at the onset of the Little Ice Age in the Alps: New evidence from Mont Miné and Morteratsch glaciers. *The Holocene*, 32(7), 624-638. DOI: https://doi.org/10.1177/09596836221088247.

Oldroyd, D. R. and Grapes, R. H. (2008). Contributions to the history of geomorphology and Quaternary geology: an introduction. In: *History of Geomorphology and Quaternary Geology*. Geological Society, London, Special Publications, 301, 1-17. DOI: 10.1144/SP301.1.

Otto, J.-Ch. and Dikau, R. (2004). Geomorphologic System Analysis of a High Mountain Valley in the Swiss Alps. *Zeitschrift für Geomorphologie*, 48, 323-341. DOI: 10.1127/zfg/48/2004/323.

Otto, J.-Chr. and Sass, O. (2006). Comparing geophysical methods for talus slope investigations in the Turtmann Valley (Swiss Alps). *Geomorphology*, 76(3-4), 257-272. DOI: https://doi.org/10.1016/j.geomorph.2005.11.008.

Otto, J.-Ch., Schrott, L., Jaboyedoff, M. and Dikau, R. (2009). Quantifying sediment storage in a high alpine valley (Turtmanntal, Switzerland). *Earth Surface Processes and Landforms*, 34, 1726 - 1742. DOI: 10.1002/esp.1856.

Penck, A. and Brückner, E. (1901/1909). Die Alpen im Eiszeitalter. Tauchnitz, Leipzig.

Phillips, M., Haberkorn, A., Kenner, R., & Nötzli, J. (2020). Current changes in mountain permafrost based on observations in the Swiss Alps. *Swiss-Bulletin für angewandte Geologie*, 25(1-2), 53-63.

Playfair, J. (1802). Illustrations of the Huttonian theory of the Earth. Cambridge University Press. DOI: https://doi.org/10.3931/e-rara-12144.

Posit PBC (2024). R Studio Desktop. URL: https://posit.co/download/rstudio-desktop/ [last access 09.09.2024].

QGIS Geographic Information System (Version 3.34.3-Prizen) (2023). Open Source Geospatial Foundation Project. Retrieved from https://www.qgis.org. [last access: 09.09.2024].

Rinntech (n.d.). TSAP-Win^{TM}, URL: https://rinntech.info/products/tsap-win/ [last access 09.09.2024].

Rydgren, K., Halvorsen, R., Töpper, J. P. and Njøs, J. M. (2014). Glacier foreland succession and the fading effect of terrain age. *Journal of Vegetation Science*, 25, 1367-1380. DOI: https://doi.org/10.1111/jvs.12184.

Reinthaler, J. (2024). Digital reconstruction of Little Ice Age glacier extents and surfaces. Dissertation for the degree of Doctor of Natural Sciences (Dr sc. nat.) submitted to the Faculty of Mathematics and Natural Sciences of the University of Zurich. DOI: https://doi.org/10.5167/uzh-261311.

Rist, A., Roth, L. and Veit, H. (2020). Elevational ground/air thermal gradients in the Swiss inner Alpine Valais. *Arctic, Antarctic, and Alpine Research*, 52 (1), 341-360. DOI : 10.1080/15230430.2020.1742022.

Roer, I. and Nyenhuis, M. (2007). Rockglacier activity studies on a regional scale: comparison of geomorphological mapping and photogrammetric monitoring. *Earth Surface Processes and Landforms*, 32, 1747-1758. DOI: https://doi.org/10.1002/esp.1496.

Saderi, S., Rathgeber, C. B. K., Rozenberg, P. and Fournier, M. (2019). Phenology of wood formation in larch (Larix decidua Mill.) trees growing along a 1000-m elevation gradient in the French Southern Alps. *Annals of Forest Science*, 76(89). DOI: https://doi.org/10.1007/s13595-019-0866-3.

Schweingruber, F. H. (1988). Tree Rings: Basics and Applications of Dendrochronology. Kluwer Academic Publishers.. DOl: 10.1007/978-94-009-1273-1

Schweingruber, F. H. (1996). Tree Rings and Environment. Dendroecology. Ed. by S. Swiss Federal Institute for Forest, Landscape Research. Birmensdorf, 609.

Steinemann, O., Ivy-Ochs, S., Hippe, K., Christl, M., Haghipour, N. and Synal, H.-A. (2021). Glacial erosion by the Trift glacier (Switzerland): Deciphering the development of riegels, rock basins and gorges. *Geomorphology*, 375, 107533. DOI: https://www.sciencedirect.com/science/article/pii/S0169555X20305067?via%3Dihub.

Swisstopo (Federal Office of Topography) (n.d.). map.geo.admin.ch: Swiss spatial data platform. URL: https://map.geo.admin.ch [last access: 28.09.2024].

Swisstopo (Federal Office of Topography) (2017). SwissAlti^{3D}. The high precision digital elevation model of Switzerland. URL: https://www.swisstopo.admin.ch/en/height-model-swissalti3d [accessed: 2023/2024]. Documentation: https://backend.swisstopo.admin.ch/fileservice/sdweb-docs-prod-swisstopoch-files/files/2023/11/14/6d40e558-c3df-483a-bd88-99ab93b88f16.pdf [last access: 09.09.2024]. [Documentation is in German].

Swisstopo (Federal Office of Topography) (2024a). SWISSIMAGE 10 cm. The Digital Color Orthophotomosaic of Switzerland. URL: https://www.swisstopo.admin.ch/en/orthoimage-swissimage-10 [accessed: 2023/2024]. Documentation: https://backend.swisstopo.admin.ch/fileservice/sdweb-docs-prod-swisstopoch-files/files/2023/11/14/a84642dc-5feb-48e5-af6b-55df4ae7a10b.pdf accessed [last access: 09.09.2024]. [Documentation is in German].

Swisstopo (Federal Office of Topography) (2024b). SWISSIMAGE HIST. The historical (before 1998) black and white Orthophotomosaic of Switzerland. URL: https://www.swisstopo.admin.ch/en/orthoimage-swissimage-hist [accessed: 2023/2024]. Documentation: https://backend.swisstopo.admin.ch/fileservice/sdweb-docs-prod-swisstopoch-files/files/2023/11/14/a84642dc-5feb-48e5-af6b-55df4ae7a10b.pdf [last access: 09.09.2024]. [Documentation is in German].

Swisstopo (Federal Office of Topography) (2024c). SWISSIMAGE HIST 1946. The historical black and white Orthophotomosaic of Switzerland from 1946. URL: https://www.swisstopo.admin.ch/en/orthoimage-swissimage-hist-1946 [accessed: 2023/2024]. Documentation: https://backend.swisstopo.admin.ch/fileservice/sdweb-docs-prod-swisstopoch-files/files/2023/11/14/a84642dc-5feb-48e5-af6b-55df4ae7a10b.pdf [last access: 09.09.2024]. [Documentation is in German].

Swisstopo (Federal Office of Topography) (2024d). Historical maps “Journey through time” on map.geo.admin. URL: https://www.swisstopo.admin.ch/en/historical-map [accessed: 2023/2024].

Swisstopo (Federal Office of Topography) (2024e). Swiss Map Raster 10 on map.geo.admin. URL: https://www.swisstopo.admin.ch/de/landeskarte-swiss-map-raster-10 [accessed: 2023/2024]. Documentation: https://backend.swisstopo.admin.ch/fileservice/sdweb-docs-prod-swisstopoch-files/files/2023/11/14/2c3c70c9-1729-42b2-9d89-32d179fded9a.pdf [last access: 09.09.2024]. [Documentation is in German].

Swisstopo (Federal office of Topography) (2024f). SwissTLM3D. The large-scale topographic landscape model of Switzerland. URL: https://www.swisstopo.admin.ch/de/landschaftsmodell-swisstlm3d [accessed: 2024]. Documentation: https://backend.swisstopo.admin.ch/fileservice/sdweb-docs-prod-swisstopoch-files/files/2023/11/14/ac809790-d483-4735-a4f6-153bfea35ff3.pdf [last access: 09.09.2024]. [Documentation is in German].

Swisstopo (Federal Office of Topography) (2024g). Geological atlas of Switzerland 1:25'000. URL: https://www.swisstopo.admin.ch/en/geological-atlas-of-switzerland-1-25000 [last access: 09.09.2024]. With the legend in: https://api3.geo.admin.ch/static/images/legends/ch.swisstopo.geologie-geologische_karte_en_big.pdf (last access: 30.09.2024).

Swisstopo (2024h). Dufourkarte. URL: https://www.swisstopo.admin.ch/de/dufourkarte [last access: 09.09.2024].

Swisstopo (2024i). Siegfriedkarte. URL: https://www.swisstopo.admin.ch/de/siegfriedkarte [last access: 09.09.2024].

Theler, D., Reynard, E., Lambiel, C. and Bardou, E. (2010). The contribution of geomorphological mapping to sediment transfer evaluation in small alpine catchments. *Geomorphology*, 124(3-4), 113-123. DOI: https://doi.org/10.1016/j.geomorph.2010.03.006.

Van der Meer, J. J. M. (1997). Short-lived streamlined bedforms (annual small flutes) formed under clean ice, Turtmann Glacier, Switzerland. *Sedimentary Geology*, 111, 107-118. DOI: https://doi.org/10.1016/S0037-0738(97)00009-2.

Van Tatenhove, F. and Dikau, R. (1990). Past and Present Permafrost Distribution in the Turtmann Valley, Wallis, Swiss Alps. *Arctic and Alpine Research*, 22(3), 302–316. DOI: https://doi.org/10.2307/1551593.

Walliser Bote (2003). 75 Jahre Turtmannhütte. URL: https://www.aloisgrichting.ch/data/Module/archive/25-natur-wissen-reisen-1/00000013.pdf [last access: 12.09.2024]. [in German].

Wanner, H., Pfister, C. and Neukom, R. (2022). The variable European Little Ice Age. *Quaternary Science Reviews*, 287, 107531. DOI: https://doi.org/10.1016/j.quascirev.2022.107531.

Wilford, D. J., Cherubini, P. and Sakals, M. E. (2005). Dendroecology: a guide for using trees to date geomorphological and hydrologic events. B.C. Min. For., Res. Br., Victoria, B.C. Land Manage. Handb. No. 58. URL: http://www.for.gov.bc.ca/hfd/pubs/Docs/Lmh/Lmh58.htm [last access: 23.09.2024].

Wojcik, R., Eichel, J., Bradley, J. and Benning, L. (2021). How allogenic factors affect succession in glacier forefields. *Earth-Science Reviews*, 218, 103642. DOI: https://doi.org/10.1016/j.earscirev.2021.103642.

Yang, D., Yang, F., Niu, Z., Shi, F. and Wang, N. (2021). Tree ring evidence of the retreat history of the Zepu glacier on the southeastern Tibetan Plateau since the Little Ice Age. *Quaternary International*, 604, 60-67. DOI: https://doi.org/10.1016/j.quaint.2021.06.004.

Zemp, M., Paul, F., Hoelzle, M. and Haeberli, W. (2008). Glacier fluctuations in the European Alps, 1850–2000: an overview and spatio-temporal analysis of available data. In: Orlove, B. et al. Darkening Peaks: Glacier Retreat, Science, and Society. Berkeley, US: University of California Press, 152-167. DOI: https://doi.org/10.5167/uzh-9024.

Zhu, H., Xu, P., Shao, X. and Luo, H. (2013). Little Ice Age glacier fluctuations reconstructed for the southeastern Tibetan Plateau using tree rings. Quaternary International, 283, 134-138, DOI: https://doi.org/10.1016/j.quaint.2012.04.011.

Appendix

TABLE A 1 DATA USED FOR THE GEOMORPHOLOGICAL MAPPING IN QGIS. THE RESOLUTION AS WELL AS THE CURRENT STATE OF ACTUALITY AS YEAR IS SHOWN.

data where used	**purpose**	**source**	**current state**
SWISSIMAGE 0.1 m GIS	base map for geomorphological mapping spatial resolution: 0.1 m	swisstopo (Swisstopo, 2024a)	2020 (used in this master thesis)
SWISSIMAGE HIST online	analysing landscape development and glacier position over the years spatial resolution: 1958 - 1998: 0.5 m ± 1 m 1999 - 2005: 0.5 m ± 0.5 m 2005 - 2016: 0.25 m ± 0.25 m or 0.5 m ± 0.5 m 2017: 0.25 m ± 0.1 m	swisstopo (Swisstopo, 2024b)	2022 - 1958
SWISSIMAGE HIST 1946 «Amerikabefliegung» online	analysing landscape development and glacier position over the years spatial resolution: 1 m ± 5 - 10 m	swisstopo (Swisstopo, 2024c)	1946
swissALTI^{3D} GIS	creating the shaded relief and contour lines for observation of landforms spatial resolution: 0.5 - 2 m ± 1 - 3 m	swisstopo (Swisstopo, 2017)	2016/2017
Permafrost and ground ice map GIS	analysing possible places for permafrost	Kenner et al. (2019), developed at SLF (Swisstopo, n.d.)	2019
Historical map collection by Swisstopo online	analysing the landscape and landforms	Dufour map, Siegfried map, series of national maps by Swisstopo (Swisstopo, 2024d; 2024h; 2024i)	1844 - 2024
SWISS Map Raster 10 (LK10) GIS	background for orientation 1:10'000	swisstopo (Swisstopo, 2024d)	2016/2017 (with some individual additions after 2017)
Hydrology swissTML3D online	analysing the landscape and landforms	swisstopo (online map viewer) (Swisstopo, n.d.)	2016/2017

GeoCover (based on GA25) online	analysing the landscape and landforms	swisstopo (online map viewer) (Swisstopo, 2024g) based on the Geological atlas of Switzerland 1:25'000 - sheets Vissoie (CN 1307) and St. Niklaus (LK 1308)	Vissoie (CN 1307): 2008 St. Niklaus (LK 1308): 1980

TABLE A 2 OVERVIEW OF THE GERMINATION AGES AND THE AGES IN YEARS OF THE SAMPLED TREES IN THIS THESIS. IT IS VISIBLE WHICH TREE SAMPLES WERE USED FOR THE CHRONOLOGY.

tree	minimum start of growth	age as of 2023 [years old]	are sample -A and -B part of the chronology in the analysis?
L001	1950	73	yes
L002	1972	51	yes
L003	2004	19	yes
L004	1991	32	yes
L005	1976	47	yes
L006	1991	32	only L006B
L007	1969	54	yes
L008	1970	53	yes
L009	1967	56	yes
L010	1977	46	yes
L011	1974	49	yes
L012	1984	39	yes
L013	1971	52	yes
L014	1976	47	yes
L015	1951	72	yes
L016	1962	61	yes
L017	1992	31	yes
L018	1980	43	yes
L019	1964	59	yes
L020	1960	63	yes
L021	1961	62	yes
L022	2000	23	no, outlier
L023	1990	33	yes
L024	1966	57	yes
L025	1972	51	yes
L026	1974	49	yes

tree	minimum start of growth	age as of 2023 [years old]	are sample -A and -B part of the chronology in the analysis?
L027	1991	32	no, outlier
L028	1966	57	yes
L029	1959	64	yes
L030	1952	71	yes
L031	1961	62	yes
L032	1964	59	yes
L033	2003	20	yes
L034	1967	56	only L034A
L035	1946	77	yes
L036	2002	21	yes
L037	1971	52	yes
L038	1976	47	yes
L039	1963	60	yes
L040	1961	62	yes
L041	1961	62	yes
L042	1983	40	yes
L043	1962	61	yes
L044	1949	74	yes
L045	1976	47	yes
L046	1968	55	yes
L047	1815	208	no, outside the study site
L048	1722	301	no, outside the study site
L049	/	/	/
L050	1842	181	no, outside the study site
L051	1826	197	no, outside the study site

R Code

```
#load firstly the script "allfunctionsdavid23.R"
#loading all these packages
library(dplR)
library(lattice)
library(latticeExtra)
library(zoo)
library(tidyverse)
library(MASS)
library(dyn)
library(readr)

### part 1: tree data ###


# get all the individual tree data, as they are in their own cvs files. need to put them together
in a list here.
# the pattern is L0 for every file
cf_all <- list.files(path = "trees_all", pattern = "L0", full.names = TRUE, recursive = TRUE,
ignore.case = TRUE)

# read each file into a list of data frames
all_data_all <- lapply(cf_all, function(file) {
  read_delim(file, delim = ",", escape_double = FALSE, trim_ws = TRUE)
})

# convert each data frame to a time series object. #ts is time series
ts_list_all <- lapply(all_data_all, function(df) {
  tryCatch({
    ts(df[,2], start = df$Year[1])
  }, error = function(e) {
    message("Error processing file: ", e$message)
    NULL
  })
})

# to remove NULL elements if any files failed to convert I could do following code with the
Filter
# ts_list <- Filter(Negate(is.null), ts_list)

# combine all time series into one time series object
all_data_table_all <- do.call(ts.union, ts_list_all)

# then convert ts.union object to data frame (because later on I need it for the detrending of
the curves)
all_data_df_all <- as.data.frame(all_data_table_all)

# set row names to the years and set column names to the names
row.names(all_data_df_all) <- 1949:2023
colnames(all_data_df_all) <- basename(sub("L0_", "", cf_all))


# do detrending to have a more precise way to correlate them
```

```
# 30y-spline is kind of a "standard" flexible high frequency detrending, retaining the decadal
variability.
# with my amount of trees and the age of the trees, 10 years makes more sense than 30 years
all_data_D_all <- detrend(all_data_df_all, method = "Spline", nyrs = 10)

# If the detrending fails, I would check the structure of all_data_df
# str(all_data_df)


# make a mean of the detrended twr
# tbrm is the function for the weighted mean
mean_chrono_all <- ts(apply(all_data_D_all, 1, tbrm),start = 1949)

# to see the mean curve, I can plot it and to see if it has time attributes I can do the other
2 lines
ts.plot(mean_chrono_all, xlab = "year", ylab = "relative TRW growth", main = "mean chronology
of all trees")
print(range(mean_chrono_all, na.rm = TRUE))

# explicitly convert detrended data frame back to a time series (for the ts.plot)
all_data_D_ts_all <- ts(all_data_D_all, start = 1949, frequency = 1)

# determine the range for the y-axis to ensure it includes all data
y_range_all <- range(all_data_D_ts_all, mean_chrono_all, na.rm = TRUE)

# plot all my detrended curves together with the mean curve overlaying it
ts.plot(all_data_D_ts_all, col = "grey", lty = 1, xlab = "year", ylab = "relative TRW growth",
main = "time series in the Turtmann Valley", ylim = y_range_all)
lines(mean_chrono_all, col="black", lwd = 2)



# plot all my detrended curves together with the mean curve of the chronology and the outliers
overlaying it
ts.plot(all_data_D_ts_all, col = "grey", lty = 1, xlab = "year", ylab = "relative TRW growth",
main = "time series in the Turtmann Valley", ylim = y_range_all)
lines(mean_chrono_all, col="black", lwd = 2)
lines(mean_chrono_out, col="red", lwd= 1)


### part 2: climate ###

# read the climate data into R
climate <- library(readr)
climate <- read_delim("nbcn-monthly_GRC_previous.csv",
                      delim = ";", escape_double = FALSE, trim_ws = TRUE)

# need to take out the year and month
climate <- climate %>%
  mutate(
    year = as.numeric(substr(date, 1, 4)),
    month = as.numeric(substr(date, 5, 6))
  )
```

```
# temperature with the columns for the months and the year for the row
# temperatue only for the years from 1949 on
temp <- pivot_wider(data = climate[,-1:-2], names_from = month, values_from = tre200m0)
temp49 <- filter(temp, year > 1948)

# plot each month to see if it works (month 2 = january, 3 = february...), this is an example:
ts.plot(temp49[,3])

# precipitation with the columns for the months and the year for the row
# precipitation only for the years from 1949 on
prec <- pivot_wider(data = climate[,c(-1,-3)] , names_from = month, values_from = rre150m0)
prec49 <- filter(prec, year > 1948)

# plot each month to see if it works (month 2 = january, 3 = february...), this is an example:
ts.plot(prec49[,3])


# need the temperature and precipitation data as numbers (and as a data frame)
temp49[,-1] <- lapply(temp49[,-1], as.numeric)
prec49[,-1] <- lapply(prec49[,-1], as.numeric)

temp49 <- as.data.frame(temp49)
prec49 <- as.data.frame(prec49)


### part 3: climate correlation with tree ring data ###

# comment by Stefan: for this I created two nice functions over the last years to explore
climate-growth relationships
# comment by Stefan: first one is to average monthly data to larger seasons up to 12 months,
therefore you need to load the climate dataset


# runningclimate function #

runningclimate_new<-function(climate,stat = c("mean","sum"),length = 12){
  x.ts<-ts(climate[,2:13],start=climate[1,1]) #transform CRU style climate data into time-series
format
  x.lag<-stats::lag(x.ts,k=-1) #create lag1 series
  x1<-ts.union(x.lag,x.ts) #combine lagged and original series
  length<-12  #default to 12 months
  stat<-match.arg(stat) #no default is given
  seasons<-rep(list(x1),length)
  for(i in 2:length){
    seasons[[i]]<-ts(cbind(matrix(rep(rep(NA,nrow(x1)),i-1),ncol=i-1),t(rollapply(t(sea-
sons[[i]]),i,stat,align='right'))),start=climate[1,1])
    seasons[[i]]<-ts.union(stats::lag(seasons[[i]][,13:24],k=-1),seasons[[i]][,13:24])
    colnames(seasons[[i]])<-c(paste0("p",month.abb),month.abb)
  }

  output<-seasons
}
```

```
runningclimate_new <- function(climate, stat = c("mean", "sum"), length = 12) {
  stat <- match.arg(stat)
  x.ts <- ts(climate[, -1], start = climate$year[1])  # Create time series from climate data
  x.lag <- stats::lag(x.ts, k = -1)
  x1 <- ts.union(x.lag, x.ts)

  seasons <- list()
  for (i in 1:length) {
    rolled <- rollapply(t(x1), i, stat, align = 'right')
    seasons[[i]] <- ts(t(rolled), start = climate$year[1])
    colnames(seasons[[i]]) <- c(paste0("p", month.abb), month.abb)
  }
  return(seasons)
}

temp.dataset <- runningclimate_new(temp49, stat = "mean") #this does not work but i do not know
why; but I do not need it
prec.dataset <- runningclimate_new(prec49, stat = "mean") #this does not work but i do not know
why; but I do not need it

# comment by Stefan: for correlations it does not matter if you choose "mean" or "sum". That's
for another script where it might matter.
# comment by Stefan: this returns a list of 12, where [[1]] is still the original monthly data,
[[2]] two-months averages, and so on! Columns range from pJan to current Dec. The alignment is
"right", so your timeseries e.g. [[List3]][,column20] would be JuneJulyAugust of current year
# comment by Stefan: second is the nice correlation plot with end months in columns and win-
dow/season lengths in rows

# Climate Plot with correlations #

Climateplot_new <- function(TRW, Climatesite, fyr, lyr, detrended = c("Yes", "No"), method =
c("pearson", "spearman"), spline.length) {
  detrended <- match.arg(detrended)
  METHOD <- match.arg(method)

  climatecor <- vector("list", length(Climatesite))

  if (detrended == "Yes") {
    tsstart <- tsp(Climatesite[[1]])[1]
    for (i in 1:length(Climatesite)) {
      Climatesite[[i]] <- ts(apply(Climatesite[[i]], 2, function(x) {
        if (sum(complete.cases(x)) > 3) {
          spline.det(ts(x), spline.length)$residualarray
        } else {
          rep(NA, length(x))
        }
      }), start = tsstart)
      climatecor[[i]] <- cor(ts.union(Climatesite[[i]], window(TRW, start = fyr, end = lyr)),
use = "p", method = METHOD)
    }
  } else {
    for (i in 1:length(Climatesite)) {
```

```
      climatecor[[i]] <- cor(ts.union(Climatesite[[i]], window(TRW, start = fyr, end = lyr)),
use = "p", method = METHOD)
    }
  }

  levelplotmatrix <- matrix(NA, length(Climatesite), 22)
  for (i in 1:length(Climatesite)) {
    levelplotmatrix[i, ] <- climatecor[[i]][1:22, ncol(Climatesite[[i]]) + 1]
  }

  rownames(levelplotmatrix) <- 1:length(Climatesite)
  colnames(levelplotmatrix) <- c(paste0("p", month.abb), month.abb[1:10])

  return(levelplotmatrix)
}

# example usage
fyr <- 1949
lyr <- 2023
TRW_all <- all_data_D_all

# ensure TRW is a time series, in case it does not work
TRW_all <- ts(apply(TRW_all, 1, tbrm), start = fyr)


#run latticeExtra again for the function + to work for the plot
library(latticeExtra)

# climate correlation plots for temperature
silly_cor <- Climateplot_new(TRW_all, temp.dataset, fyr = fyr, lyr = lyr, detrended = "Yes",
spline.length = 10, method = "spearman")

title <- "correlation of TWR with temperature in the Turtmann Valley"
P1_all <- contourplot(t(silly_cor), region = TRUE, contour = FALSE, scales = list(tck = c(1,
0)), main = title, par.settings = list(fontsize = list(text = 8, points = 10)), lwd = 0.4,
axis.text = list(cex = 0.5), labels = list(cex = 0.5), col.regions = colorRampPalette(c("red",
"yellow", "white", "lightblue", "blue")), at = seq(-0.825, 0.825, 0.05), xlab = "End months",
ylab = "Season length")
P2_all <- contourplot(t(silly_cor), col.regions = FALSE, scales = list(tck = c(1, 0)), par.set-
tings = list(fontsize = list(text = 8, points = 10)), axis.text = list(cex = 0.5), labels =
list(cex = 0.5), cex = 0.5, region = FALSE, lwd = 0.4, at = seq(-0.80, 0.80, 0.1))

combined_plot_temp <- P1_all + as.layer(P2_all)
print(combined_plot_temp)


# climate correlation plots for precipitation
silly_cor <- Climateplot_new(TRW, prec.dataset, fyr = fyr, lyr = lyr, detrended = "Yes",
spline.length = 10, method = "spearman")

title <- "correlation of TWR with precipitation in the Turtmann Valley"
P3_all <- contourplot(t(silly_cor), region = TRUE, contour = FALSE, scales = list(tck = c(1,
0)), main = title, par.settings = list(fontsize = list(text = 8, points = 10)), lwd = 0.4,
axis.text = list(cex = 0.5), labels = list(cex = 0.5), col.regions = colorRampPalette(c("red",
```

```
"yellow", "white", "lightblue", "blue")), at = seq(-0.825, 0.825, 0.05), xlab = "End months",
ylab = "Season length")
P4_all <- contourplot(t(silly_cor), col.regions = FALSE, scales = list(tck = c(1, 0)), par.set-
tings = list(fontsize = list(text = 8, points = 10)), axis.text = list(cex = 0.5), labels =
list(cex = 0.5), cex = 0.5, region = FALSE, lwd = 0.4, at = seq(-0.80, 0.80, 0.1))

combined_plot_prec <- P3_all + as.layer(P4_all)
print(combined_plot_prec)
```

Personal Declaration

I hereby declare that the submitted thesis is the result of my own, independent work. All external sources are explicitly acknowledged in the thesis.

Zürich, 30.09.2024

Location, Date

Ariane Dieth